Study of Kaon Bag Parameter with Wilson Fermion using Gradient Flow

著者（英）	Asobu Suzuki
year	2019
その他のタイトル	Gradient Flowを用いたWilsonフェルミオンでのK中間子Bagパラメータの研究
学位授与大学	筑波大学 (University of Tsukuba)
学位授与年度	2018
報告番号	12102甲第8934号
URL	http://doi.org/10.15068/00156551

Study of Kaon Bag Parameter with Wilson Fermion using Gradient Flow

Asobu Suzuki

February 2019

Study of Kaon Bag Parameter with Wilson Fermion using Gradient Flow

Asobu Suzuki
Doctoral Program in Physics

Submitted to the Graduate School of
Pure and Applied Sciences
in Partial Fulfillment of the Requirements
for the Degree of Doctor of Philosophy in Science
at the University of Tsukuba

Contents

1 Introduction

The study of the $K_0 - \overline{K}_0$ mixing is very important phenomena to study the indirect CP-violation, because the CKM matrix elements emerges in the Feynman diagrams. The mission of the lattice QCD is the calculation of the QCD correction of the diagrams, such quantity is called as the kaon bag parameter. There were many efforts to calculate the kaon bag parameter, however, it tends to struggle in the calculation using the Wilson-type fermions. This problem relates to the chiral symmetry breaking which makes us to perform an extra renormalization. We discuss about the kaon physics and its relation with the $K_0 - \overline{K}_0$ mixing in the section 2.1.

In this thesis, we suggest that the gradient flow works for the calculation of the kaon bag parameter. The gradient flow is a recent new effort of the lattice QCD, it considers a fictitious time and the developments of fields towards that direction. Moreover, the gradient flow has a property that it removes the ultraviolet divergence from the theory, in other words, we can regard the gradient flow as a certain renormalization scheme. From the previous researches, we know the way to define the renormalized operator via the gradient flow scheme, which is called as the small flow time expansion. It is also known that the background field method can be applied to the flowed theory and it makes calculations slightly easy. We will review these techniques of the gradient flow in the section 3.1.

The gradient flow made many contributions to the lattice QCD. For example, the energy momentum tensor is successfully defined even on the lattice via the gradient flow. The energy momentum tensor is a convenient origin of the thermodynamical quantities and is defined as a Noether current of the translational symmetry. Since the translational symmetry is broken on the lattice, it has the important meaning that the gradient flow removes the details of the lattice. In addition, the computation of the topological susceptibility provides a new perspective for calculations with the Wilson fermion. The topological susceptibility is involved with the axion and known as one of the targets of the finite temperature lattice QCD. The topological susceptibility can be defined via the two different ways, however, one of them uses the chiral Ward-Takahashi identity. The previous work tells that the two definitions have good agreement with each other. From the fact that the Wilson fermion breaks the chiral symmetry, the gradient flow makes the great assistance of the renormalization even for the Wilson fermion.

We would like to use the consequence above to the other computation. In especially, the aim of this study is calculation of the kaon bag parameter with the Wilson fermion using the gradient flow. We must calculate a transition amplitude of the $\Delta S = 2$ four fermion operator, $O^{\Delta S=2} = (\overline{s}\gamma_\mu^L d)(\overline{s}\gamma_\mu^L d)$, to calculate the kaon bag parameter. When we consider the renormalization of the $\Delta S = 2$ four fermion operator, however, it must be contaminated by another operators which have same parity and other chirality with the original $\Delta S = 2$ four fermion operator.

$$O_{Ren.}^{\Delta S=2} = ZO^{\Delta S=2} + \sum_i Z_i O_i.$$

Our prospectus is that the gradient flow undertakes this bothersome renormalization.

To substantiate our claim, we numerically study about the meson correlation functions in the section 3.3 and 3.5. In particular, we estimate meson masses, pion decay constant and PCAC mass using the gradient flow. In especially, the calculation of PCAC mass is important from the viewpoint of chiral symmetry, because it is defined via the PCAC relation which is a kind of the chiral Ward-Takahashi identity. Our numerical results were consistent with the Schrödinger functional scheme, therefore, the gradient flow works well for the lattice calculation.

In this study, we will consider the matching factor of the $\Delta S = 2$ operator. Calculations with the gradient flow is very convenient, however, what we want to calculate are operators renormalized in the $\overline{\text{MS}}$ scheme. Such transformation can be done by the small flow time expansion method [37],[120]-[123]. According to the small flow time expansion method, we can evaluate the matching factor with the perturbation theory. For the fermion bi-linear operators, the matching factor have been calculated. Since our new calculation is in relation to the four fermion operators, we calculate it in the section 4.1. The calculation of four fermion operator needs several techniques, dimensional reduction scheme and Fierz rearrangement. We will review these techniques at the same time. We also challenge to the calculation of the $\Delta S = 1$ operator which is important for the $K \to \pi\pi$ decay in the section 4.2. $\Delta S = 1$ operator includes so-called penguin diagrams. We will evaluate them with the gradient flow.

2 Kaon Bag Parameter

The purpose of the lattice QCD is to ”solve” the QCD from the view point of first principle numerical study. For example, the nucleon-nucleon potential is one of the recent achievements of the lattice QCD and the finite density lattice QCD challenges to drive the confinement/deconfinement phase transition of the QCD phase diagram. It is also important to study the CP violation phenomena, because it is involved with the undecided parameter of the Standard Model.

Historically, CP violation is deeply involved with the kaon physics. The kaon has been discovered in 1947 and contributed to the discovery of CP violation in 1964. After that, the kaon physics has been active as a prove of the CP violation. Even in the 21st century, the NA48 and the KTeV experiments detected the direct CP violation from the kaon decay.

The neutral kaon has an unique property that it oscillate to its antiparticle pair with each other. This phenomena is called as the $K^0 - \overline{K^0}$ mixing and gives an indirect evidence of the CP violation. The kaon bag parameter also relates to the CP violation phenomena, since it gives QCD corrections of the $K^0 - \overline{K^0}$ mixing. There are many works to attacking the bag parameter, however, it tends to suffer from the operator mixing for the Wilson type fermions.

The lattice QCD is one of the most powerful framework to attack the QCD in a non-perturvative way, however, we must take care to artifacts called doublers. It is known that the lattice action which describes one particle corresponds to 16 particles in the naive discretization method. The Wilson fermions add the extra term which vanishes in the continuum limit and succeed to remove the doublers in exchange for the chiral symmetry. This effort is useful for many observables, however, if an observable relates to the chiral symmetry we must perform an extra renormalization to obtain the correct result. The kaon bag parameter just corresponds to this case.

In this section, we will discuss about the mechanism of the operator mixing. The section 2.1 shows the definition of the bag parameter and its relation with the CP violation via the $K^0 - \overline{K^0}$ mixing. The section 2.2 shows an brief introduction to the lattice QCD with the Wilson fermion, in which we will see the explicit chiral symmetry breaking and its effect.

2.1 Standard Model Parameter

The Standard Model describes strong, electromagnetic and weak interactions based on the $SU(3)_C \times SU(2)_L \times U(1)_Y$ gauge theory [1]-[9]. In 2012, the Standard model Higgs boson was detected by ATLAS and CMS collaborations [10][11], and the Standard Model was established. However, there are some parameters which cannot be fixed from the original theory. The CKM mixing angles and the CP violation phase are included in such the undecided parameters. In this section, we will start from the CP violation phenomena and reach to the kaon bag parameter which describes the QCD correction of the $K_0 - \overline{K}_0$ mixing.

2.1.1 CP Violation

In our Universe, the matter exists overwhelmingly more than the antimatter. It indicates that the CP symmetry is broken under the development of the Universe. The CKM matrix takes into account about the CP violation in the Standard Model.

The CP violation deeply relates to the kaon physics. The experiment which firstly found the CP violation detected the process in kaon decays [12]. The K^0 state is constructed from the $\overline{s}$ quark and the d quark. It has an antiparticle pair $\overline{K^0}$ and they are related via the CP transformation as

$$CP\left|K^0\right\rangle = -\left|\overline{K^0}\right\rangle. \tag{2.1}$$

From this relation, we can construct eigenstates of the CP transformation,

$$K_1 = \frac{1}{\sqrt{2}}\left(K^0 - \overline{K^0}\right), \tag{2.2}$$

$$K_2 = \frac{1}{\sqrt{2}}\left(K^0 + \overline{K^0}\right). \tag{2.3}$$

They have eigenvalue ± 1. Let us assume that the weak interactions do not change the CP symmetry and consider a decay process to two pion state. Because the two pion state is CP even,

$$CP\left|\pi\pi\right\rangle = +\left|\pi\pi\right\rangle, \tag{2.4}$$

only the K_1 can decays to the two pion state. However, the experiment [12] detected that the K_2 can decay to the two pion state via a state called as K_L.

Let us next regard the K_0 and $\overline{K^0}$ as the two state system and consider their time evolution via the Hamiltonian,

$$H = M - \frac{i}{2}\Gamma = \begin{pmatrix} M_{11} - \frac{i}{2}\Gamma_{11} & M_{12} - \frac{i}{2}\Gamma_{12} \\ M_{12}^* - \frac{i}{2}\Gamma_{12}^* & M_{22} - \frac{i}{2}\Gamma_{22} \end{pmatrix}. \tag{2.5}$$

Because of the CPT, we can assume symmetry that

$$H_{11} = H_{22}. \tag{2.6}$$

From the Schrödinger equation,

$$i\frac{\mathrm{d}}{\mathrm{d}t}\psi = H\psi, \tag{2.7}$$

we obtain the time evolution of the each state as

$$\begin{aligned} i\frac{\mathrm{d}}{\mathrm{d}t}K_1 &= \left[H_{11} - M_{12} + \frac{i}{2}\mathrm{Re}\left\{\Gamma_{12}\right\}\right]K_1 + \frac{1}{2}\mathrm{Im}\left\{\Gamma_{12}\right\}K_2 \\ i\frac{\mathrm{d}}{\mathrm{d}t}K_2 &= \left[H_{11} + M_{12} - \frac{i}{2}\mathrm{Re}\left\{\Gamma_{12}\right\}\right]K_2 - \frac{1}{2}\mathrm{Im}\left\{\Gamma_{12}\right\}K_1. \end{aligned} \tag{2.8}$$

Therefore, K_1 and K_2 do not diagonalize the Hamiltonian (2.5) and are mixed with each other. Since K_1 has even parity and K_2 has odd parity for the CP transformation CP is no longer conserved under this Hamiltonian.

2.1.2 CKM matrix

As we saw in the previous section, the mixing, in other words the CP violation, comes from the complex number. The Cabbibo-Kobayashi-Maskawa matrix $\{V_{ij}\}$ describes the mixture between the other generations of quarks, which explains the CP violation [14][15]. By using the CKM matrix we can write the coupling of the W gauge bosons as

$$-\frac{g}{2\sqrt{2}}W_\mu^- \begin{pmatrix} \bar{u}^\alpha & \bar{c}^\alpha & \bar{t}^\alpha \end{pmatrix} \gamma^\mu(1-\gamma_5) \begin{pmatrix} V_{ud} & V_{us} & V_{ub} \\ V_{cd} & V_{cs} & V_{cb} \\ V_{td} & V_{ts} & V_{tb} \end{pmatrix} \begin{pmatrix} d_\alpha \\ s_\alpha \\ b_\alpha \end{pmatrix}. \tag{2.9}$$

Because of the unitarity of the CKM matrix, it has 9 free parameters. Because some of the parameters can be absorbed into the phase of the quark fields it is enough to consider 4 parameters as

$$\begin{pmatrix} c_{12}c_{13} & s_{12}c_{13} & s_{13}e^{-i\delta_{13}} \\ -s_{12}c_{23} - c_{12}s_{23}s_{13}e^{i\delta_{13}} & c_{12}c_{23} - s_{12}s_{23}s_{13}e^{i\delta_{13}} & s_{23}c_{13} \\ s_{12}s_{23} - c_{12}c_{23}s_{13}e^{i\delta_{13}} & -c_{12}c_{23} - s_{12}c_{23}s_{13}e^{i\delta_{13}} & c_{23}c_{13} \end{pmatrix}, \tag{2.10}$$

where we denoted as

$$c_{ij} = \cos(\theta_{ij}),\ s_{ij} = \sin(\theta_{ij}), \tag{2.11}$$

and the 4 free parameters as θ_{12}, θ_{23}, θ_{13} and δ_{13}[1]. Because the experimental data show that

$$s_{13} \ll s_{23} \ll s_{12}, \tag{2.12}$$

[1]This parameterization is called as standard parameterization [16].

we can parameterize that

$$s_{12} = \lambda,\ s_{23} = A\lambda^2,\ s_{13}e^{i\delta_{13}} = A\lambda^3(\rho - i\eta), \tag{2.13}$$

with the parameters λ, A, ρ and η[2]. The CKM matrix becomes

$$\begin{pmatrix} 1-\frac{1}{2}\lambda^2 & \lambda & A\lambda^3(\rho - i\eta) \\ -\lambda & 1-\frac{1}{2}\lambda^2 & A\lambda^2 \\ A\lambda^3(1-\rho-i\eta) & -A\lambda^2 & 1 \end{pmatrix}, \tag{2.14}$$

for $\mathcal{O}\left(\lambda^4\right)$.

Note that the complex numbers emerge in the matrix elements V_{ub} and V_{td} denote the CP violation in the Standard Model.

2.1.3 $\mathbf{K^0 - \overline{K^0}}$ mixing

In the section 2.1.1, we dealt the $K^0 - \overline{K^0}$ system and mixing. The eigenstates which diagonalize the Hamiltonian are not K_1 and K_2. The correct ones are given as

$$|K_S\rangle = \frac{1}{\sqrt{1+\epsilon^2}}\left(|K_1\rangle + \epsilon\,|K_2\rangle\right), \tag{2.15}$$

$$|K_L\rangle = \frac{1}{\sqrt{1+\epsilon^2}}\left(|K_2\rangle + \epsilon\,|K_1\rangle\right). \tag{2.16}$$

The subscripts S/L mean the short/long living particle. The K_S mainly decays to the two pion CP even state, on the other hand, the K_S mainly decays to the three pion CP odd state. However, because of the mixing K_L can also decays to the two pion state although such process is rare.

Let us consider the box diagrams in Figure 1 which describe the $K^0 - \overline{K^0}$ mixing. It is important

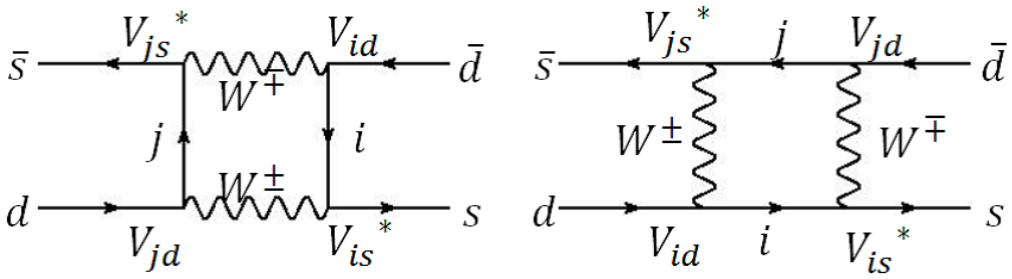

Figure 1: Box diagrams of the $K^0 - \overline{K^0}$ mixing.

that at the vertex there are the complex CKM matrix elements V_{ub} and V_{td}. In the Standard Model, we cannot apply the perturbation theory to the QCD part since the coupling constant becomes large

[2]This parameterization is called as Wolfenstein parameterization [17].

at low energy scale. To take out the QCD part from the diagrams, [18] and [19] integrate out heavier particles and obtain the effective Hamiltonian as

$$\mathcal{H}_{\text{eff.}}^{\Delta S=2} \propto \int \mathrm{d}^4x\, O^{\Delta S=2}(x), \tag{2.17}$$

$$O^{\Delta S=2} = \left(\bar{s}\gamma_\mu(1-\gamma_5)d\right)\left(\bar{s}\gamma_\mu(1-\gamma_5)d\right). \tag{2.18}$$

The bag parameter our target of this study characterize the matrix element of the $\Delta S = 2$ operator as

$$B_K = \frac{\left\langle \overline{K^0}\left| O^{\Delta S=2}\right| K^0\right\rangle}{\frac{8}{3}\left|\left\langle 0\left|\bar{s}\gamma_\mu(1-\gamma_5)d\right| K^0\right\rangle\right|^2} = \frac{\left\langle \overline{K^0}\left| O^{\Delta S=2}\right| K^0\right\rangle}{\frac{8}{3}m_K^2 f_K^2}, \tag{2.19}$$

where m_K and f_K mean the mass and decay constant of the kaon. We need the lattice QCD calculation to obtain the bag parameter.

In this section, we considered the CP violation in the viewpoint of the kaon system. Since the $K^0 - \overline{K^0}$ mixing does not describe the end state of the decay process, it is called as the indirect CP violation. The bag parameter relates to the QCD part of the $K^0 - \overline{K^0}$ mixing and it is necessary to use the lattice calculation.

2.2 Lattice Fermion and Chiral Symmetry

The lattice regularization has two important meanings for the field theory. One is that the lattice regularization provides a non-perturbative formulation of the theory. It is well known that the Wilsonian renormalization group approach brought a big progress in the analysis of the critical phenomenon. One is that the lattice, discrete space time, is compatible with numerical calculations. The lattice QCD is almost the only numerical method that gives non-perturbative calculations, and becomes a big field in the elementary particle theory nowadays. We focus on the later property and consider an application to the bag parameter. We will review some problems specific to the lattice QCD in the progress.

2.2.1 Naive discretization

In this section, we will see the most naive discretization procedure of the QCD. Since QCD needs the gauge invariance of the theory, it is natural to put quarks on the site and put gluon on the link[3]. Along with that, the gauge fields are defined through the link variable,

$$U_\mu(x) = e^{ig_0 A_\mu(x+\hat{\mu}/2)}. \tag{2.20}$$

The gauge transformations are defined as

$$\begin{aligned}
\psi(x) &\rightarrow \Omega(x)\psi(x), && (2.21)\\
\bar{\psi}(x) &\rightarrow \bar{\psi}(x)\Omega^\dagger(x), && (2.22)\\
U_\mu(x) &\rightarrow \Omega(x+\hat{\mu}a)U_\mu(x)\Omega^\dagger(x), && (2.23)\\
\Omega(x) &\in SU(3), && (2.24)
\end{aligned}$$

on the lattice. When we take the naive continuum limit $a \rightarrow 0$ the gauge transformation (2.23) reproduces the correct gauge transformation, because

$$\begin{aligned}
&1 + ig_0 a A_\mu(x) + O(a^2)\\
&\rightarrow 1 + ig_0 a \left\{ \Omega(x) A_\mu \Omega^\dagger(x) - \frac{i}{g}\Omega(x)\partial_\mu \Omega^\dagger(x) \right\} + O(a^2). \qquad (2.25)
\end{aligned}$$

By using the link variable, we can construct the gauge invariant plaquette action as

$$\begin{aligned}
S_w(U) &= \frac{1}{g_0^2}\sum_{x,\mu,\nu} \mathrm{Re\,tr}\left[U_{\mu\nu} + U\mu\nu^\dagger(x)\right], && (2.26)\\
U_{\mu\nu}(x) &= U_\mu(x)U_\nu(x+\hat{\mu})U_\mu^\dagger(x+\hat{\nu})U_\nu^\dagger(x), && (2.27)
\end{aligned}$$

[3]Gauge fields $A_\mu(x)$ depends not only on the coordinate x but also on the direction μ!

where $U_{\mu\nu}$ is called as the plaquette which is the simplest gauge invariant quantity. We can also show that when we take a naive continuum limit $a \to 0$ the plaquette action becomes the gluon action as

$$S_g[U] = \frac{6}{g_0^2}\sum_{x;\mu<\nu}\left\{1-\frac{1}{6}Tr\left(U_{\mu\nu}(x)+U\mu\nu^{\dagger}(x)\right)\right\} \tag{2.28}$$

$$= \int dx\, F^a_{\mu\nu}(x)F^a_{\mu\nu}(x)+O(a^2). \tag{2.29}$$

In practice, the rectangular action[4] (2.30) is often used, because it can get closer to the continuum limit earlier than the plaquette action.

$$S_g[U] = \frac{1}{g_0^2}\sum_{x;\mu\neq\nu} Tr\left\{(1-8C)U_{\mu\nu}(x)+C\left(R_{\mu\mu\nu}(x)+R_{\nu\nu\mu}(x)\right)\right\}, \tag{2.30}$$

$$R_{\mu\mu\nu}(x) = U_\mu(x)U_\mu(x+\hat{\mu}a)U_\nu(x+2\hat{\mu}a)U^\dagger_\mu(x+\hat{\mu}a+\hat{\nu}a)U^\dagger_\mu(x+\hat{\nu}a)U^\dagger_\nu(x), \tag{2.31}$$

where $R_{\mu\mu\nu}$ is the 2×1 rectangular plaquette.

The naive discretization of the fermion action is given by

$$S^0_F[U,\psi,\overline{\psi}] = \sum_x \overline{\psi}'(x)\left\{\sum_\mu \frac{\gamma_\mu}{2}\left(U_\mu(x)\psi'(x+\hat{\mu})-U_\mu(n-\hat{\mu})\psi'(x-\hat{\mu})\right)\right\} + m\sum_x \overline{\psi}(x)\psi(x). \tag{2.32}$$

Note that we rewrite the quark field $\psi' = a^{3/2}\psi$ and the quark mass $M = ma$ to erase the dimension. This action return to the continuum action in $a \to 0$,

$$S^0_F[U,\psi,\overline{\psi}] \to \int \mathrm{d}^4x\ \left\{\overline{\psi}(x)\gamma_\mu D_\mu\psi(x)+m\overline{\psi}(x)\psi(x)\right\}, \tag{2.33}$$

however, it includes the doublers which are extra degrees of freedom. To indicate the doublers explicitly, let us take

$$U_\mu(x) = 1. \tag{2.34}$$

With this condition, the naive fermion action becomes

$$S^0_F[U=1,\psi,\overline{\psi}] = \sum_x \overline{\psi}'(x)\left\{\sum_\mu \frac{\gamma_\mu}{2}\left(\psi'(x+\hat{\mu})-\psi'(x-\hat{\mu})\right)\right\} + M\sum_x \overline{\psi}'(x)\psi'(x)$$

$$= \int_p \overline{\psi}'(-p)\left(i\gamma_\mu \sin(p_\mu a)+m\right)\psi'(p), \tag{2.35}$$

[4] $C = -0.331$ is known as the Iwasaki gauge action[106].

where we denoted

$$\int_p (\cdots) = \int \frac{1}{(2\pi)^4} \mathrm{d}^4 p \, (\cdots). \tag{2.36}$$

In the naive continuum limit, the quark propagator is given by

$$\left\langle \psi(x)\overline{\psi}(y) \right\rangle = \sum_{\bar{p}} e^{i\bar{p}\cdot\frac{x-y}{a}} \int_p \frac{-i\sum_\mu e^{i\bar{p}_\mu}\gamma_\mu \tilde{p}_\mu + m}{\tilde{p}^2 + m^2} e^{ip\cdot(x-y)}, \tag{2.37}$$

$$\tilde{p}_\mu = \frac{1}{a}\sin(p_\mu a) \tag{2.38}$$

where we denoted $\bar{p}$ as the momenta runs in $2^D = 16$ vertices of the hyper-cubic lattice,

$$\bar{p} \in \{(0,0,0,0), (\pi,0,0,0), (\cdots), (\pi,\pi,0,0), (\cdots), (\pi,\pi,\pi,0), (\cdots), (\pi,\pi,\pi,\pi)\}, \tag{2.39}$$

where $(\cdots)$ means possible permutations. These 15 extra degrees of freedom are called doubler, which must be removed from the lattice theory.

2.2.2 Nielsen-Ninomiya theorem

The fermion doubling problem is not failure of the lattice formulation. We can understand it as a property the lattice formalization essentially has. Such property is known as Nielsen-Ninomiya theorem [26]. The statement of the theorem is that if the lattice fermion satisfy the assumptions below the doubling problem must occur.

- translational invariance on the lattice
- chiral symmetry
- hermitian symmetry
- bi-linear form of the fermion field
- locality

One can find the proof of this theorem, for example, in [27] and [28], in which the Poincáre-Hopf index theorem is used.

2.2.3 Wilson fermion

The Nielsen-Ninomiya theorem seems to impose the strong restriction to the lattice theory. However, if we use it in the reverse sense there are possibilities to avoid the fermion doubling problem.

The Wilson fermion realizes it by giving up the chiral symmetry of the fermion action.

The chiral transformation is defined by

$$\psi \rightarrow e^{i\theta\gamma_5}\psi \tag{2.40}$$

$$\overline{\psi} \rightarrow \overline{\psi}e^{i\theta\gamma_5}. \tag{2.41}$$

Since the γ_5 anti-commutes with the other gamma matrices γ_μ the naive fermion action (2.33) is surely invariant with respect to the chiral transformation. Besides, half of the doublers,

$$\bar{p} \in \{(0,0,0,0), (\pi,\pi,0,0), (\cdots), (\pi,\pi,\pi,\pi)\}, \tag{2.42}$$

have positive chirality and the other half of the doublers

$$\bar{p} \in \{(\pi,0,0,0), (\cdots), (\pi,\pi,\pi,0), (\cdots)\}, \tag{2.43}$$

have negative chirality.

The Wilson fermion is defined as

$$\begin{aligned} S_F^{\text{Wilson}}[U,\psi,\overline{\psi}] &= S_F^0[U,\psi,\overline{\psi}] \\ &- \frac{r}{2}\sum_{x;\mu}\left\{\overline{\psi}'(x)U_\mu(x)\psi'(x+\hat{\mu}) + \overline{\psi}'(x+\hat{\mu})U_\mu^\dagger(x)\psi'(x) - 2\overline{\psi}'(x)\psi'(x)\right\} \end{aligned} \tag{2.44}$$

The additive term corresponds to $O(a)$ term,

$$-ar\int \mathrm{d}^4x\,\overline{\psi}(x)D^2\psi(x), \tag{2.45}$$

and it will be vanished in the naive continuum limit. Simultaneously, it can be seen that the additive term breaks the chiral symmetry explicitly. Let us consider the quark propagator again. We can write down it as

$$\left\langle\psi(x)\overline{\psi}(y)\right\rangle = \sum_{\bar{p}} e^{i\bar{p}\cdot\frac{x-y}{a}}\int_p \frac{-i\sum_\mu e^{i\bar{p}_\mu}\gamma_\mu\tilde{p}_\mu + m(p)}{\tilde{p}^2 + m^2(p)}e^{ip\cdot(x-y)}, \tag{2.46}$$

$$m(p) = m + \frac{2r}{a}\sum_\mu \sin^2(p_\mu a/2). \tag{2.47}$$

We can see that the pole mass is changed from (2.37). The mass $m(p)$ returns to the bare mass m in the continuum limit. On the other hand, $m(p)$ diverges as $1/a$ at the 15 edges of the Brillouin zone. In this way, the doublers are removed from the theory at the expense of the chiral symmetry for the Wilson fermion.

Practically, the Wilson-clover fermion [105] is frequently used,

$$S_F^{\text{Wilson-clover}}[U,\psi,\bar{\psi}] = S_F^{\text{Wilson}}[U,\psi,\overline{\psi}] - C_{sw}\sum_{\mu<\nu}\frac{\bar{\psi}'(x)[\gamma_\mu,\gamma_\nu]}{2i}\hat{F}_{\mu\nu}(x)\psi'(x), \tag{2.48}$$

where we defined the "clover" term as

$$\hat{F}_{\mu\nu}(x) \;:=\; -\frac{i}{8}(U_{\mu\nu}(x) + U_{\mu-\nu}(x) + U_{-\mu\nu}(x) + U_{-\mu-\nu}(x) - (\mu \longleftrightarrow \nu)). \tag{2.49}$$

This additional term is $O(a)$ improvement of the action and it approaches to

$$-aC_{sw}\int d^4x\, \bar{\psi}(x)\frac{[\gamma_\mu,\gamma_\nu]}{2i}F_{\mu\nu}(x)\psi(x), \tag{2.50}$$

in the continuum limit.

There are some kinds of fermions besides the Wilson fermion. The Kogut Susskind fermion [29] doubles the effective lattice spacing to reduce the Brillouin zone. The doublers reduce to half, however, the chiral symmetry also breaks. The overlap fermion [32] which satisfies the Ginsparg Wilson relation [30] and the domain wall fermion [31] which uses the five dimensional heavy quarks are new efforts of the lattice QCD. They avoid the fermion doubling problem and realize the lattice chiral symmetry at the same time in exchange for computational costs.

2.2.4 Operator mixing

The Wilson fermion explicitly breaks the chiral symmetry as we saw in the previous section. This breaking emerges as artifacts which have different chirality on the calculation of the bag parameter. To see this, let us consider for a four fermion operator,

$$O^{\pm}_{\Gamma\Gamma'} = \frac{1}{2}\left(\left(\overline{\psi}_1\Gamma\psi_2\right)\left(\overline{\psi}_3\Gamma'\psi_4\right) \pm \left(\overline{\psi}_1\Gamma\psi_4\right)\left(\overline{\psi}_3\Gamma'\psi_2\right)\right), \tag{2.51}$$

and its chirality. It is convenient to take the interpolate operators Γ and Γ' as

$$\begin{aligned}(\Gamma,\Gamma') \in \{&VV+AA, VV-AA, SS+PP, SS-PP, TT\\ &VA+AV, VA-AV, SP+PS, SP-PS, T\tilde{T}\}\end{aligned} \tag{2.52}$$

When we consider the discrete chiral transformation as

$$\chi_{24} = \begin{cases} \psi_2 \to i\gamma_5\psi_2, & \overline{\psi}_2 \to i\overline{\psi}_2\gamma_5, \\ \psi_4 \to i\gamma_5\psi_4, & \overline{\psi}_4 \to i\overline{\psi}_4\gamma_5, \end{cases} \tag{2.53}$$

and

$$\chi_{12} = \begin{cases} \psi_1 \to i\gamma_5\psi_1, & \overline{\psi}_1 \to i\overline{\psi}_1\gamma_5, \\ \psi_1 \to i\gamma_5\psi_2, & \overline{\psi}_2 \to i\overline{\psi}_2\gamma_5. \end{cases} \tag{2.54}$$

Under these transformations, the each four fermion operators are transformed as

$$O^{\pm}_{VV+AA} \xrightarrow{\chi_{24}} -O^{\pm}_{VV+AA} \quad , \quad O^{\pm}_{VV+AA} \xrightarrow{\chi_{12}} +O^{\pm}_{VV+AA}, \tag{2.55}$$

$$O^{\pm}_{VV-AA} \xrightarrow{\chi_{24}} +O^{\pm}_{VV-AA} \quad , \quad O^{\pm}_{VV-AA} \xrightarrow{\chi_{12}} +O^{\mp}_{VV-AA}, \tag{2.56}$$

$$O^{\pm}_{SS-PP} \xrightarrow{\chi_{24}} +O^{\pm}_{SS-PP} \quad , \quad O^{\pm}_{SS-PP} \xrightarrow{\chi_{12}} -O^{\mp}_{SS-PP}, \tag{2.57}$$

$$O^{\pm}_{SS+PP} \xrightarrow{\chi_{24}} -O^{\pm}_{SS+PP} \quad , \quad O^{\pm}_{SS+PP} \xrightarrow{\chi_{12}} -O^{\pm}_{SS+PP}, \tag{2.58}$$

$$O^{\pm}_{TT} \xrightarrow{\chi_{24}} -O^{\pm}_{\tilde{T}\tilde{T}} \quad , \quad O^{\pm}_{TT} \xrightarrow{\chi_{12}} -O^{\pm}_{\tilde{T}\tilde{T}}, \tag{2.59}$$

$$O^{\pm}_{VA+AV} \xrightarrow{\chi_{24}} -O^{\pm}_{VA+AV} \quad , \quad O^{\pm}_{VA+AV} \xrightarrow{\chi_{12}} +O^{\pm}_{VA+AV}, \tag{2.60}$$

$$O^{\pm}_{VA-AV} \xrightarrow{\chi_{24}} +O^{\pm}_{VA-AV} \quad , \quad O^{\pm}_{VA-AV} \xrightarrow{\chi_{12}} +O^{\mp}_{VA-AV}, \tag{2.61}$$

$$O^{\pm}_{SP-PS} \xrightarrow{\chi_{24}} +O^{\pm}_{SP-PS} \quad , \quad O^{\pm}_{SP-PS} \xrightarrow{\chi_{12}} -O^{\mp}_{SP-PS}, \tag{2.62}$$

$$O^{\pm}_{SP+PS} \xrightarrow{\chi_{24}} -O^{\pm}_{SP+PS} \quad , \quad O^{\pm}_{SP+PS} \xrightarrow{\chi_{12}} -O^{\pm}_{SP+PS}, \tag{2.63}$$

$$O^{\pm}_{T\tilde{T}} \xrightarrow{\chi_{24}} -O^{\pm}_{T\tilde{T}} \quad , \quad O^{\pm}_{T\tilde{T}} \xrightarrow{\chi_{12}} -O^{\pm}_{T\tilde{T}}. \tag{2.64}$$

Therefore, the bag parameter which has the chirality $VV + AA$ does not mix with the other operator in the massless limit. However, the chiral symmetry breaking contributes to the renormalization factor as

$$O^{\text{ren.}}_{VV+AA} = \sum_i Z_{VV+AA,i} O^0_i, \tag{2.65}$$

where subscript i runs in $\{VV + AA, VV - AA, SS + PP, SS - PP, TT\}$ and $Z_{VV+AA,i}$ means the mixing coefficients for the bare operator O^0_i with $VV + AA$.

For the domain wall fermions, it is suggested that the mixing coefficients with the wrong chirality $Z_{VV+AA,i}$, $i \neq VV + AA$ are $O\left((am)^2\right)$ [93][94], in which the Rome-Southampton method [92] works well to calculate the bag parameter.

2.2.5 Previous works

The kaon bag parameter has been calculated with the domain wall fermions, the improved staggered fermion and the twisted mass Wilson fermion[5]. There is no mixing of operators for the domain wall fermion, however, it is hard to increase the number of statistics. The staggered fermion also suffers from the chiral symmetry breaking.

For the Wilson fermion, there are two approaches to the kaon bag parameter. The first method uses the chiral Ward-Takahashi identity to determine the mixing coefficients [89] and the second method uses the twisted mass approach [99][100]. The first one tends to struggle with the unwanted operators as in Figure 2 and 3. ETMC collaboration has used the twisted mass approach for $n_f = 2 + 1 + 1$ flavor QCD [102] and succeeded to calculate the kaon bag parameter with high precision.

[5]One can find the recent progress of the bag parameter in the figures of [95] or [102] for examples.

Figure 4 shows their results.

In this thesis, we propose to use the gradient flow method to the kaon bag parameter. Since the

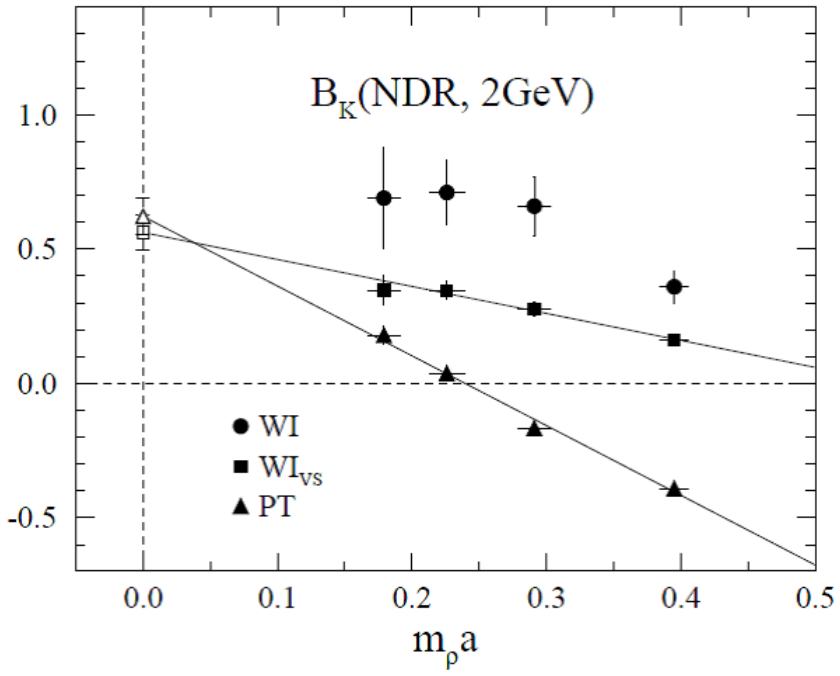

Figure 2: The bag parameter calculated in [89].

unwanted mixing is originally lattice artifacts, it will be vanished by applying the gradient flow in prospect. To support our claim, we will see the details of the gradient flow in the next chapter.

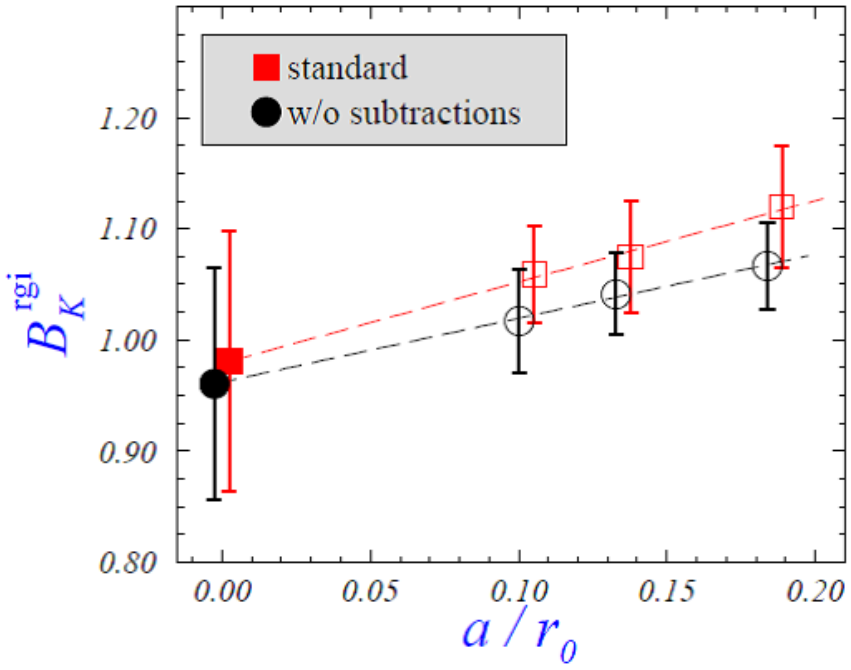

Figure 3: The bag parameter calculated in [91].

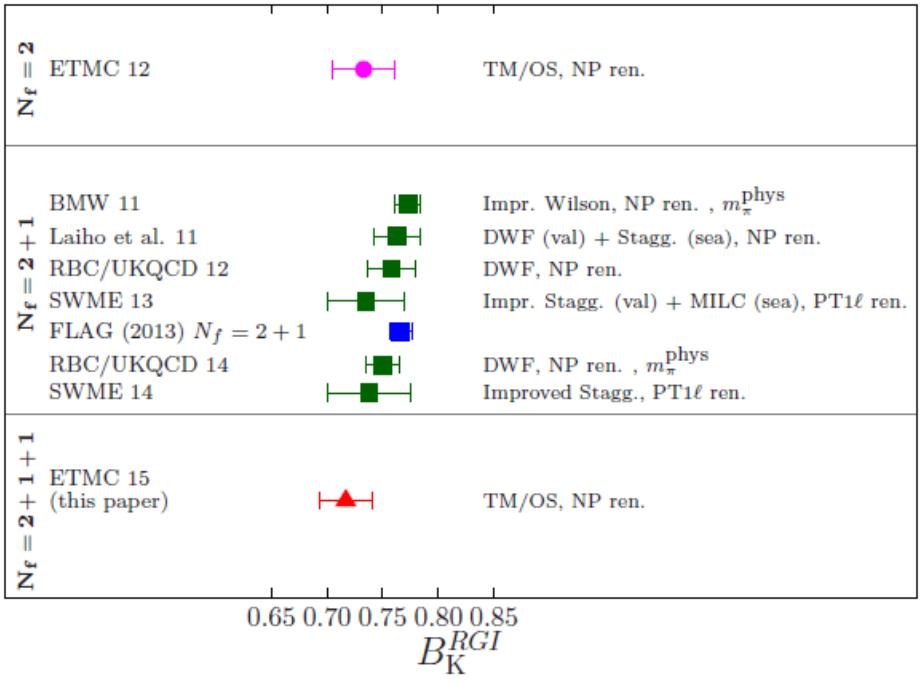

Figure 4: The bag parameter calculated in [102].

3 Gradient Flow

In recent years, the gradient flow method [33]-[38] provides many advantages to the Lattice QCD calculation. The concepts of the gradient flow have been expanded even for the quark fields, and use range was also expanded significantly, definition of the energy momentum tensor, setting a scale to the lattice, computation of the chiral susceptibility, studying the topological susceptibility, and so on[39]-[57]. Especially for the computation of the topological susceptibility [49] provides a new perspective for calculations with the Wilson fermion. Since the Wilson type fermion explicitly breaks the chiral symmetry at the finite lattice spacing, it is hard to define the topological susceptibility in naive ways. However, they successfully used the property that the gradient flow can present a correct renormalization for operators even it is related to the chiral symmetry. They suggested two definitions for the topological susceptibility which coincide throughout the chiral Ward-Takahashi identity, and their numerical results had a very good agreement. Therefore, the gradient flow makes the great assistance of the renormalization even for the Wilson fermion.

In this chapter, we firstly introduce the gradient flow and see the matching factor of forming bilinear operators as simple examples. When we use the gradient flow method is there is need to transfer an expectation value to the $\overline{\text{MS}}$ scheme. According to the renormalization group argument, perturbative calculations are justified, however, the gradient flow increases the number of Feynman diagrams and makes the calculation difficult. Since such calculations are generally tough, we will put the first half of this chapter into it.

In the later part of the chapter, we will see numerical examples of the gradient flow. As the concrete examples of lattice QCD, we will treat the meson mass and the decay constant in the section 3.3. They do not relate to the chiral symmetry, however, we make sure that the gradient flow correctly renormalize the hadronic observables. In the section 3.4 and 3.5, we finally proceed to calculations of the quantity which is related to some symmetry. We will see the numerical study of the energy momentum tensor, the topological charge, the chiral condensate and the PCAC mass. The energy momentum tensor is the Noether current of the translational symmetry and it is hard to calculate on the lattice. Because the topological susceptibility and the PCAC mass can be defined via the chiral Ward-Takahashi identity, it is also hard to calculate with the Wilson fermion. The chiral condensate needs a nontrivial additive renormalization for the Wilson fermion. We will see that the gradient flow solves such the problems. Finally, note that the results in the section 3.4 are short review and in the section 3.5 are our original results.

3.1 Definition and Techniques

In the gradient flow method, we consider a time evolution to the fictitious time direction. If the original theory is defined on the 4 dimensional space time we add one dimension and consider a 4 + 1 dimensional "flowed" theory. The time evolution equations are originally defined via the variation of the action,

$$\partial_t \phi(t,x) = -\frac{\delta S[\phi]}{\delta \phi(t,x)}. \tag{3.1}$$

This method was a great success in Yang-Mills theory [35] and the other theories. For examples, super Yang-Mills theory [60][61] and $O(N)$ non-linear sigma model [62]. In these theories, it is known that the right hand side of (3.1) takes a form like a thermal diffusion equation. The idea was also incorporated into QCD and the flow equation for the quark fields were also written down [36].

At the same time, computational techniques were developed, the small flow time expansion method and the background field method. The small flow time expansion provides us a way to transfer the gradient flow scheme to the other renormalization scheme and the background field theory makes perturbative calculations slightly easy. In this section, we will review and introduce them in a practical way.

3.1.1 Flow equations

The gradient flow for the $SU(N)$ gauge group is called as the Wilson flow [35], and is defined via a flow equation,

$$\begin{aligned}
\partial_t B_\mu(t,x) &= D_\nu G_{\nu\mu}(t,x), \quad B_\mu(t=0,x) = A_\mu(x), && (3.2)\\
G_{\mu\nu}(t,x) &= \partial_\mu B_\nu(t,x) - \partial_\nu B_\mu(t,x) + [B_\mu(t,x), B_\nu(t,x)], && (3.3)\\
D_\mu &= \partial_\mu + [B_\mu(t,x), \cdot]. && (3.4)
\end{aligned}$$

We denote the fundamental gauge field as $A_\mu(x)$ and its flowed field as $B_\mu(t,x)$. The right hand side of the flow equation (3.2) is nothing but the gradient of the Yang-Mills action,

$$\begin{aligned}
S_{YM} &= -\frac{1}{2g_0^2}\int \mathrm{d}^D x \ \mathrm{tr}[F_{\mu\nu}(x)F_{\mu\nu}(x)], && (3.5)\\
F_{\mu\nu}(x) &= \partial_\mu A_\nu(x) - \partial_\nu A_\mu(x) + [A_\mu(x), A_\nu(x)]. && (3.6)
\end{aligned}$$

Note that the symbol t means the flow time and x means four dimensional coordinates[6]. Let us consider the gauge transformation of the flow equation. If the gauge transformation does not depend on the flow time,

$$B_\mu(t,x) \to V(x)\left(B_\mu(t,x) + \partial_\mu\right) V^{-1}(x), \tag{3.7}$$

[6]We distinguish the coordinate time from the flow time and write it as x_0.

the flow equation obviously covariant. To consider the flow time dependent gauge transformation, it is convenient that we regard the original flow equation (3.2) as a special case of the generalized flow equation,

$$\partial_t B_\mu(t,x) = D_\nu G_{\nu\mu}(t,x) + \alpha_0 D_\mu \partial_\nu B_\nu(t,x). \tag{3.8}$$

If we choose the gauge parameter α_0 as 0, the flow equation (3.8) returns to the original one (3.2). We can show that (3.8) is also covariant for the flow time dependent gauge transformation,

$$B_\mu(t,x) \to V(t,x)\left(B_\mu(t,x) + \partial_\mu\right) V^{-1}(t,x), \tag{3.9}$$

where the transfer matrix $V(t,x)$ satisfies

$$\partial_t V(t,x) = -\alpha_0 \partial_\nu B_\nu(t,x) V(t,x) \ , \quad V(t=0,x) = \mathbb{1}. \tag{3.10}$$

In particular, (3.9) can be changed to an infinitesimal gauge transformation

$$B_\mu(t,x) \to B_\mu(t,x) + D_\mu \omega(t,x), \tag{3.11}$$

where the transfer matrix $\omega(t,x)$ satisfies

$$\partial_t \omega(t,x) = \alpha_0 D_\nu \partial_\nu \omega(t,x) - \delta\alpha_0 \partial_\nu B_\nu(t,x) \ , \quad \omega(t=0,x) = 0. \tag{3.12}$$

This infinitesimal gauge transformation changes the gauge parameter α_0 to $\alpha_0 + \delta\alpha_0$.

The flow equation (3.8) can be separated to a linear part and a nonlinear part as

$$\partial_t B_\mu(t,x) = \partial^2 B_\mu(t,x) + (\alpha_0 - 1)\partial_\mu \partial_\nu B_\nu(t,x) + R_\mu(t,x), \tag{3.13}$$

where R_μ means the nonlinear part,

$$\begin{aligned} R_\mu(t,x) &= 2[B_\nu(t,x), \partial_\nu B_\mu(t,x)] - [B_\nu(t,x), \partial_\mu B_\nu(t,x)] \\ &\quad + (\alpha_0 - 1)[B_\mu(t,x), \partial_\nu B_\nu(t,x)] + [B_\nu(t,x), [B_\nu(t,x), B_\mu(t,x)]] \end{aligned} \tag{3.14}$$

To construct the formal solution, we define the heat kernel

$$K_t(x)_{\mu\nu} = \int_p \frac{1}{p^2} \left\{ \left(\delta_{\mu\nu} p^2 - p_\mu p_\nu\right) e^{-tp^2} + p_\mu p_\nu e^{-\alpha_0 t p^2} \right\} e^{ipx}. \tag{3.15}$$

If we choose the gauge parameter α_0 to 1, the heat kernel reduces to a Gaussian damping factor

$$K_t(x)_{\mu\nu}|_{\alpha_0=1} = \int_p \delta_{\mu\nu} e^{-tp^2} e^{ipx} = \delta_{\mu\nu} \frac{e^{-x^2/4t}}{(4\pi t)^{D/2}}. \tag{3.16}$$

According to the general solution of differential equations, the solution of (3.8) is constructed by the solution for linear part,

$$B_\mu(t,x)^{\text{linear}} = \int \mathrm{d}^D y \, K_t(x-y)_{\mu\nu} A_\nu(y), \tag{3.17}$$

and the particular solution for the nonlinear part,

$$B_\mu(t,x)^{\text{non-linear}} = \int \mathrm{d}^D y \int_0^t \mathrm{d}s\, K_{t-s}(x-y)_{\mu\nu} R_\nu(s,y), \tag{3.18}$$

$$B_\mu(t,x) = B_\mu(t,x)^{\text{linear}} + B_\mu(t,x)^{\text{non-linear}}. \tag{3.19}$$

The gradient flow can be expanded for the quark field[36]. The gradient flow is originally defined via the variation of the action, however, we give the flow equation in the form of a thermal diffusion equation,

$$\partial_t \chi(t,x) = D^2 \chi(t,x) - \alpha_0 \partial_\nu B_\nu(t,x)\chi(t,x), \tag{3.20}$$

$$\partial_t \overline{\chi}(t,x) = \overline{\chi}(t,x)\overleftarrow{D^2} + \alpha_0 \overline{\chi}(t,x)\partial_\nu B_\nu(t,x), \tag{3.21}$$

and the initial condition

$$\chi(t=0,x) = \psi(x)\ , \quad \overline{\chi}(t=0,x) = \overline{\psi}(x). \tag{3.22}$$

The covariant derivative is act for the quark field as

$$D_\mu = \partial_\mu + B_\mu(t,x). \tag{3.23}$$

We can also discuss about the flow time dependent infinitesimal gauge transformation

$$\chi(t,x) \to (1 + i\omega(t,x))\, \chi(t,x), \tag{3.24}$$

$$\overline{\chi}(t,x) \to \overline{\chi}(t,x)(1 - i\omega(t,x)). \tag{3.25}$$

If the gauge transfer matrix $\omega(t,x)$ satisfies (3.12) the flow equations for the quark field are also covariant.

To construct the formal solution of the flow equation (3.20), we separate it as

$$\partial_t \chi(t,x) = \partial^2 \chi(t,x) + \Delta' \chi(t,x), \tag{3.26}$$

$$\Delta' = (1-\alpha_0)\partial_\nu B_\nu(t,x) + 2B_\nu(t,x)\partial_\nu + B_\nu(t,x)B_\nu(t,x). \tag{3.27}$$

At this time, we define the heat kernel as

$$K_t(x) = \int_p e^{-tp^2} e^{ipx} = \frac{e^{-x^2/4t}}{(4\pi t)^{D/2}}. \tag{3.28}$$

and obtain the formal solution,

$$\chi(t,x) = \int \mathrm{d}^D y \left\{ K_t(x-y)\psi(y) + \int_0^t \mathrm{d}s\, K_{t-s}(x-y)\Delta' \chi(s,y) \right\}. \tag{3.29}$$

We can also construct the formal solution for the flow equation with respect to the anti-quark field (3.21) as

$$\overline{\chi}(t,x) = \int \mathrm{d}^D y \left\{ \overline{\psi}(y) K_t(x-y) + \int_0^t \mathrm{d}s\, \overline{\chi}(s,y) \overleftarrow{\Delta'} K_{t-s}(x-y) \right\}, \tag{3.30}$$

$$\overleftarrow{\Delta'} = -(1-\alpha_0)\partial_\nu B_\nu(t,x) - 2\overleftarrow{\partial}_\nu B_\nu(t,x) + B_\nu(t,x) B_\nu(t,x). \tag{3.31}$$

In the next section, we will adopt a perturbative calculation of the gradient flow. Since the formal solutions (3.19), (3.29) and (3.30) take the simplest form we will set the gauge parameter to 1, $\alpha_0 = 1$ for the perturbation. By contrast, we will set the gauge parameter to 0, $\alpha_0 = 0$ for numerical calculation exclusively. Numerical study of the gradient flow is discussed in the section 3.3.1.

3.1.2 Renormalization and gradient flow

The gradient flow has the property that the gradient flow makes an expectation value of a composite operator become free from the ultra violet divergence. The general proof is subject to [37][59] and we see the flowed energy,

$$E(t) = \frac{1}{4} \int \mathrm{d}^D x \left\langle G^a_{\mu\nu}(t,x) G^a_{\mu\nu}(t,x) \right\rangle, \tag{3.32}$$

as an example. We use the dimensional regularization scheme, $D = 4 - 2\epsilon$, and consider one loop perturbation theory. As we mentioned, the gauge parameter is set to 1 for simplicity. Therefore, the flowed gauge field is given as

$$B_\mu(t,x) = \int \mathrm{d}^D y \left\{ K_t(x-y) A_\mu(y) + \int_0^t \mathrm{d}s\, K_{t-s}(x-y) R_\mu(s,y) \right\}, \tag{3.33}$$

$$R_\mu(t,x) = 2[B_\nu(t,x), \partial_\nu B_\mu(t,x)](t,x)] - [B_\nu(t,x), \partial_\mu B_\nu + [B_\nu(t,x), [B_\nu(t,x), B_\mu(t,x)]], \tag{3.34}$$

with the heat kernel

$$K_t(x) = \int_p e^{-tp^2} e^{ipx}. \tag{3.35}$$

Note that the formal solution above is a recursive representation and we can separate the flowed gauge field as

$$B_\mu(t,x) = \sum_{k=1,2,3,\cdots} B_{\mu,k}(t,x), \tag{3.36}$$

$$B_{\mu,1}(t,x) = \int \mathrm{d}^D y\, K_t(x-y) A_\mu(y), \tag{3.37}$$

$$B_{\mu,2}(t,x) = \int \mathrm{d}^D y \int_0^t \mathrm{d}s\, K_{t-s}(x-y) \left(2[B_{\nu,1}(s,y), \partial_\nu B_{\mu,1}(s,y)] - [B_{\nu,1}(s,y), \partial_\mu B_{\nu,1}(s,y)]\right), \tag{3.38}$$

$$\begin{aligned} B_{\mu,3}(t,x) = \int \mathrm{d}^D y \int_0^t \mathrm{d}s\, K_{t-s}(x-y) \Big(&2[B_{\nu,2}(s,y), \partial_\nu B_{\mu,1}(s,y)] - [B_{\nu,2}(s,y), \partial_\mu B_{\nu,1}(s,y)] \\ &+2[B_{\nu,1}(s,y), \partial_\nu B_{\mu,2}(s,y)] - [B_{\nu,1}(s,y), \partial_\mu B_{\nu,2}(s,y)] + [B_{\nu,1}(s,y), [B_{\nu,1}(s,y), B_{\mu,1}(s,y)]]\Big). \end{aligned} \tag{3.39}$$

The higher order terms of the flowed gauge field, $B_{\mu,k>3}$, are $O(g_0^6)$ and we omit them. The each

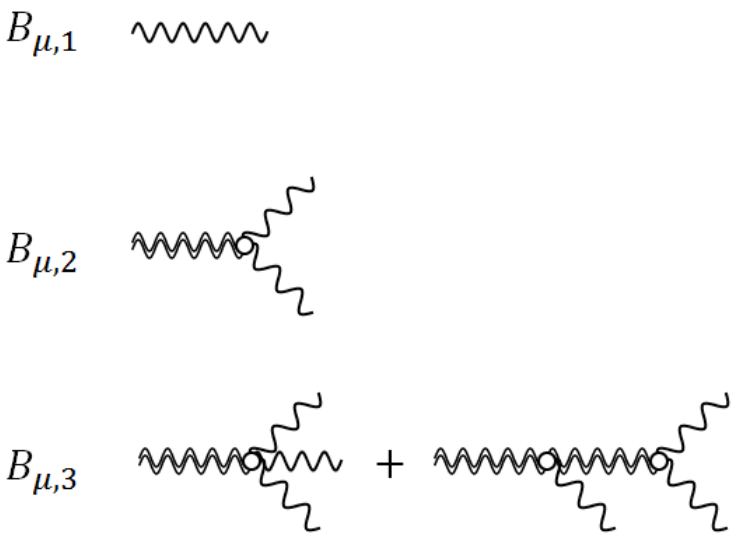

Figure 5: Diagrammatic representation of the flowed gauge field.

term (3.37)-(3.39) are also diagrammatically represented as in the Figure 5. The heat kernel is pictured as a double wavy line. By using these picture, we can also describe the flowed energy, $E = \left\langle G_{\mu\nu} G_{\mu\nu} \right\rangle / 4$, diagrammatically as shown in the Figure 6, where the black spots mean the usual QCD vertices.

One can calculate the flowed energy as

$$E(t) = \frac{(N^2-1)(D-1)}{2(8\pi t)^{D/2}} g_0^2 \left[1 + \frac{(8t)^\epsilon}{(4\pi)^2} g_0^2 \left\{ \left(\frac{11}{3} N - \frac{2}{3} N_f \right) \frac{1}{\epsilon} + (\text{finite}) \right\} + O(g_0^4) \right]. \tag{3.40}$$

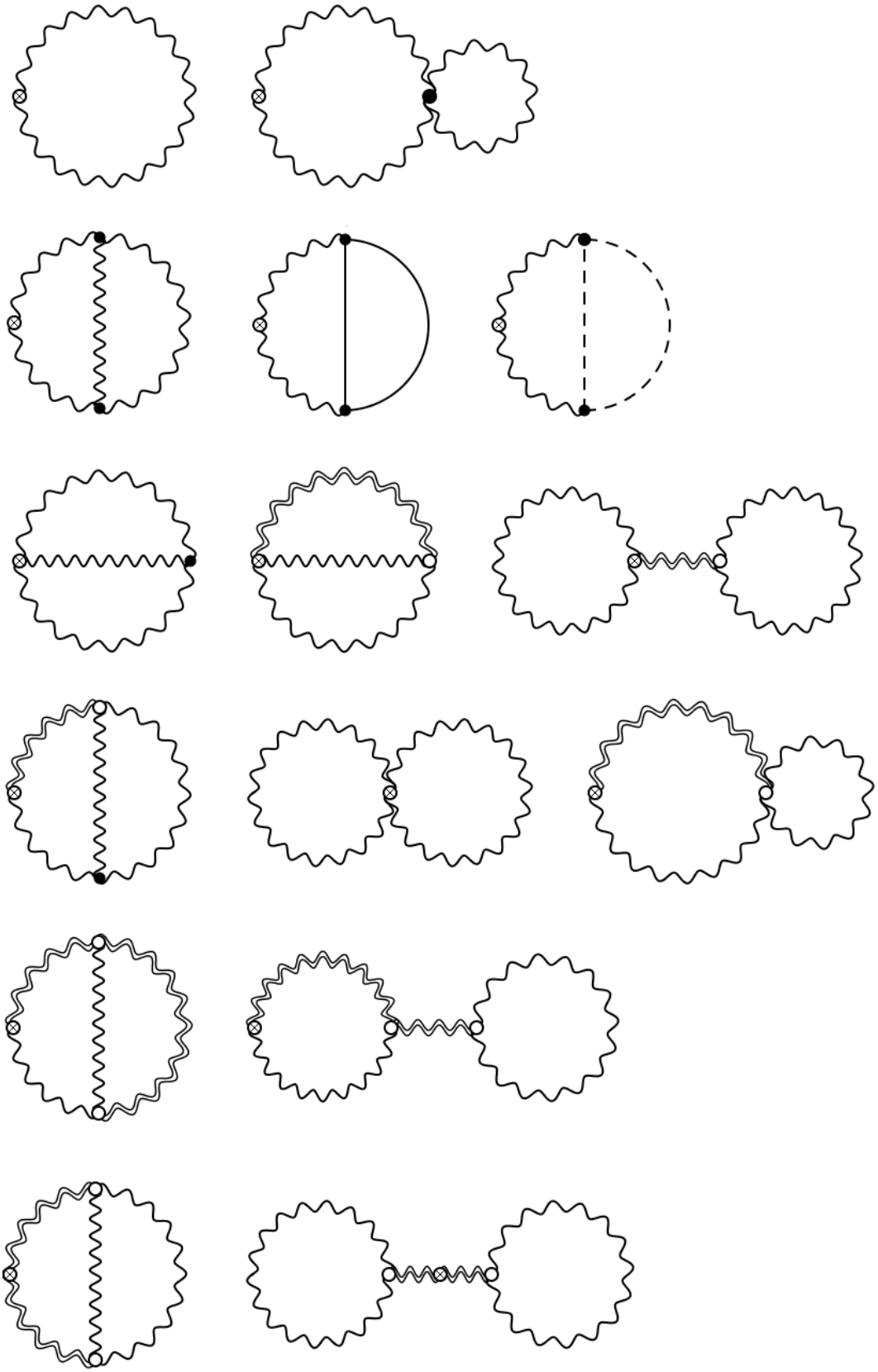

Figure 6: One loop diagrams for the energy $E = \left\langle G_{\mu\nu} G_{\mu\nu} \right\rangle / 4$.

The ultraviolet divergence can be absorbed into the gauge coupling,

$$g_0^2 = g^2\mu^{2\epsilon}\left(4\pi e^{-\gamma}\right)^{-\epsilon}\left\{1 - \frac{1}{(4\pi)^2}g^2\left(\frac{11}{3}N - \frac{2}{3}N_f\right)\frac{1}{\epsilon} + O(g^4)\right\}. \tag{3.41}$$

This cancellation is not a coincidence but a general property. Lüscher and Weisz [37] provided a general proof for the renormalizability of the gradient flow. In this thesis, we admit the renormalizability of the gradient flow and proceed to concrete calculation methods.

Note that when we include the flowed quark fields χ and $\overline{\chi}$ we must impose the field strength renormalization in addition to the gauge coupling and the quark mass. In [123], it is suggested that a useful choice of the field strength renormalization is given by

$$\mathring{\chi}(t,x) = \sqrt{\varphi(t)}\chi(t,x), \tag{3.42}$$

$$\mathring{\overline{\chi}}(t,x) = \sqrt{\varphi(t)}\overline{\chi}(t,x), \tag{3.43}$$

where $\mathring{\chi}$ and $\mathring{\overline{\chi}}$ are renormalized quark field and the coefficient φ is defined by

$$\varphi(t) = \frac{-6}{(4\pi)^2 t^2\left\langle\overline{\chi}(t,x)\gamma_\mu\overleftrightarrow{D}_\mu\chi(t,x)\right\rangle}, \quad \overleftrightarrow{D}_\mu = D_\mu - \overleftarrow{D}_\mu. \tag{3.44}$$

We will discuss the perturbative evaluation of the renormalization factor (3.44) in the section 3.2.1.

3.1.3 Small flow time expansion

The small flow time expansion method provides us a way to "match" an expectation value calculated in the gradient flow scheme to the other renormalization scheme. Since the general choice is the $\overline{\text{MS}}$ scheme we particularly consider the matching factor for the $\overline{\text{MS}}$ scheme later. The first step of the small flow time expansion is calculating the relation between the bare operator and the flowed operator. When we consider the $t \to 0$ limit, because of the symmetry, we can demand the relation as

$$O(\chi,\overline{\chi},B) \sim c(t)O(\psi,\overline{\psi},A)\ , \quad (\text{for } t \to 0), \tag{3.45}$$

where $O(\psi,\overline{\psi},A)$ means the bare operator and $O(\chi,\overline{\chi},B)$ means its flowed operator[7]. The coefficient $c(t)$ connects the bare operator and the flowed operator. To obtain the coefficient $c(t)$, let us

[7] As an example, if we choose the bare operator as the scalar density,

$$O(\psi,\overline{\psi},A) = \overline{\psi}T^a\psi,$$

its flowed operator is given by

$$O(\chi,\overline{\chi},B) = \overline{\chi}T^a\chi.$$

consider the one particle irreducible vertex correction of the difference $O(\chi,\overline{\chi},B) - O(\psi,\overline{\psi},A)$. In generally, it would be proportional to the vertex function Γ[8]

$$\left\langle O(\chi,\overline{\chi},B) - O(\psi,\overline{\psi},A)\right\rangle_{\rm 1PI} = I_{\rm GF}(t)\Gamma, \tag{3.46}$$

where we denote the proportional constant as $I_{\rm GF}(t)$. The left hand side will be

$$\begin{aligned}\left\langle O(\chi,\overline{\chi},B) - O(\psi,\overline{\psi},A)\right\rangle_{\rm 1PI} &= (c(t)-1)\left\langle O(\psi,\overline{\psi},A)\right\rangle_{\rm 1PI} \\ &= (c(t)-1)Z_O\Gamma \sim (c(t)-1)\Gamma \end{aligned}\tag{3.47}$$

In the second line, we considered one loop perturbation theory and used the fact that $c(t)-1$ is $O(g^2)$, because the tree level contributions of the flowed operator and the bare operator are same,

$$\langle O(\chi,\overline{\chi},B)\rangle_{\rm 1PI}|_{\rm tree} = \Gamma\ , \quad (\text{for } t\to 0), \tag{3.48}$$

$$\left\langle O(\psi,\overline{\psi},A)\right\rangle_{\rm 1PI}|_{\rm tree} = \Gamma. \tag{3.49}$$

Comparing them and the right hand side of the (3.45), we obtain the representation of the small flow time expansion as

$$O(\chi,\overline{\chi},B) \sim (1 + I_{\rm GF}(t))O(\psi,\overline{\psi},A) + O(t)\ , \quad (\text{for } t\to 0). \tag{3.50}$$

We will see concrete examples of the coefficient $I_{\rm GF}(t)$ in the section 3.2.

As we mentioned, we must renormalize the quark field by the useful choice,

$$\mathring{\chi}(t,x) = \sqrt{\varphi(t)}\chi(t,x), \tag{3.51}$$

$$\mathring{\overline{\chi}}(t,x) = \sqrt{\varphi(t)}\overline{\chi}(t,x), \tag{3.52}$$

$$\varphi(t) = \frac{-6}{(4\pi)^2 t^2\left\langle \overline{\chi}_f(t,x)\gamma_\mu \overleftrightarrow{D}_\mu \chi(t,x)\right\rangle}. \tag{3.53}$$

Therefore, the flowed operator must be written as $O(\mathring{\chi},\mathring{\overline{\chi}},B)$[9]. If the operator O includes a quark field $O(\mathring{\chi},\mathring{\overline{\chi}},B)$ and $O(\chi,\overline{\chi},B)$ are related to

$$O(\mathring{\chi},\mathring{\overline{\chi}},B) = \varphi^{n/2}(t)O(\chi,\overline{\chi},B). \tag{3.54}$$

[8]For the scalar density,

$$\Gamma = T^a.$$

[9]For the scalar density,

$$O(\mathring{\chi},\mathring{\overline{\chi}},B) = \mathring{\overline{\chi}}T^a\mathring{\chi}.$$

Finally, we have

$$O(\mathring{\chi},\mathring{\overline{\chi}},B) = \varphi^{n/2}(t)(1+I_{\rm GF}(t))O(\psi,\overline{\psi},A), \tag{3.55}$$

for the small flow time. Renormalizing the bare operator as

$$O(\psi,\overline{\psi},A) = \frac{1}{Z_O^{\overline{\rm MS}}\left(Z_\psi^{\overline{\rm MS}}\right)^{n/2}} O^{\overline{\rm MS}}(\psi_{\overline{\rm MS}},\overline{\psi}_{\overline{\rm MS}},A), \tag{3.56}$$

we obtain the matching factor,

$$Z^{{\rm GF}\to\overline{\rm MS}}(t) = \frac{Z_O^{\overline{\rm MS}}}{1+I_{\rm GF}(t)}\left(\frac{Z_\psi^{\overline{\rm MS}}}{\varphi(t)}\right)^{n/2}. \tag{3.57}$$

By using this matching factor, we can define the $\overline{\rm MS}$ operator via the gradient flow as

$$Z^{{\rm GF}\to\overline{\rm MS}}(t)O(\mathring{\chi},\mathring{\overline{\chi}},B). \tag{3.58}$$

The point for calculation of the matching factor (3.57) is $I_{\rm GF}(t)$, in other words, the one particle irreducible vertex correction of the difference $O(\chi,\overline{\chi},B) - O(\psi,\overline{\psi},A)$. However, there are many diagrams specific to the gradient flow. We can reduce some diagrams by using the background field method. We will discuss it in the next section.

3.1.4 Background field method

To calculate the matching factor (3.57), we must consider the one particle irreducible vertex correction. Since the formal solution of the gauge field and the quark fields are recursive representation the number of diagrams increases. Moreover, it is also difficult to evaluate the integration in general. The background field method provides a way to reduce the number of diagrams to evaluate.

The background field method [63]-[67] is originally adopted for general field theory including QCD. It improves the perspective of the perturbative calculation by separating the fields to background fields and quantum fields. Especially for QCD, the gauge field A_μ and the quark field $\psi,\overline{\psi}$ are separated to

$$A_\mu(x) = \hat{A}_\mu(x) + a_\mu(x), \tag{3.59}$$

$$\psi(x) = \hat{\psi}(x) + p(x), \tag{3.60}$$

$$\overline{\psi}(x) = \hat{\overline{\psi}}(x) + \overline{p}(x). \tag{3.61}$$

We denote the background fields as $\hat{A}_\mu$, $\hat{\psi}$, $\hat{\overline{\psi}}$ and the quantum fields as a_μ, p, $\overline{p}$. In actual calculation, we can fix the background fields to some constant value and regard the quantum fields as the integration variables for the path integral.

Let us consider the flow time evolution of the each field[121]. From here on, we denote the flowed background fields as $\hat{B}_\mu$, $\hat{\chi}$, $\hat{\overline{\chi}}$ and the flowed quantum fields as b_μ, k, $\overline{k}$. Of course, the sum of the background and the quantum fields return to the original fields,

$$B_\mu(x) = \hat{B}_\mu(x) + b_\mu(x), \tag{3.62}$$
$$\chi(x) = \hat{\chi}(x) + k(x), \tag{3.63}$$
$$\overline{\chi}(x) = \hat{\overline{\chi}}(x) + \overline{k}(x). \tag{3.64}$$

We naturally assume that the background fields evolve along the form of original flow equation with $\alpha_0 = 0$,

$$\partial_t \hat{B}_\mu(t,x) = \hat{D}_\nu \hat{G}_{\nu\mu}(t,x) \ , \quad \hat{B}_\mu(t=0,x) = \hat{A}_\mu(x), \tag{3.65}$$
$$\partial_t \hat{\chi}(t,x) = \hat{D}^2 \hat{\chi}(t,x) \ , \quad \hat{\chi}(t=0,x) = \hat{\psi}(x), \tag{3.66}$$
$$\partial_t \hat{\overline{\chi}}(t,x) = \hat{\overline{\chi}}(t,x)\overleftarrow{\hat{D}}^2 \ , \quad \hat{\overline{\chi}}(t=0,x) = \hat{\overline{\psi}}(x), \tag{3.67}$$

where we defined that the field strength of the background field

$$\hat{G}_{\mu\nu}(t,x) = \partial_t \hat{B}_\nu(t,x) - \partial_t \hat{B}_\mu(t,x) + [\hat{B}_\mu(t,x),\, \hat{B}_\nu(t,x)], \tag{3.68}$$

and the covariant derivative with the background field

$$\hat{D}_\mu = \partial_\mu + [\hat{B}_\mu(t,x), \cdot\,] \ , \text{(for gauge fields)}, \tag{3.69}$$
$$\hat{D}_\mu = \partial_\mu + \hat{B}_\mu(t,x) \quad , \text{(for quark fields)}. \tag{3.70}$$

Let us suppose that the background gauge field $\hat{A}_\mu(x)$ satisfies the equation of motion,

$$\hat{D}_\nu \hat{F}_{\nu\mu}(x) = 0. \tag{3.71}$$

In such situation, the background gauge field does not flow and we can write

$$\hat{B}_\mu(t,x) = \hat{A}_\mu(x). \tag{3.72}$$

The solutions for the background fermion flow also simplified as

$$\hat{\chi}(t,x) = e^{t\hat{D}^2}\hat{\psi}(x), \tag{3.73}$$
$$\hat{\overline{\chi}}(t,x) = \hat{\overline{\psi}}(x)e^{t\overleftarrow{\hat{D}}^2}. \tag{3.74}$$

The formal solutions for the background fields take greatly simple form, however, the quantum field part must take more complicated structure.

Because of the equations (3.62)-(3.64), the flow equations for the quantum fields must be remaining part of the original flow equation as

$$\begin{aligned}
\partial_t b_\mu(t,x) &= \{\delta_{\mu\nu}\hat{D}^2 + (\alpha_0 - 1)\hat{D}_\mu\hat{D}_\nu\} b_\nu(t,x) + 2[\hat{G}_{\mu\nu}(t,x),\, b_\nu(t,x)] + \hat{R}_\mu(t,x), && (3.75)\\
\partial_t k(t,x) &= \left\{D^2 - \alpha_0\hat{D}_\mu b_\mu(t,x)\right\} k(t,x) \\
&\quad + \left\{(1-\alpha_0)\hat{D}_\mu b_\mu(t,x) + 2b_\mu(t,x)\hat{D}_\mu + b^2(t,x)\right\}\hat{\chi}(t,x), && (3.76)\\
\partial_t \overline{k}(t,x) &= \overline{k}(t,x)\left\{\overleftarrow{D}^2 + \alpha_0\hat{D}_\mu b_\mu(t,x)\right\} \\
&\quad + \hat{\overline{\chi}}(t,x)\left\{-(1-\alpha_0)\hat{D}_\mu b_\mu(t,x) - 2\hat{\overleftarrow{D}}_\mu b_\mu(t,x) + b^2(t,x)\right\}, && (3.77)
\end{aligned}$$

with the initial conditions,

$$\begin{aligned}
b_\mu(t=0,x) &= a_\mu(x), && (3.78)\\
k(t=0,x) &= p(x), && (3.79)\\
\overline{k}(t=0,x) &= \overline{p}(x), && (3.80)
\end{aligned}$$

where we defined the higher order term as

$$\begin{aligned}
\hat{R}_\mu(t,x) &= +2[b_\nu(t,x),\, \hat{D}_\nu b_\mu(t,x)] - [b_\nu(t,x),\, \hat{D}_\mu b_\nu(t,x)] \\
&\quad + (\alpha_0 - 1)[b_\mu(t,x),\, \hat{D}_\nu b_\nu(t,x)] + \left[b_\nu(t,x),\, \left[b_\nu(t,x),\, b_\mu(t,x)\right]\right]. && (3.81)
\end{aligned}$$

Note that when we clearly indicate the color index the higher order term become

$$\begin{aligned}
\hat{R}^a_\mu(t,x) &= 2f^{abc}b^b_\nu(t,x)\hat{\mathcal{D}}^{cd}_\nu b^d_\mu(t,x) - f^{abc}b^b_\nu(t,x)\hat{\mathcal{D}}^{cd}_\mu b^d_\nu(t,x) \\
&\quad + f^{abc}f^{cde}b^b_\nu(t,x)b^d_\nu(t,x)b^e_\mu(t,x). && (3.82)
\end{aligned}$$

We can construct the formal solution for these flow equations with the same assumption (3.71) and the gauge fixing $\alpha_0 = 1$,

$$\begin{aligned}
b^a_\mu(t,x) &= \int \mathrm{d}^D y\, \left\{K^{ab}_t(x,y)_{\mu\nu}a^b_\nu(y) + \int_0^t \mathrm{d}s\, K^{ab}_{t-s}(x,y)_{\mu\nu}\hat{R}^b_\nu(s,y)\right\}, && (3.83)\\
k(t,x) &= e^{t\hat{D}^2}p(x) \\
&\quad + \int_0^t \mathrm{d}s\, e^{(t-s)\hat{D}^2}\left\{2b_\mu(s,x)\hat{D}_\mu + b^2(s,x)\right\}\left\{e^{s\hat{D}^2}\hat{\psi}(x) + k(s,x)\right\}, && (3.84)\\
\overline{k}(t,x) &= \overline{p}(x)e^{t\hat{\overleftarrow{D}}^2} \\
&\quad + \int_0^t \mathrm{d}s\, \left\{\hat{\overline{\psi}}(x)e^{s\hat{\overleftarrow{D}}^2} + \overline{k}(s,x)\right\}\left\{-2\hat{\overleftarrow{D}}_\mu b_\mu(s,x) + b^2(s,x)\right\}e^{(t-s)\hat{\overleftarrow{D}}^2}, && (3.85)
\end{aligned}$$

where we defined the heat kernel $K^{ab}_t(x,y)$ by

$$\begin{aligned}
K_t(x,y) &= e^{t\left\{\hat{\mathcal{D}}_x + 2\hat{\mathcal{F}}(x)\delta(x-y)\right\}}, && (3.86)\\
\hat{\mathcal{D}}^{ab}_\mu &= \delta^{ab}\partial_\mu + \hat{B}^c_\mu(t,x)f^{acb}, && (3.87)\\
\hat{\mathcal{F}}^{ab}_{\mu\nu}(x) &= \hat{F}^c_{\mu\nu}(x)f^{acb}. && (3.88)
\end{aligned}$$

In this section, we constructed the formal solutions for the background (3.72), (3.73), (3.74) and the quantum flow equations (3.83), (3.84), (3.85). The results above will be used for the calculations of bi-linear operators in the next section and the four fermion operators in the next chapter.

3.2 Example : Fermion Bi-linear Operator

In this section, we will see two examples of the matching factor of fermion bi-linear operators [120][123]. We deal with the axial vector current and the scalar density for the later convenience. We will view the PCAC relation via evaluating the axial vector current and the pseudo scalar density numerically in the section 3.5. At first, we evaluate the renormalization factor of the quark field (3.44) which is necessary for the renormalization. Although the calculation is complicated, it will be a good exercise for the gradient flow.

For the fermion bi-linear operators, the calculation itself has no difficulty, however, we must take care to the infrared divergence. We will see that the order of the integration is sensitive. We will discuss about them in the end of this section.

3.2.1 Quark field renormalization

As we mentioned, we must consider the renormalization of the field in the case of quarks. When we choose the prescription,

$$\mathring{\chi}(t,x) = \sqrt{\varphi(t)}\chi(t,x), \tag{3.89}$$

$$\mathring{\overline{\chi}}(t,x) = \sqrt{\varphi(t)}\overline{\chi}(t,x), \tag{3.90}$$

$$\varphi(t) = \frac{-6}{(4\pi)^2 t^2 \left\langle \overline{\chi}(t,x)\gamma_\mu \overleftrightarrow{D}_\mu \chi(t,x)\right\rangle}, \tag{3.91}$$

we must evaluate the expectation value,

$$\left\langle \overline{\chi}(t,x)\gamma_\mu \overleftrightarrow{D}_\mu \chi(t,x)\right\rangle. \tag{3.92}$$

We evaluate the expectation value (3.92) with one-loop perturbation. We set the gauge parameter $\alpha_0 = 1$ for simplicity. As we did in the section 3.1.2, the flowed quark field can be decomposed into

$$\chi(t,x) = \sum_{k=1,2,3,\cdots} \chi_k(t,x), \tag{3.93}$$

$$\chi_1(t,x) = \int \mathrm{d}^D y\, K_t(x-y)\psi(y), \tag{3.94}$$

$$\chi_2(t,x) = \int \mathrm{d}^D y \int_0^t \mathrm{d}s\, K_{t-s}(x-y) 2B_{\nu,1}(s,y)\partial_\nu \chi_1(s,y), \tag{3.95}$$

$$\chi_3(t,x) = \int \mathrm{d}^D y \int_0^t \mathrm{d}s\, K_{t-s}(x-y)\left(2B_{\nu,1}(s,y)\partial_\nu \chi_2(s,y) + B_{\nu,1}(s,y)B_{\nu,1}(s,y)\chi_1(s,y)\right), \tag{3.96}$$

where $B_{\mu,1}$ means the linear term of the flowed gauge field,

$$B_{\mu,1}(t,x) = \int \mathrm{d}^D y\, K_t(x-y)A_\mu(y), \tag{3.97}$$

and K_t means the heat kernel,

$$K_t(x) = \int_p e^{-tp^2} e^{ipx} = \frac{e^{-x^2/4t}}{(4\pi t)^{D/2}}. \tag{3.98}$$

The each term (3.94)-(3.96) can be diagrammatically represented as in the Figure 7. The heat

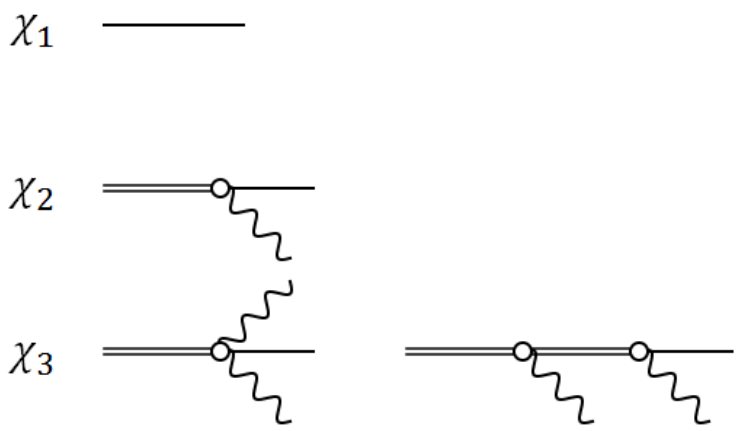

Figure 7: Diagrammatic representation of the flowed quark field.

kernel is pictured as a double line. By using these pictures, we can also describe the expectation value (3.92) as in the Figure 8. Since the propagator of the linear term of the flowed gauge fields can be calculated as

$$\left\langle B^a_{\mu,1}(t,x) B^b_{\nu,1}(s,y) \right\rangle = g_0^2 \frac{-e^{(t+s)\partial_x^2}}{\partial_x^2} \delta^{ab} \delta_{\mu\nu} \delta(x-y), \tag{3.99}$$

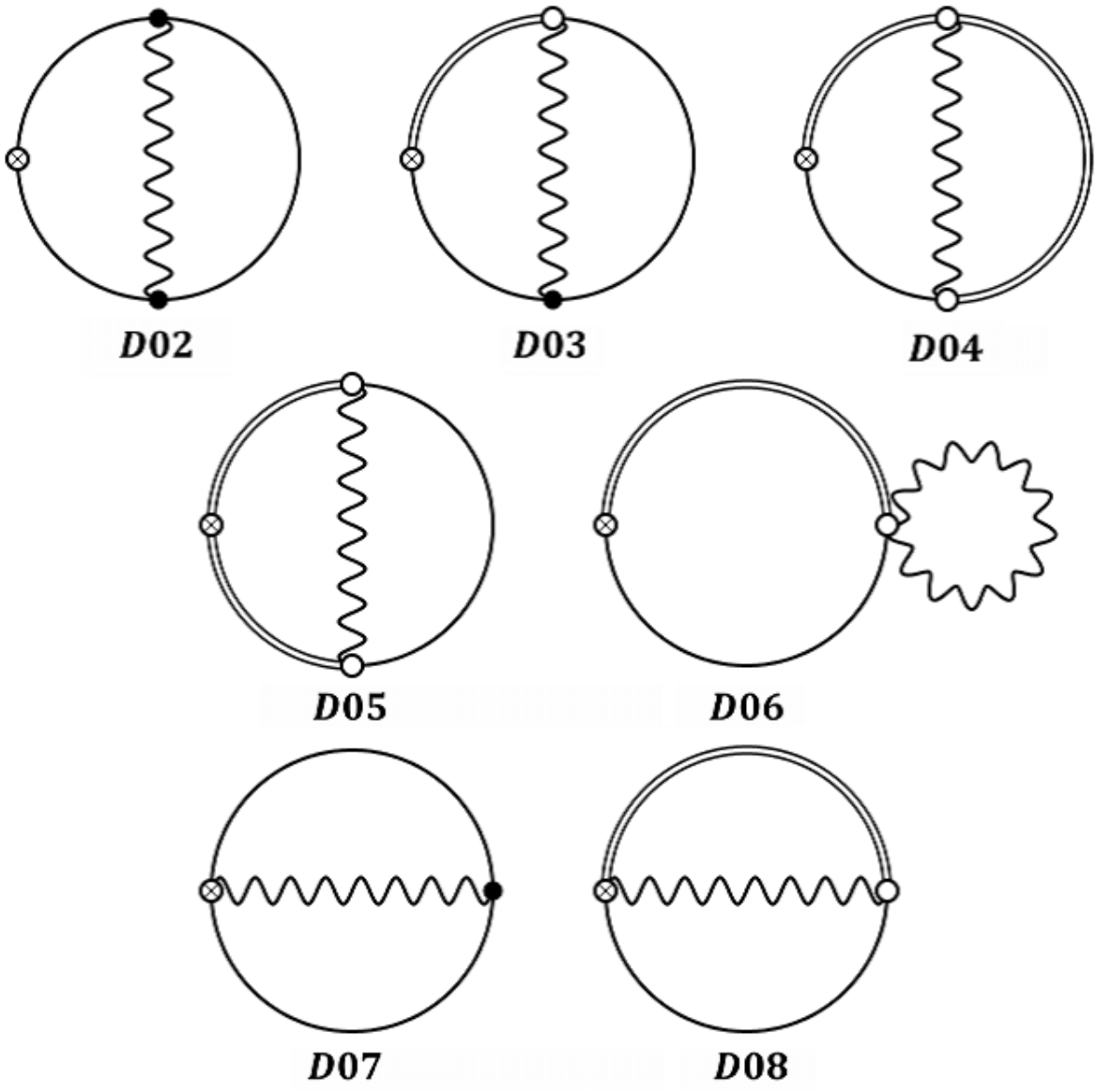

Figure 8: One loop diagrams for the quark renormalization factor.

the each diagram in the Figure 8 are denoted as

$$D02 \;:\; (-ip_\mu)e^{-2tp^2}S_{F\nu}(p)S_{F\rho}(p-l)S_{F\sigma}(p)G^{ab}_{\alpha\beta}(l)T^aT^b\mathrm{tr}\left[\gamma_\mu\gamma_\nu\gamma_\alpha\gamma_\rho\gamma_\beta\gamma_\sigma\right], \tag{3.100}$$

$$D03 \;:\; \int_0^t \mathrm{d}s(-ip_\mu)e^{-(t-s)p^2}e^{-s(p-l)^2}e^{-tp^2}S_{F\nu}(p)S_{F\sigma}(p-l) \tag{3.101}$$
$$\times(-2i(p-l)_\lambda)G^{ab}_{\rho\lambda}(s,0;l)T^aT^b\mathrm{tr}\left[\gamma_\mu\gamma_\nu\gamma_\rho\gamma_\sigma\right],$$

$$D04 \;:\; \int_0^t \mathrm{d}s\int_0^s \mathrm{d}u(-ip_\mu)S_{F\nu}(p)e^{-(t-s)p^2}e^{-(s-u)(p-l)^2}e^{-up^2}e^{-tp^2}$$
$$\times(-2i(p-l)_\rho)(-2ip_\lambda)G^{ab}_{\rho\lambda}(s,u;l)T^aT^b\mathrm{tr}\left[\gamma_\mu\gamma_\nu\right], \tag{3.102}$$

$$D05 \;:\; \int_0^t \mathrm{d}s\int_0^t \mathrm{d}u(-ip_\mu)S_{F\nu}(p-l)e^{-(t-s)p^2}e^{-(t-u)p^2}e^{-(s+u)(p-l)^2}$$
$$\times(-2i(p-l)_\rho)(2i(p-l)_\sigma)G^{ab}_{\rho\sigma}(s,u;l)T^aT^b\mathrm{tr}\left[\gamma_\mu\gamma_\nu\right], \tag{3.103}$$

$$D06 \;:\; \int_0^t \mathrm{d}s(-ip_\mu)S_{F\nu}(p)e^{-(t-s)p^2}e^{-sp^2}e^{-tp^2}G^{ab}_{\rho\rho}(s,s;l)T^aT^b\mathrm{tr}\left[\gamma_\mu\gamma_\nu\right], \tag{3.104}$$

$$D07 \;:\; e^{-tp^2}e^{-tl^2}e^{-t(p+l)^2}S_{F\rho}(p)S_{F\lambda}(p+l)G^{ab}_{\mu\nu}(t,0;l)T^aT^b\mathrm{tr}\left[\gamma_\mu\gamma_\rho\gamma_\nu\gamma_\lambda\right], \tag{3.105}$$

$$D08 \;:\; \int_0^t \mathrm{d}s\, e^{-(t-s)p^2}e^{-(t+s)(p+l)^2}(-2i(p-l)_\rho)S_{F\nu}(p+l)G^{ab}_{\mu\rho}(t,s;l)T^aT^b\mathrm{tr}\left[\gamma_\mu\gamma_\nu\right], \tag{3.106}$$

with the quark and gluon propagator,

$$S_{F\mu}(l) = -i\frac{l_\mu}{l^2}, \tag{3.107}$$

$$G^{ab}_{\mu\nu}(t,s;l) = g_0^2e^{-(t+s)l^2}\frac{1}{l^2}\delta^{ab}\delta_{\mu\nu}. \tag{3.108}$$

Calculations specifically to the gradient flow are the internal momentum integral and the each ones are denoted as

$$I_{D02} = \int_{l,p} \frac{1}{l^2(p-l)^2} e^{-2tp^2}, \tag{3.109}$$

$$I_{D03} = \int_{l,p} \int_0^t \mathrm{d}s \, \frac{1}{l^2} e^{-tp^2} e^{-s(p-l)^2} e^{-sl^2} e^{-(t-s)p^2} \tag{3.110}$$

$$I_{D04} = \int_{l,p} \int_0^t \mathrm{d}s \int_0^s \mathrm{d}u \, \frac{p\cdot(p-l)}{l^2} e^{-(t-s)p^2} e^{-(s-u)(p-l)^2} e^{-up^2} e^{-tp^2} e^{-(s+u)l^2} \tag{3.111}$$

$$I_{D05} = \int_{l,p} \int_0^t \mathrm{d}s \int_0^t \mathrm{d}u \, \frac{p\cdot(p-l)}{l^2} e^{-(t-s)p^2} e^{-(t-u)p^2} e^{-(s+u)(p-l)^2} e^{-(s+u)l^2} \tag{3.112}$$

$$I_{D06} = \int_{l,p} \int_0^t \mathrm{d}s \, \frac{1}{l^2} e^{-(t-s)p^2} e^{-sp^2} e^{-tp^2} e^{-2sl^2} \tag{3.113}$$

$$I_{D07(1)} = \int_{l,p} \frac{1}{l^2(p+l)^2} e^{-tp^2} e^{-tl^2} e^{-t(p+l)^2} \tag{3.114}$$

$$I_{D07(2)} = \int_{l,p} \frac{p\cdot l}{p^2 l^2 (p+l)^2} e^{-tp^2} e^{-tl^2} e^{-t(p+l)^2} \tag{3.115}$$

$$I_{D08} = \int_{l,p} \int_0^t \mathrm{d}s \, \frac{1}{l^2} e^{-(t-s)p^2} e^{-(t+s)l^2} e^{-(t+s)(p+l)^2}. \tag{3.116}$$

The each integrals are calculated as follows.

We use the Feynman parameter integral for I_{D02}.

$$\begin{aligned} I_{D02} &= \int_{l,p} \int_0^1 \mathrm{d}x \, \frac{1}{\{(l-px)^2 + x(1-x)p^2\}^2} e^{-2tp^2} \\ &= \int_{l,p} \int_0^1 \mathrm{d}x \, \frac{1}{\{l^2 + x(1-x)p^2\}^2} e^{-2tp^2} \\ &= \frac{\Gamma(2-D/2)}{(4\pi)^{D/2}} \int_0^1 \mathrm{d}x \, x^{D/2-2}(1-x)^{D/2-1} \int_p \left(p^2\right)^{D/2-2} e^{-2tp^2} \\ &= \frac{1}{2(2t)^2(4\pi)^4} \left\{ \frac{1}{\epsilon} + 2\log(8\pi t) + 1 \right\}, \end{aligned} \tag{3.117}$$

where we used the representation of the beta function

$$B(x,y) = \int_0^1 \mathrm{d}x \, t^{x-1}(1-t)^{y-1} = \frac{\Gamma(x)\Gamma(y)}{\Gamma(x+y)}. \tag{3.118}$$

The other integrals can be performed straightforwardly.

$$\begin{aligned}
I_{D03} &= \int_{l,p}\int_0^t \mathrm{d}s\ \frac{1}{l^2}e^{-2t\left(p-\frac{s}{2t}l\right)^2}e^{-\left(2s-\frac{s^2}{2t}\right)l^2} \\
&= \frac{1}{(2t)(4\pi)^D}\frac{\Gamma(D/2-1)}{\Gamma(D/2)}\int_0^t \mathrm{d}s\ \left(4ts-s^2\right)^{1-D/2} \\
&= \frac{2(2t)^{2-D}}{(4\pi)^D}\frac{\Gamma(D/2-1)}{\Gamma(D/2)}2^{2-D}\int_0^{1/4}\mathrm{d}x\ \left(x-x^2\right)^{1-D/2} \\
&= \frac{2(2t)^{2-D}}{(4\pi)^D}\frac{\Gamma(D/2-1)}{\Gamma(D/2)}2^{1-D}\left\{\int_0^{1/4}\mathrm{d}x\ \left(x-x^2\right)^{1-D/2}+\int_{3/4}^1\mathrm{d}x\ \left(x-x^2\right)^{1-D/2}\right\} \\
&= \frac{2(2t)^{2-D}}{(4\pi)^D}\frac{\Gamma(D/2-1)}{\Gamma(D/2)}2^{1-D}\left\{B(\epsilon,\epsilon)-\int_{1/4}^{3/4}\mathrm{d}x\ \frac{1}{x(1-x)}\right\} \\
&= \frac{1}{2(2t)^2(4\pi)^4}\left\{\frac{1}{\epsilon}+2\log(8\pi t)+1+2\log(2)-\log(3)\right\}, \qquad (3.119)
\end{aligned}$$

where we replaced $s = 4tx$ in the third line and took a limit

$$\lim_{\epsilon\to 0}\int_{1/4}^{3/4}\mathrm{d}x\ \left(x-x^2\right)^{1-D/2}. \qquad (3.120)$$

D04 and D05 do not diverge with $\epsilon \to 0$.

$$\begin{aligned}
I_{D04} &= \int_{l,p}\int_0^t \mathrm{d}s\int_0^s \mathrm{d}u\ \frac{p\cdot(p-l)}{l^2}e^{-2t\left(p-\frac{s-u}{2t}l\right)^2}e^{\frac{(s-u)^2}{2t}l^2}e^{-2sl^2} \\
&= \int_{l,p}\int_0^t \mathrm{d}s\int_0^s \mathrm{d}u\ \frac{1}{l^2}\left\{p^2+\frac{(s-u)(s-u-2t)}{4t^2}l^2\right\}e^{-2tp^2}e^{\frac{(s-u)^2}{2t}l^2}e^{-2sl^2} \\
&= \frac{1}{(2t)^2(4\pi)^4}\int_0^t \mathrm{d}s\int_0^s \mathrm{d}u\ \left[\frac{2}{4ts-(s-u)^2}+\frac{(s-u)(s-u-2t)}{\{4ts-(s-u)^2\}^2}\right] \\
&= \frac{1}{2(2t)^2(4\pi)^4}\left\{4\log(3)-5\log(2)\right\}, \qquad (3.121)
\end{aligned}$$

and

$$\begin{aligned}
I_{D05} &= \int_{l,p}\int_0^t \mathrm{d}s\int_0^t \mathrm{d}u\ \frac{p\cdot(p-l)}{l^2}e^{-2t\left(p-\frac{s+u}{2t}l\right)^2}e^{\frac{(s+u)^2}{2t}l^2}e^{-2sl^2} \\
&= \int_{l,p}\int_0^t \mathrm{d}s\int_0^t \mathrm{d}u\ \frac{1}{l^2}\left\{p^2+\frac{(s+u)(s+u-2t)}{4t^2}l^2\right\}e^{-2tp^2}e^{\frac{(s+u)^2}{2t}l^2}e^{-2sl^2} \\
&= \frac{1}{(2t)^2(4\pi)^4}\int_0^t \mathrm{d}s\int_0^t \mathrm{d}u\ \left[\frac{2}{(s+u)(4t-s-u)}+\frac{(s+u)(s+u-2t)}{\{(s+u)(4t-s-u)\}^2}\right] \\
&= \frac{1}{4(2t)^2(4\pi)^4}\left\{12\log(2)-5\log(3)\right\}, \qquad (3.122)
\end{aligned}$$

where we took $\epsilon \to 0$ in the middle.

D06 must be calculated on the D dimension, because it diverges as

$$\begin{aligned} I_{D06} &= \int_{l,p} \int_0^t \mathrm{d}s \, \frac{1}{l^2} e^{-2tp^2} e^{-2sl^2} \\ &= \frac{1}{(4\pi)^D} \frac{\Gamma(D/2-1)}{\Gamma(D/2)} \int_0^t \mathrm{d}s \, (2t)^{-D/2} (2s)^{1-D/2} \\ &= \frac{(2t)^{2-D}}{(4\pi)^D} \frac{\Gamma(D/2-1)}{\Gamma(D/2)} \int_0^1 \mathrm{d}x \, x^{1-D/2} \\ &= \frac{1}{(2t)^2 (4\pi)^4} \left\{ \frac{1}{\epsilon} + 2\log(8\pi t) + 1 \right\}. \end{aligned} \tag{3.123}$$

D07 and D08 do not also diverge.

$$\begin{aligned} I_{D07(1)} &= \int_{l,p} \int_0^\infty \mathrm{d}\alpha \, \frac{1}{l^2} e^{-tp^2} e^{-tl^2} e^{-(t+\alpha)(p+l)^2} \\ &= \frac{1}{(4\pi)^4} \int_0^\infty \mathrm{d}\alpha \, \frac{1}{2t+\alpha} \frac{1}{3t^2+2t\alpha} \\ &= \frac{1}{t^2 (4\pi)^4} \left\{ 2\log(2) - \log(3) \right\}, \end{aligned} \tag{3.124}$$

and

$$\begin{aligned} I_{D07(2)} &= \int_{l,p} \int_0^\infty \mathrm{d}\alpha \mathrm{d}\beta \, \frac{p \cdot l}{l^2} e^{-(t+\beta)p^2} e^{-tl^2} e^{-(t+\alpha)(p+l)^2} \\ &= \frac{-1}{(4\pi)^4} \int_0^\infty \mathrm{d}\alpha \mathrm{d}\beta \, \frac{t+\alpha}{2t+\alpha+\beta} \frac{1}{\{3t^2+2t(\alpha+\beta)+\alpha\beta\}^2} \\ &= \frac{-1}{2t^2 (4\pi)^4} \left\{ 2\log(2) - \log(3) \right\}, \end{aligned} \tag{3.125}$$

and

$$\begin{aligned} I_{D08} &= \int_{l,p} \int_0^t \mathrm{d}s \, \frac{1}{l^2} e^{-2tp^2} e^{-\frac{3t^2-s^2+2ts}{2t} l^2} \\ &= \frac{1}{(4\pi)^4} \int_0^t \mathrm{d}s \, \frac{1}{2t} \frac{1}{3t^2+2ts} \\ &= \frac{1}{4t^2 (4\pi)^4} \log(3). \end{aligned} \tag{3.126}$$

Combining them with the spinor factor, we have

$$D02 \quad : \quad -\frac{1}{\epsilon} - 2\log(8\pi t), \tag{3.127}$$

$$D03 \quad : \quad 2\frac{1}{\epsilon} + 4\log(8\pi t) + 2 + 4\log 2 - 2\log 3, \tag{3.128}$$

$$D04 \quad : \quad -20\log(2) + 16\log(3), \tag{3.129}$$

$$D05 \quad : \quad 12\log(2) - 5\log(3), \tag{3.130}$$

$$D06 \quad : \quad -4\frac{1}{\epsilon} - 8\log(8\pi t) - 2, \tag{3.131}$$

$$D07 \quad : \quad 8\log(2) - 4\log(3), \tag{3.132}$$

$$D08 \quad : \quad -2\log(3), \tag{3.133}$$

in the unit of

$$\frac{-8N_f}{(4\pi)^2 t^2}\frac{g_0^2}{(4\pi)^2}\frac{N^2-1}{2N}. \tag{3.134}$$

Finally, we obtain that

$$\varphi(t) \quad = \quad (8\pi t)^{-\epsilon}\left\{1 + \frac{g^2}{(4\pi)^2}\,\frac{N^2-1}{2N}\left(\frac{3}{\epsilon} + 3\log\left(8\pi\mu^2 t\right) - \log\left(432\right)\right)\right\}. \tag{3.135}$$

3.2.2 Axial vector current

We evaluate the matching factor for the axial vector current in this section. This time, we will use the background field method. The formal solutions for the background are (3.72), (3.73), (3.74) and for the quantum flow equations are (3.83), (3.84), (3.85). Since we can freely choose the background fields we set the gauge field to be 0 and the quark fields to be constant,

$$\hat{B}(t,x) \quad = \quad \hat{A}(x) = 0, \tag{3.136}$$

$$\hat{\chi}(t,x) \quad = \quad \hat{\psi}(x) = (\text{const.}), \tag{3.137}$$

$$\hat{\overline{\chi}}(t,x) \quad = \quad \hat{\overline{\psi}}(x) = (\text{const.}). \tag{3.138}$$

According to the small flow time expansion method, it is important to calculate the expansion coefficient $I_{\rm GF}$, in other words, the one particle irreducible vertex correction of the difference $O(\chi,\overline{\chi},B) - O(\psi,\overline{\psi},A)$. Since we are using the background field method the coefficient $I_{\rm GF}$ will appear as

$$\left\langle \overline{\chi}(t)\gamma_\mu\gamma_5 T^a \chi(t) - \overline{\psi}\gamma_\mu\gamma_5 T^a \psi \right\rangle_{\rm 1PI} \quad = \quad I_{\rm GF}(t)\hat{\overline{\psi}}\gamma_\mu\gamma_5 T^a\hat{\psi}. \tag{3.139}$$

We evaluate (3.139) in the one-loop order. It is enough to consider the quantum quark fields as

$$k(t,x) \quad \sim \quad e^{t\partial^2}p(x) + \int_0^t \mathrm{d}s\; e^{(t-s)\partial^2}\left(b^2(s,x)\hat{\psi} + 2b_\mu(s,x)\partial_\mu e^{s\partial^2}p(x)\right), \tag{3.140}$$

$$\overline{k}(t,x) \quad \sim \quad \overline{p}(x)\, e^{t\overleftarrow{\partial^2}} + \int_0^t \mathrm{d}s\; \left(\hat{\overline{\psi}}b^2(s,x) - 2\overline{p}(x)\, e^{s\overleftarrow{\partial^2}}\overleftarrow{\partial}_\mu b_\mu(s,x)\right) e^{(t-s)\overleftarrow{\partial^2}}. \tag{3.141}$$

With the same conditions, the propagator of the gauge field is evaluated as

$$\left\langle b_\mu^a(t,x) b_\nu^b(s,y) \right\rangle \sim g_0^2 \frac{-e^{(t+s)\partial_x^2}}{\partial_x^2} \delta^{ab} \delta_{\mu\nu} \delta(x-y). \tag{3.142}$$

By using these representations (3.140)-(3.142), we can calculate the left hand side of the (3.139), diagramatically it is described as in the Figure 9. We denoted the QCD quark-gluon vertex as the

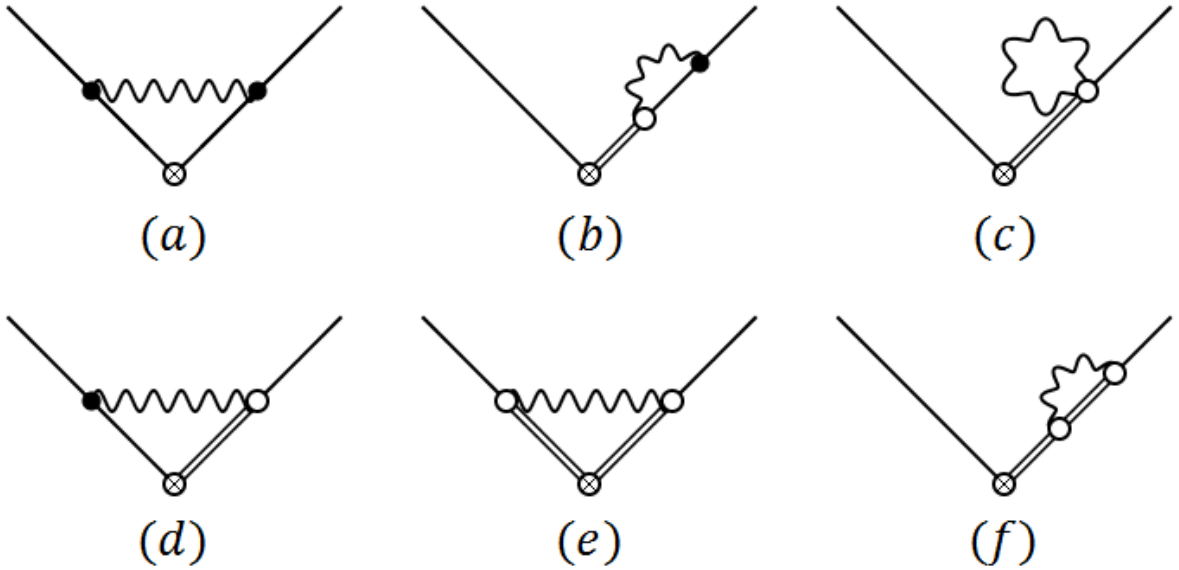

Figure 9: One loop diagrams for the fermion bi-linear operators.

black solid point and the flowed vertex as the white solid point. The heat kernel of the gradient flow is described by the double line. When we set the all of the external momentum to 0 the diagrams (d), (e) and (f) in the Figure 9 are vanished, because, the each diagrams are proportional to the external momentum. The other diagrams can be expressed as

$$(a) \quad : \quad \int_l \hat{\bar{\psi}} V_{1\nu}^b \gamma_\rho \gamma_\mu \gamma_5 T^a \gamma_\lambda V_{1\sigma}^c \hat{\psi} \left(e^{-2tl^2} - 1 \right) S_{F\rho}(l) S_{F\lambda}(l) G_{\nu\sigma}^{bc}(l), \tag{3.143}$$

$$(b) \quad : \quad 2 \int_0^t \mathrm{d}s \int_l \hat{\bar{\psi}} \gamma_\mu \gamma_5 T^a (-i l_\nu) T^b \gamma_\lambda V_{1\rho}^c \hat{\psi} e^{-sl^2} S_{F\lambda}(l) G_{\nu\rho}^{bc}(s.0;l), \tag{3.144}$$

$$(c) \quad : \quad \int_0^t \mathrm{d}s \int_l \hat{\bar{\psi}} \gamma_\mu \gamma_5 T^a T^b T^c \hat{\psi} G_{\nu\nu}^{bc}(s,s;l), \tag{3.145}$$

where we used the symbols below,

$$S_{F\mu}(l) = -i \frac{l_\mu}{l^2}, \tag{3.146}$$

$$V_{1\mu}^a = \gamma_\mu T^a, \tag{3.147}$$

$$G_{\mu\nu}^{ab}(t,s;l) = g_0^2 e^{-(t+s)l^2} \frac{1}{l^2} \delta^{ab} \delta_{\mu\nu}. \tag{3.148}$$

Note that when we calculate the diagram (a) (3.143) we must replace

$$e^{-2tl^2} - 1 = -2l^2 \int_0^t \mathrm{d}s\, e^{-2sl^2}, \tag{3.149}$$

and perform the internal momentum integration first. This procedure is related to the infrared divergence, and we will discuss about them in the section 3.2.4. Anywhere, the contribution from the diagram (a) become

$$(a) \quad : \quad \int_0^t \mathrm{d}s \int_l \overline{\hat{\psi}} V^b_{1\nu} \gamma_\rho \gamma_\mu \gamma_5 T^a \gamma_\lambda V^c_{1\sigma} \hat{\psi} (-2l^2) e^{-2sl^2} S_{F\rho}(l) S_{F\lambda}(l) G^{bc}_{\nu\sigma}(l). \tag{3.150}$$

Since the form of the internal momentum integrals are same it is enough to consider that

$$\int \frac{\mathrm{d}^D l}{(2\pi)^D} \frac{1}{l^2} e^{-tl^2} = \frac{t^{1-D/2}}{(4\pi)^{D/2}} \frac{\Gamma(D/2-1)}{\Gamma(D/2)}, \tag{3.151}$$

and we obtain that

$$(a) \quad : \quad \frac{g_0^2}{(4\pi)^2} \frac{N^2-1}{2N} (-1) \left\{ \frac{1}{\epsilon} + \log(8\pi t) + \frac{7}{2} \right\} \overline{\hat{\psi}} \gamma_\mu \gamma_5 T^a \hat{\psi}, \tag{3.152}$$

$$(b) \quad : \quad \frac{g_0^2}{(4\pi)^2} \frac{N^2-1}{2N} (+2) \left\{ \frac{1}{\epsilon} + \log(8\pi t) + 1 \right\} \overline{\hat{\psi}} \gamma_\mu \gamma_5 T^a \hat{\psi}, \tag{3.153}$$

$$(c) \quad : \quad \frac{g_0^2}{(4\pi)^2} \frac{N^2-1}{2N} (-4) \left\{ \frac{1}{\epsilon} + \log(8\pi t) + \frac{1}{2} \right\} \overline{\hat{\psi}} \gamma_\mu \gamma_5 T^a \hat{\psi}. \tag{3.154}$$

Therefore, the coefficient of the small flow time expansion become

$$I_{\mathrm{GF}}(t) = \frac{g_0^2}{(4\pi)^2} \frac{N^2-1}{2N} (-3) \left\{ \frac{1}{\epsilon} + \log(8\pi t) + \frac{7}{6} \right\}. \tag{3.155}$$

Since the axial vector current does not require the renormalization this ultraviolet divergence will be canceled by the quark field strength renormalization. In reality, because of the small flow time expansion

$$\overline{\mathring{\chi}}(t) \gamma_\mu \gamma_5 T^a \mathring{\chi}(t) = \left\{ 1 + \frac{g^2}{(4\pi)^2} \frac{N^2-1}{2N} \left(\frac{7}{2} - \log(432) \right) \right\} \overline{\psi} \gamma_\mu \gamma_5 T^a \psi, \tag{3.156}$$

for the small flow time. To obtain the relation (3.156), we used the renormalization of the coupling constant

$$g_0^2 = \mu^{2\epsilon} g^2. \tag{3.157}$$

Comparing with the $\overline{\mathrm{MS}}$ renormalized operator [119],

$$\left\{ \overline{\psi} \gamma_\mu \gamma_5 T^a \psi \right\}_{\overline{\mathrm{MS}}} = \left\{ 1 + \frac{g^2}{(4\pi)^2} \frac{N^2-1}{2N} (-4) \right\} \overline{\psi} \gamma_\mu \gamma_5 T^a \psi, \tag{3.158}$$

we obtain the matching factor as

$$Z^{\mathrm{GF}\to\overline{\mathrm{MS}}}(t)_{\mathrm{axial}} = 1 + \frac{g^2}{(4\pi)^2}\frac{N^2-1}{2N}\left(-\frac{1}{2} + \log(432)\right). \tag{3.159}$$

We can also replace the coupling constant g by the running coupling constant $\overline{g}(q)$, because the matching factor (3.159) is independent of the renormalization group flow as discussed in [120]. Moreover, we can set the scale $q = 1/\sqrt{8t}$ and obtain

$$Z^{\mathrm{GF}\to\overline{\mathrm{MS}}}(t)_{\mathrm{axial}} = 1 + \frac{\overline{g}(1/\sqrt{8t})^2}{(4\pi)^2}\frac{N^2-1}{2N}\left(-\frac{1}{2} + \log(432)\right). \tag{3.160}$$

3.2.3 Pseudo scalar density

In the previous section, we saw the matching factor of the axial vector current. Since it does not require the renormalization there is no divergence derived from ϵ. In this section, we will consider the pseudo scalar density. We can see the mechanism of the renormalization well, since the pseudo scalar density requires the renormalization.

$$\left\langle \overline{\chi}(t)\gamma_5 T^a \chi(t) - \overline{\psi}\gamma_5 T^a \psi \right\rangle_{\mathrm{1PI}} \quad = \quad I_{\mathrm{GF}}(t)\hat{\overline{\psi}}\gamma_5 T^a \hat{\psi}. \tag{3.161}$$

The Feynman diagrams take the same form of the axial vector current. At this time, non-zero contributions from the each diagram of the Figure 9 can be represented as

$$(a) \quad : \quad \int_l \hat{\overline{\psi}} V^b_{1\nu}\gamma_\rho\gamma_5 T^a \gamma_\lambda V^c_{1\sigma}\hat{\psi}\left(e^{-2tl^2}-1\right) S_{F\rho}(l) S_{F\lambda}(l) G^{bc}_{\nu\sigma}(l), \tag{3.162}$$

$$(b) \quad : \quad 2\int_0^t \mathrm{d}s \int_l \hat{\overline{\psi}}\gamma_5 T^a (-il_\nu) T^b \gamma_\lambda V^c_{1\rho}\hat{\psi} e^{-sl^2} S_{F\lambda}(l) G^{bc}_{\nu\rho}(s.0;l), \tag{3.163}$$

$$(c) \quad : \quad \int_0^t \mathrm{d}s \int_l \hat{\overline{\psi}}\gamma_5 T^a T^b T^c \hat{\psi} G^{bc}_{\nu\nu}(s,s;l). \tag{3.164}$$

We can see that the internal momentum integral is same with the previous one and the difference comes from the spinor index. The results are

$$(a) \quad : \quad \frac{g_0^2}{(4\pi)^2}\frac{N^2-1}{2N}(-4)\left\{\frac{1}{\epsilon} + \log(8\pi t) + \frac{1}{2}\right\}\hat{\overline{\psi}}\gamma_5 T^a\hat{\psi}, \tag{3.165}$$

$$(b) \quad : \quad \frac{g_0^2}{(4\pi)^2}\frac{N^2-1}{2N}(+2)\left\{\frac{1}{\epsilon} + \log(8\pi t) + 1\right\}\hat{\overline{\psi}}\gamma_5 T^a\hat{\psi}, \tag{3.166}$$

$$(c) \quad : \quad \frac{g_0^2}{(4\pi)^2}\frac{N^2-1}{2N}(-4)\left\{\frac{1}{\epsilon} + \log(8\pi t) + \frac{1}{2}\right\}\hat{\overline{\psi}}\gamma_5 T^a\hat{\psi}. \tag{3.167}$$

The result of the diagram (b) and (c) are not changed. It can be considered that the diagram (b) and (c) belong to the self energy part, in other words, the field strength renormalization and the

diagram (a) is a composite type contribution of the operator. Combining them with the quark field renormalization, we obtain the coefficient

$$I_{\rm GF}(t) = \frac{g_0^2}{(4\pi)^2}\frac{N^2-1}{2N}(-6)\left\{\frac{1}{\epsilon} + \log(8\pi t) + \frac{4}{3}\right\}. \tag{3.168}$$

and the relation

$$\overset{\circ}{\overline{\chi}}(t)\gamma_5 T^a \overset{\circ}{\chi}(t) = \left\{1 + \frac{g^2}{(4\pi)^2}\frac{N^2-1}{2N}\left(-\frac{3}{\epsilon} - 3\log(8\pi\mu^2 t) - 2 - \log(432)\right)\right\}\overline{\psi}\gamma_5 T^a\psi. \tag{3.169}$$

We again compare with the $\overline{\rm MS}$ renormalized operator,

$$\left\{\overline{\psi}\gamma_5 T^a\psi\right\}_{\overline{\rm MS}} = \left\{1 + \frac{g^2}{(4\pi)^2}\frac{N^2-1}{2N}\left(-\frac{3}{\epsilon} + 3\gamma - 3\log(4\pi) + 4\right)\right\}\overline{\psi}\gamma_5 T^a\psi, \tag{3.170}$$

and we have

$$Z^{\rm GF\to\overline{MS}}(t)_{\rm pseudo} = 1 + \frac{g^2}{(4\pi)^2}\frac{N^2-1}{2N}\left\{3\log(8t\mu^2) + 3\gamma - 2\log(2) + 6 + \log(432)\right\}. \tag{3.171}$$

When we set the scale $q = 1/\sqrt{8t}$,

$$Z^{\rm GF\to\overline{MS}}(t)_{\rm pseudo} = 1 + \frac{\overline{g}(1/\sqrt{8t})^2}{(4\pi)^2}\frac{N^2-1}{2N}\left\{3\gamma - 6\log(2) + 6 + \log(432)\right\}\frac{\overline{m}(1/\sqrt{8t})}{\overline{m}}. \tag{3.172}$$

Note that we add the factor $\overline{m}(1/\sqrt{8t})/\overline{m}$ to the matching factor to apply the renormalization group argument.

We can see that the divergence of the flowed operator (3.169) is canceled by the operator renormalization (3.170). Therefore, the gradient flow scheme and the $\overline{\rm MS}$ scheme are connected by the finite renormalization.

3.2.4 Infrared divergence

In the previous sections, we put off the discussion about the infrared divergence. We considered the subtraction between the flowed operator and the bare operator. The meaning of this representation is that $e^{2tl^2} - 1$ is rewritten by an integration of the flow time,

$$e^{-2tl^2} - 1 = -2l^2\int_0^t ds\, e^{-2sl^2}. \tag{3.173}$$

This replacement cares the infrared divergence and we will see it directly by introducing a gluon mass to the propagator. Such evaluation appears in the Figure 9. and the integration of the internal momentum is given by

$$\int_l \frac{1}{l^2(l^2+\lambda^2)}\left(e^{-2tl^2} - 1\right), \tag{3.174}$$

where we introduced the gluon mass $\lambda > 0$. We can show that

$$\int_l \frac{1}{l^2(l^2+\lambda^2)} e^{-2tl^2} = \frac{1}{(4\pi)^2}\left\{-\log\left(2t\lambda^2\right) - \gamma\right\}, \tag{3.175}$$

$$\int_l \frac{1}{l^2(l^2+\lambda^2)} = \frac{1}{(4\pi)^2}\left\{\frac{1}{\epsilon} - \gamma + \log\left(\frac{4\pi}{\lambda^2}\right) + 1\right\}. \tag{3.176}$$

Since the second equation (3.176) is easy, let us proof the first one (3.175)

$$\begin{aligned}
\int_l \frac{1}{l^2(l^2+\lambda^2)} e^{-2tl^2} &= \int_l \int_0^\infty d\alpha\, \frac{1}{l^2}\, e^{-2tl^2} e^{-\alpha(l^2+\lambda^2)} \\
&= \frac{1}{(4\pi)^{D/2}} \frac{\Gamma(D/2-1)}{\Gamma(D/2)}\, \lambda^{D-4} \int_0^\infty d\alpha\, (\alpha + 2t\lambda^2)^{1-D/2} e^{-\alpha} \\
&= \frac{1}{(4\pi)^{D/2}} \frac{1}{1-\epsilon}\, \lambda^{-2\epsilon}\, e^{2t\lambda^2} \left(\Gamma(\epsilon) - \gamma(\epsilon, 2t\lambda^2)\right),
\end{aligned} \tag{3.177}$$

where $\gamma(z,p)$ means a lower incomplete gamma function which is defined by

$$\gamma(z,p) := \int_0^p dx\, x^{z-1} e^{-x}. \tag{3.178}$$

We know the power series expansion of it. (3.178) is expanded as

$$\gamma(z,p) = e^{-p} \sum_{n=0}^{\infty} \frac{p^{z+n}}{z(z+1)\cdots(z+n)}. \tag{3.179}$$

Using equation (3.179), we obtain that

$$\int_l \frac{1}{l^2(l^2+\lambda^2)}\, e^{-2tl^2} = \frac{1}{(4\pi)^2}\, \left(-\gamma - \log\left(2t\lambda^2\right)\right). \tag{3.180}$$

When we consider the subtraction between these two integrations above, the infrared divergence $\log(\lambda^2)$ is just canceled out.

As we mentioned that

$$\int_0^t \mathrm{d}s \int_l \frac{1}{l^2}\, e^{-2sl^2} \neq \int_l \int_0^t \mathrm{d}s\, \frac{1}{l^2}\, e^{-2sl^2}, \tag{3.181}$$

because the right hand side is ill-defined. However, we can proof that

$$\int_0^t \mathrm{d}s \int_l \frac{1}{l^2+\lambda^2}\, e^{-2sl^2} = \int_l \int_0^t \mathrm{d}s\, \frac{1}{l^2+\lambda^2}\, e^{-2sl^2}. \tag{3.182}$$

Since we calculated the right hand side of (3.182) we must calculate the left hand side of (3.182),

$$\begin{aligned}
\int_0^t \mathrm{d}s \int_l \frac{1}{l^2+\lambda^2}\, e^{-2sl^2} &= \frac{1}{(4\pi)^{D/2}} \lambda^{D-2} \int_0^\infty d\alpha \int_0^t ds\, (\alpha + 2s\lambda^2)^{-D/2} e^{-\alpha} \\
&= \frac{1}{2(4\pi)^2} \left(\frac{4\pi}{\lambda^2}\right)^{\epsilon} (1+\epsilon) \int_0^\infty d\alpha\, \left\{(\alpha + 2t\lambda^2)^{1-D/2} - \alpha^{1-D/2}\right\} e^{-\alpha} \\
&= \frac{-1}{2(4\pi)^2} \left(\frac{4\pi}{\lambda^2}\right)^{\epsilon} (1+\epsilon) \left(\frac{1}{\epsilon} + \log\left(2t\lambda^2\right)\right) \\
&= \frac{-1}{2(4\pi)^2} \left(\frac{1}{\epsilon} + \log\left(8\pi t\right) + 1\right).
\end{aligned} \tag{3.183}$$

It is just the right hand side of (3.182). In other words, we can exchange the gluon mass to 0 limit and the internal momentum integral on the left hand side of (3.182),

$$\lim_{\lambda\to 0}\int_0^t \mathrm{d}s \int_l \frac{1}{l^2+\lambda^2}\, e^{-2sl^2} = \int_0^t \mathrm{d}s \int_l \lim_{\lambda\to 0}\frac{1}{l^2+\lambda^2}\, e^{-2sl^2}, \tag{3.184}$$

while cannot exchange them in the right hand side of (3.182),

$$\lim_{\lambda\to 0}\int_l\int_0^t \mathrm{d}s\, \frac{1}{l^2+\lambda^2}\, e^{-2sl^2} \neq \int_l \lim_{\lambda\to 0}\int_0^t \mathrm{d}s\, \frac{1}{l^2+\lambda^2}\, e^{-2sl^2}.. \tag{3.185}$$

This result shows that the gluon mass λ correctly cares the infrared divergence, in other words, the right hand side of (3.181) is contaminated by the infrared divergence. Moreover, it is emphasized that we can evaluate the integration (3.175) in four dimensional space time because it has no divergence derived from ϵ. This property will be helpful for the calculation of the Penguin diagram in the section 4.2.

As the end of this section, let us calculate the renormalization factor of the quark field with the gluon mass. We will confirm that the gluon mass does not contribute to the renormalization factor[10]. There is no need to calculate the diagrams $D04$, $D05$, $D07$ and $D08$ in the Figure 8, because they do not have divergence originally. The other diagrams are denoted as

$$D02 \;:\; (-ip_\mu)e^{-2tp^2}S_{F\nu}(p)S_{F\rho}(p-l)S_{F\sigma}(p)G^{ab}_{\alpha\beta}(l)T^aT^b\mathrm{tr}\left[\gamma_\mu\gamma_\nu\gamma_\alpha\gamma_\rho\gamma_\beta\gamma_\sigma\right], \tag{3.186}$$

$$D03 \;:\; \int_0^t \mathrm{d}s(-ip_\mu)e^{-(t-s)p^2}e^{-s(p-l)^2}e^{-tp^2}S_{F\nu}(p)S_{F\sigma}(p-l) \tag{3.187}$$
$$\times(-2i(p-l)_\lambda)G^{ab}_{\rho\lambda}(s,0;l)T^aT^b\mathrm{tr}\left[\gamma_\mu\gamma_\nu\gamma_\rho\gamma_\sigma\right],$$

$$D06 \;:\; \int_0^t \mathrm{d}s(-ip_\mu)S_{F\nu}(p)e^{-(t-s)p^2}e^{-sp^2}e^{-tp^2}G^{ab}_{\rho\rho}(s,s;l)T^aT^b\mathrm{tr}\left[\gamma_\mu\gamma_\nu\right], \tag{3.188}$$

where we denote the gluon propagator including the gluon mass as

$$G^{ab}_{\mu\nu}(s,t;l) = \frac{g_0^2}{l^2+\lambda^2}\, e^{-(s+t)l^2}\delta^{ab}\delta_{\mu\nu}. \tag{3.189}$$

We can see that integration of the internal momentum l of the diagram $D06$ does not suffer from the infrared divergence, and we can remove the gluon mass λ from this calculation.

$$D06 \;:\; -4\frac{1}{\epsilon} - 8\log(8\pi t) - 2 \tag{3.190}$$

The diagrams $D02$ and $D03$ need the gluon mass, and the form of their momentum integration can be written as

$$D02 \;:\; \int_{p,l} \frac{p\cdot(p-l)}{p^2\,(p-l)^2}\frac{1}{l^2+\lambda^2}\, e^{-2tp^2}, \tag{3.191}$$

$$D03 \;:\; \int_{p,l}\int_0^t \mathrm{d}s\, \frac{1}{l^2+\lambda^2}\, e^{-s(p-l)^2}e^{-tp^2}e^{-sl^2}. \tag{3.192}$$

[10]One can skip the calculation (3.186)-(3.208), since it is just a confirmation.

Let us evaluate eq.(3.191) first. We can decompose the integrand as

$$\frac{p\cdot(p-l)}{p^2\,(p-l^2)} = \frac{1}{2}\left\{\frac{1}{p^2}+\frac{1}{(p-l)^2}-\frac{l^2}{p^2(p-l)^2}-\frac{1}{l^2}+\frac{1}{l^2}\right\}. \tag{3.193}$$

We added $0 = l^{-2} - l^{-2}$ for later calculation. We can evaluate that

$$\int_{p,l}\left\{\frac{1}{(p-l)^2}-\frac{1}{l^2}\right\}\frac{1}{l^2+\lambda^2}\,e^{-2tp^2}, \tag{3.194}$$

in four dimensional space time, because they do not have a divergence derived from ϵ

$$\begin{aligned}&\lim_{\epsilon\to 0}\int_{p,l\in\mathcal{R}^D}\left\{\frac{1}{(p-l)^2}-\frac{1}{l^2}\right\}\frac{1}{l^2+\lambda^2}\,e^{-2tp^2}\\ &\quad=\int_{p,l\in\mathcal{R}^4}\left\{\frac{1}{(p-l)^2}-\frac{1}{l^2}\right\}\frac{1}{l^2+\lambda^2}\,e^{-2tp^2}.\end{aligned} \tag{3.195}$$

When we integrate out the internal momentum p, we get

$$\int_{p,l\in\mathcal{R}^4}\frac{1}{l^2}\,\frac{1}{l^2+\lambda^2}\,e^{-2tp^2} = \frac{1}{(4\pi)^2}\,\frac{1}{(2t)^2}\int_l\frac{1}{l^2(l^2+\lambda^2)} \tag{3.196}$$

and

$$\begin{aligned}\int_{p,l\in\mathcal{R}^4}\frac{1}{(p-l)^2}\,\frac{1}{l^2+\lambda^2}\,e^{-2tp^2} &= \int_{p,l}\int_0^\infty d\alpha\; e^{-\alpha(p-l)^2}\,\frac{1}{l^2+\lambda^2}\,e^{-2tp^2}\\ = \frac{1}{(4\pi)^2}\int_l\int_0^\infty d\alpha\,\frac{1}{(\alpha+2t)^2}\,e^{-\frac{2t\alpha}{\alpha+2t}\,l^2} &= \frac{1}{(4\pi)^2(2t)^2}\int_l\frac{1-e^{-2tl^2}}{l^2(l^2+\lambda^2)}.\end{aligned} \tag{3.197}$$

The other integration must be done in $D = 4-2\epsilon$ dimension, however, we can show that

$$\begin{aligned}&\lim_{\lambda\to 0}\int_{p,l\in\mathcal{R}^D}\left\{\frac{1}{p^2}-\frac{l^2}{p^2(p-l)^2}\right\}\frac{1}{l^2+\lambda^2}\,e^{-2tp^2}\\ &\quad=\int_{p,l\in\mathcal{R}^D}\left\{\frac{1}{p^2\,l^2}-\frac{1}{p^2(p-l)^2}\right\}e^{-2tp^2}=0.\end{aligned} \tag{3.198}$$

To sum up eq.(3.196) to eq.(3.198), we obtain

$$\begin{aligned}&\int_{p,l}\left\{\frac{1}{p^2}+\frac{1}{(p-l)^2}-\frac{l^2}{p^2(p-l)^2}-\frac{1}{l^2}\right\}\frac{1}{l^2+\lambda^2}\,e^{-2tp^2}\\ &\quad=\frac{1}{(4\pi)^2(2t)^2}\int_l\frac{-1}{l^2(l^2+\lambda^2)}\,e^{-2tl^2}\\ &\quad=\frac{1}{(4\pi)^4(2t)^2}\left(\gamma+\log\left(2t\lambda^2\right)\right).\end{aligned} \tag{3.199}$$

It does not diverge in $\epsilon\to 0$ limit. The last integration is

$$\begin{aligned}&\int_{p,l}\frac{1}{l^2(l^2+\lambda^2)}\,e^{-2tp^2}\\ &\quad=\frac{1}{(4\pi)^4(2t)^2}\left(\frac{1}{\epsilon}-\gamma+\log\left(\frac{2t(4\pi)^2}{\lambda^2}\right)+1\right).\end{aligned} \tag{3.200}$$

Finally, we have

$$D02 \quad : \quad -\frac{1}{\epsilon} - 2\log(8\pi t). \tag{3.201}$$

Therefore, the diagram $D02$ is not changed by introducing the gluon mass. One may be wondering that there is arbitrariness in how to make 0 like

$$0 = \frac{1+\epsilon}{l^2} - \frac{1+\epsilon}{l^2}, \tag{3.202}$$

however, we can show that such construction makes obvious cancellation. In particular,

$$\begin{aligned} &\lim_{\epsilon\to 0}\int_{p,l\in\mathcal{R}^D} \left\{\frac{1}{(p-l)^2} - \frac{1+\epsilon}{l^2}\right\}\frac{1}{l^2+\lambda^2}\, e^{-2tp^2} \\ &\qquad \neq \int_{p,l\in\mathcal{R}^4} \left\{\frac{1}{(p-l)^2} - \frac{1}{l^2}\right\}\frac{1}{l^2+\lambda^2}\, e^{-2tp^2}. \end{aligned} \tag{3.203}$$

We evaluate p integration in $D = 4-2\epsilon$ dimension at this time,

$$\begin{aligned} &\int_{p,l\in\mathcal{R}^D} \left\{\frac{1}{(p-l)^2} - \frac{1}{l^2}\right\}\frac{1}{l^2+\lambda^2}\, e^{-2tp^2} \\ &= \int_{p,l\in\mathcal{R}^D}\int_0^\infty d\alpha\, \left\{e^{-\alpha(p-l)^2} - e^{-\alpha l^2}\right\}\frac{1}{l^2+\lambda^2}\, e^{-2tp^2} \\ &= \int_{l\in\mathcal{R}^D}\int_0^\infty d\alpha\, \left\{\frac{1}{(\alpha+2t)^{2-\epsilon}} e^{-\frac{2t\alpha}{\alpha+2t}l^2} - \frac{1}{(2t)^{2-\epsilon}} e^{-\alpha l^2}\right\}\frac{1}{l^2+\lambda^2}. \end{aligned} \tag{3.204}$$

It is hard to evaluate this integration, however, we can discuss whether the integrand is bounded. The most dangerous area is where $\alpha = 0$ and the integrand become 0 in there. If we choose an equation (3.202) we cannot exchange the limit and the integration.

Let us evaluate the diagram $D03$ throughout equation (3.192).

$$\begin{aligned} &\int_{p,l}\int_0^t \mathrm{d}s\, \frac{1}{l^2+\lambda^2}\, e^{-s(p-l)^2} e^{-tp^2} e^{-sl^2} \\ =\ & \frac{1}{(4\pi)^{2-\epsilon}(2t)^{2-\epsilon}}\int_{p,l}\int_0^t \mathrm{d}s\, \frac{1}{l^2+\lambda^2}\, e^{-\left(2s-\frac{s^2}{2t}\right)l^2} \\ =\ & \frac{1}{(4\pi)^{2-\epsilon}(2t)^{2-\epsilon}}\int_l \frac{1}{l^2+\lambda^2}\left\{\frac{1}{2l^2}\left(1-e^{-\frac{3}{2}tl^2}\right) + \int_0^t ds\, \frac{s}{2t}\, e^{-\left(2s-\frac{s^2}{2t}\right)l^2}\right\}, \end{aligned} \tag{3.205}$$

where we used an integration by parts. In the second term, the divergence is suppressed because the integrand is vanishing at $s = 0$. We can evaluate it as

$$\int_l\int_0^t \mathrm{d}s\, \frac{s}{2t}\, \frac{1}{l^2}\, e^{-\left(2s-\frac{s^2}{2t}\right)} = \frac{1}{(4\pi)^2}\log\left(\frac{4}{3}\right). \tag{3.206}$$

The first term will be

$$\frac{1}{(4\pi)^{2-\epsilon}(2t)^{2-\epsilon}}\int_l \frac{1}{2l^2(l^2+\lambda^2)}\left(1-e^{-\frac{3}{2}tl^2}\right)$$
$$=\frac{1}{2(4\pi)^4(2t)^2}\left(\frac{1}{\epsilon}+2\log(8\pi t)+1-\log\left(\frac{4}{3}\right)\right). \tag{3.207}$$

Therefore, there is no change with the gluon mass and we have again

$$Z_\chi = 1+\frac{g_0^2}{(4\pi)^2}\,\frac{N^2-1}{2N}\left(\frac{3}{\epsilon}+6\log(8\pi t)-\log(432)\right). \tag{3.208}$$

3.3 Hadronic Observables

In the previous sections, we reviewed the theoretical system of the gradient flow and discussed about some examples. The point is that the gradient flow can be dealt as a renormalization scheme. Gradient flow is more effective combining it with the lattice calculation. When we calculate some operator using the gradient flow on the lattice, the result is automatically renormalized in the gradient flow scheme. Since what we need to calculate is the operator renormalized in the $\overline{\text{MS}}$ scheme, we must multiply the matching factor to the numerical result.

We will discuss the numerical procedure of such operation at first. We must take care to the two important points. One is taking the Wick contraction, and one is extracting of flow time zero limit. Such discussions are given in the next section. After that, we will calculate mass and decay constant of mesons, which are practical examples of the lattice calculation.

3.3.1 Computational procedure on the lattice

In this section, we will review the computational procedure of the lattice simulation combining with the gradient flow. Since there are no differences about Hybrid Monte Carlo simulation we can use the existing configurations. We will discuss about two issues for applying the gradient flow method to the lattice simulation. One is that the gauge field is defined on the link of the lattice. We must rewrite the flow equation in terms of the link variable. The other one is caused by the fact that the integration of the quark field is already performed, in other words, the quark field does not explicitly appear in the lattice simulation. The flow equation of the quark field will be taken over by the flow kernel.

In the lattice simulation, gauge field is put on the link and defined via the link variable,

$$U_\mu(x) = e^{ig_0 A_\mu(x+\hat{\mu}/2)}. \tag{3.209}$$

Therefore, we must consider the flow equation[11] with respect to the link variable. According to the flow equation for the gauge field,

$$\begin{aligned} \partial_t B_\mu(t,x) &= D_\nu G_{\nu\mu}(t,x), \quad B_\mu(t=0,x) = A_\mu(x), && (3.210)\\ G_{\mu\nu}(t,x) &= \partial_\mu B_\nu(t,x) - \partial_\nu B_\mu(t,x) + [B_\mu(t,x), B_\nu(t,x)], && (3.211)\\ D_\mu &= \partial_\mu + [B_\mu(t,x), \cdot], && (3.212) \end{aligned}$$

we obtain that

$$\left(\partial_t V_\mu(t,x)\right) V_\mu^{-1} = -g_0^2 \partial_{x,\mu} S_w(V), \quad V_\mu(t=0,x) = U_\mu(x), \tag{3.213}$$

where we defined the plaquette action S_w

$$S_w(U) = \frac{1}{g_0^2} \sum_x \text{Re tr}\left[U_\mu(x) U_\nu(x+\hat{\mu}) U_\mu^\dagger(x+\hat{\nu}) U_\nu^\dagger(x)\right], \tag{3.214}$$

[11] Convenient choice of the gauge parameter is $\alpha_0 = 0$ for numerical studies.

and its differential

$$\partial_{x,\mu} f(U) = T^a \frac{\mathrm{d}}{\mathrm{d}s} f\left(e^{sX} U\right), \quad X(y,\nu) \begin{cases} T^a & (y,\nu) = (x,\mu), \\ 0 & \text{otherwise.} \end{cases} \tag{3.215}$$

When we rewrite the flow equations (3.213) as

$$\partial_t V_t = Z(V_t) V_t, \tag{3.216}$$

one suspect that the equation (3.216) can be solved by using the Runge-Kutta method. The Runge-Kutta method gives an approximate solution of a diffusion equation. In generally, let us consider

$$\frac{\mathrm{d}}{\mathrm{d}t} y(t) = F(t,y), \quad y(t_0) = y_0. \tag{3.217}$$

The s stage approximate solution is

$$y_{n+1} = y_n + h \sum_{i=1}^{s} b_i k_i, \tag{3.218}$$

$$k_i = f\left(t_n + c_i h, y_n + h \sum_{j=1}^{i-1} a_{ij} k_j\right), \tag{3.219}$$

where the coefficients a, b, c are defined by Butcher tableau.

However, we must solve the diffusion equation (3.216) which is defined on the Lie group. The approximate solutions also must belong to the Lie group. Such techniques are suggested in [77] and [78]. Lüscher constructed the solutions for these equations. According to [34],

$$W_0 = V_t, \tag{3.220}$$

$$W_1 = \exp\left(\frac{1}{4} Z_0\right) W_0, \tag{3.221}$$

$$W_2 = \exp\left(\frac{8}{9} Z_1 - \frac{17}{36} Z_0\right) W_1, \tag{3.222}$$

$$W_3 = \exp\left(\frac{3}{4} Z_2 - \frac{8}{9} Z_1 + \frac{17}{36} Z_0\right) W_2, \tag{3.223}$$

$$Z_i = \epsilon Z(W_i), \quad i = 0, 1, 2. \tag{3.224}$$

The flow time evolution is

$$V_{t+\epsilon} = W_3 + O(\epsilon^4). \tag{3.225}$$

The flowed quark field emerges via the propagator on the lattice. We must take care that the flowed propagator is not defined through the inverse of the flowed Dirac operator

$$\overrightarrow{\chi_{\mathrm{f}}(t)\overline{\chi}_{\mathrm{f}}}(t) \neq \{D(t) + m\}^{-1}. \tag{3.226}$$

To see the correct representation, let us consider the flow equation for the quark field with flavor f = u, d, s.

$$\partial_t \chi_{\rm f}(t,x) = \Delta\chi_{\rm f}(t,x),\ \chi_{\rm f}(t=0,x) = \psi_f(x), \tag{3.227}$$

$$\partial_t \overline{\chi}_{\rm f}(t,x) = \overline{\chi}_{\rm f}(t,x)\overleftarrow{\Delta},\ \overline{\chi}_{\rm f}(t=0,x) = \overline{\psi}_f(x), \tag{3.228}$$

where we denote

$$\Delta\chi_{\rm f}(t,x) = D_\mu D_\mu \chi(t,x), \tag{3.229}$$

$$\overline{\chi}_{\rm f}(t,x)\overleftarrow{\Delta} = \overline{\chi}_{\rm f}(t,x)\overleftarrow{D}_\mu\overleftarrow{D}_\mu, \tag{3.230}$$

$$D_\mu\chi_{\rm f}(t,x) = \left(\partial_\mu + B_\mu(t,x)\right)\chi_{\rm f}(t,x), \tag{3.231}$$

$$\chi_{\rm f}(t,x)\overleftarrow{D}_\mu = \overline{\chi}_{\rm f}(t,x)\left(\overleftarrow{\partial}_\mu - B_\mu(t,x)\right). \tag{3.232}$$

When we describe solutions of the flow equation

$$\chi_{\rm f}(t,x) = \sum_y K(t,x;0,y)\psi(y), \tag{3.233}$$

$$\overline{\chi}_{\rm f}(t,x) = \sum_y \overline{\psi}(y)K(t,x;0,y)^\dagger, \tag{3.234}$$

the flow kernel $K(t,x;s,y),\ (s \le t)$ satisfies flow equation

$$(\partial_t - \Delta_x)\,K(t,x;s,y) = 0,\ K(t,x;t,y) = \delta_{x,y,}, \tag{3.235}$$

$$K(t,x;s,y)^\dagger\left(\overleftarrow{\partial}_t - \overleftarrow{\Delta}_x\right) = 0,\ K(t,x;t,y)^\dagger = \delta_{x,y}, \tag{3.236}$$

and adjoint flow equation

$$K(t,x;s,y)\left(\overleftarrow{\partial}_s - \overleftarrow{\Delta}_y\right) = 0, \tag{3.237}$$

$$\left(\partial_s - \Delta_y\right)K(t,x;s,y)^\dagger = 0. \tag{3.238}$$

We can obtain the correct quark propagator

$$\overbrace{\chi_{\rm f}(t,x)\overline{\chi}_{\rm f}}(s,y) = \sum_{v,w} K(t,x;0,v)\left(S_f(v,w) - c_{\rm fl}\delta_{v,w}\right)K(s,y;0,w)^\dagger, \tag{3.239}$$

where $S_f(x,y)$ means the quark propagator with bare mass m_{0f} and satisfies

$$\left(D_\mu\gamma_\mu + m_{0f}\right)S_f(x,y) = 0. \tag{3.240}$$

The term including the coefficient $c_{\rm fl}$ means a $O(a)$ improvement of the Green's function and it is given at tree level perturbation as

$$c_{\rm fl} = \frac{1}{2}. \tag{3.241}$$

Finally, let us see the expectation value of the axial vector current as an example. The axial vector current at flow time t is given by

$$A^a_{\mu,\mathrm{f}}(t,x) = c_A(t)\varphi_\mathrm{f}(t)\overline{\chi}_\mathrm{f}(t,x)\gamma_\mu\gamma_5 T^a \chi_\mathrm{f}(t,x), \tag{3.242}$$

where we denote the matching factor as $c_A(t)$ and the renormalization factor of the quark field $\chi_\mathrm{f}(t)$ as $\varphi_\mathrm{f}(t)$ which is defined by

$$\varphi_\mathrm{f}(t) = \frac{-6}{(4\pi)^2 t^2 \left\langle \overline{\chi}_f(t,x)\gamma_\mu \overleftrightarrow{D}_\mu \chi(t,x)\right\rangle}, \quad \overleftrightarrow{D}_\mu = D_\mu - \overleftarrow{D}_\mu. \tag{3.243}$$

In the section 3.2.1, we calculated the matching factor $c_A(t)$ as

$$c_A(t) = 1 + \frac{\overline{g}^2(\sqrt{1/8t})}{(4\pi)^2}\frac{N^2-1}{2N}\left(-\frac{1}{2} + \log(432)\right). \tag{3.244}$$

We can estimate (3.244) numerically by using Mathematica, and some instance are listed in the Table 1[12]. We set the $\overline{\mathrm{MS}}$ reference scale to 2GeV.

flow time t	$c_A(t)$	flow time	$c_A(t)$
0.1	1.1413035695042353	1.1	1.2954060122014912
0.2	1.1644982623865360	1.2	1.3098832143525223
0.3	1.1825307239391032	1.3	1.3249219203188570
0.4	1.1983333490997918	1.4	1.3406632095394684
0.5	1.2129577533829257	1.5	1.3572681120862948
0.6	1.2269285984453740	1.6	1.3749271524269420
0.7	1.2405611222968254	1.7	1.3938730705716695
0.8	1.2540716233799060	1.8	1.4143988648626418
0.9	1.2676254449909745	1.9	1.4368847146685473
1.0	1.2813613936858140	2.0	1.4618401155811900

Table 1: Matching factor of the axial vector current.

The expectation value of the axial vector current is

$$\begin{aligned}
&\left\langle A_{\mu,\mathrm{f}}(t,x)\right\rangle \\
&\quad = -c_A(t,\mu)\varphi_\mathrm{f}(t)\mathrm{tr}\left[\gamma_\mu\gamma_5\overrightarrow{\chi_\mathrm{f}(t,x)}\overrightarrow{\chi}_\mathrm{f}(t,x)\right] \\
&\quad = -c_A(t,\mu)\varphi_\mathrm{f}(t)\sum_{v,w}\mathrm{tr}\left[\gamma_\mu\gamma_5 K(t,x;0,v)\left(S_\mathrm{f}(v,w) - c_\mathrm{fl}\delta_{v,w}\right)K(t,x;0,w)^\dagger\right].
\end{aligned} \tag{3.245}$$

[12]we set the bare gauge coupling $\beta = 2.05$.

The renormalization factor (3.243) is estimated within almost the same manner. In practice, we must take the zero flow time limit after taking the continuum limit, because there are $O(t)$ terms in the expression (3.242). In principle, we can expand the perturbative calculation to higher order and such improvement will be helpful to take the zero flow time limit. Two loop calculation and more detailed discussion can be shown in the [58].

In this section, we briefly reviewed the numerical procedure of the gradient flow method and the construction of the axial vector current as an example. We will proceed to concrete calculation in the next section.

3.3.2 Meson mass

The most easiest calculation of lattice QCD is the calculation of pion mass, since it does not need a renormalization. Therefore, if we calculate the pion mass with the gradient flow, it does not depend on the flow time. It will be a first check of our numerical procedure discussed in the previous section. We will calculate masses of pion, kaon, ρ meson, η_{ss} meson and ϕ meson as an exercise.

We use (2+1) flavor gauge configurations generated in [104], and the number of configurations is 65. Bare gauge coupling is set to $\beta = 2.05$ and hopping parameter of each quarks are $\kappa_u = \kappa_d = 0.1356$, $\kappa_s = 0.1351$, which corresponds to $a = 0.0701(29)$fm. The Lattice size is $28^3 \times 56$. The fermion action is $O(a)$ improved Wilson-clover action[105] and the gauge action is renormalization group improved Iwasaki gauge action. The reference scale of renormalization is fixed to $\mu = 2$GeV. Our purpose of this section is reproduction of the original results $m_\pi/m_\rho \sim 0.63$ and $m_{\eta_{ss}}/m_\phi \sim 0.73$.

At first, we evaluate pion mass with periodic boundary condition. It is calculated via the correlation function of

$$P^a(\vec{x},t) = \overline{\psi}(\vec{x},t)\gamma_5 T^a \psi(\vec{x},t). \tag{3.246}$$

Under the periodic boundary condition, the expectation value of some operator O is defined by

$$\langle O \rangle_{\mathrm{PBC}} = \sum_n \left\langle n | O\, e^{iHT} | n \right\rangle, \tag{3.247}$$

Where $|n\rangle$ means some complete set and T means temporal size of the lattice. Combining with the fact that

$$\mathbb{1} = |0\rangle\langle 0| + \sum_{k:\text{one particle state}} \int \frac{\mathrm{d}^3 p}{(2\pi)^3} |E_k(\vec{p})\rangle \langle E_k(\vec{p})| \frac{1}{2E_k(\vec{p})} + (\text{contribution from multi particle state}), \tag{3.248}$$

we obtain the representation of the correlation function as

$$\begin{aligned} G(t) &:= \sum_{\vec{x}} \left\langle P(\vec{0},0)P(\vec{x},t)\right\rangle_{\mathrm{PBC}} \\ &= \sum_{k:\text{one particle state}} \frac{|<0|P(0)|E_k(\vec{0})>|^2}{2m_k}\left(e^{-m_k t}+e^{-m_k(T-t)}\right) + (\text{multi particle state}). \end{aligned} \tag{3.249}$$

When we take t enough large, $t \to T/2$, contribution from the lightest particle become relevant, and we obtain

$$G(t) \sim \frac{|<0|P(0)|E_\pi(\vec{0})>|^2}{m_\pi} e^{-m_\pi T/2}\cosh\left(m_\pi(t-T/2)\right), \tag{3.250}$$

and

$$m_\pi = \cosh^{-1}\left(\frac{G(t+1)+G(t-1)}{2G(t)}\right). \tag{3.251}$$

We present the correlation function $G(t)$ for several flow time in the Figure 10. The difference of color means the difference of the flow time. The red, green and blue data mean $G(t)$ at dimensionless flow time $t/a^2 = 0.1$, 1.0 and 2.0. We can see that the value itself is different, however, the slope seems to be constant for each flow time.

Figure 11 describes the flow time dependence of pion mass. As we expected, the pion mass does not depend on the flow time, since the pion mass is not effected by the renormalization. We can realize that the gradient flow slightly improves the errors of the meson mass, because the gradient flow plays a role of smearing for the each field.

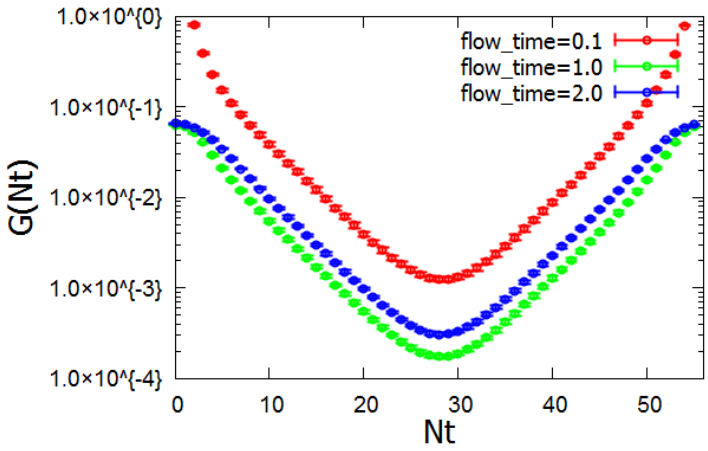

Figure 10: Correlation function $G(t)$ for several flow time.

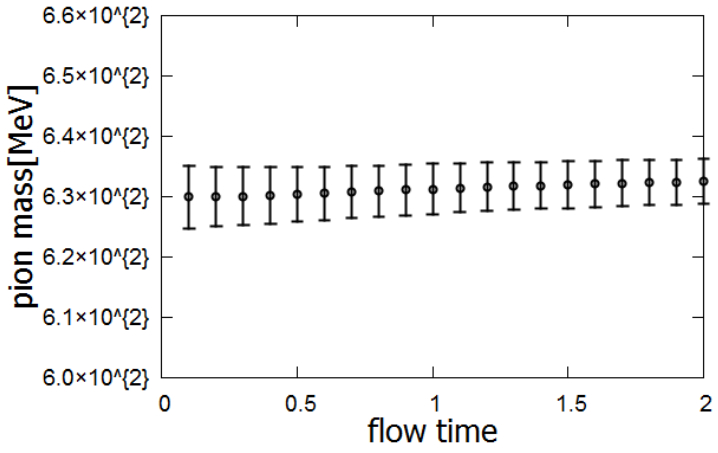

Figure 11: Flow time dependence of pion mass.

The mass of the other meson can be calculated with almost the same manner. We summarize the meson mass in the Table 2. We estimated the mass of the pseudo scalar particle, pion, kaon, η_{ss} meson, and vector meson, ρ meson, ϕ meson. Our results reproduce the original one, $m_\pi/m_\rho \sim 0.63$ and $m_{\eta_{ss}}/m_\phi \sim 0.73$. We also estimate the kaon mass which is necessary for the calculation of bag parameter.

meson	mass[MeV]
π	630.2(4.7)
K	731.7(4.8)
ρ	975.7(54.1)
η_{ss}	823.6(4.7)
ϕ	1125.0(28.3)

Table 2: Estimation of meson masses.

The gradient flow is greatly convenient method for the lattice QCD calculation, however, we need extreme caution for the each calculation. Especially for the Wick contraction of the flowed quark field (3.239), contraction must be taken at zero flow time. Our first estimates above are first check of validity.

3.3.3 Decay constant

We can also calculate the decay constant with the gradient flow. Historically, decay constant of a lot of particle have been measured[115]-[118] and such calculation will become a good exercise.

The pion decay constant is defied via the probability amplitude,

$$ip_\mu f_\pi = \left\langle 0|A_\mu(0)|E_\pi(\vec{p})\right\rangle, \tag{3.252}$$

where A_μ means the axial vector current,

$$A^a_\mu(x) \;=\; \overline{\psi}(x)\gamma_\mu\gamma_5 T^a\psi(x). \tag{3.253}$$

Note that we improved the axial vector current by

$$(A_I)^a_\mu(x) = A^a_\mu(x) + c_A\frac{1}{2}\left(P^a(x+a\hat{\mu}) - P^a(x-a\hat{\mu})\right), \tag{3.254}$$

which removes the $O(a)$ errors. The coefficient c_A is determined non-perturbatively[109], and given as

$$c_A = -0.0272(18), \tag{3.255}$$

in our parameter setup. After that, we simply denote the improved axial vector current as $A^a_\mu(x)$. As we discussed in the previous section, the correlation function of the pion operator with the periodic boundary condition is denoted by

$$\sum_{\vec{x}}\left\langle P(\vec{0},0)P(\vec{x},t)\right\rangle_{\rm PBC} \overset{t\to T/2}{\sim} \frac{|<0|P(0)|E_\pi(\vec{0})>|^2}{m_\pi}e^{-m_\pi T/2}\cosh\left(m_\pi(t-T/2)\right). \tag{3.256}$$

Similarly, the correlation function of the axial vector current and the pion operator with the periodic boundary condition is denoted by

$$\sum_{\vec{x}}\left\langle A_\mu(\vec{0},0)P(\vec{x},t)\right\rangle_{\rm PBC} \overset{t\to T/2}{\sim} \frac{<0|A_\mu(0)|E_\pi(\vec{0})><E_\pi(\vec{0})|P(0)|0>}{m_\pi}e^{-m_\pi T/2}\sinh\left(m_\pi(t-T/2)\right). \tag{3.257}$$

When we rewrite the each coefficient as

$$\sum_{\vec{x}}\left\langle P(\vec{0},0)P(\vec{x},t)\right\rangle_{\rm PBC} \overset{t\to T/2}{\sim} W_{PP}\cosh\left(m_\pi(t-T/2)\right), \tag{3.258}$$

$$\sum_{\vec{x}}\left\langle A_\mu(\vec{0},0)P(\vec{x},t)\right\rangle_{\rm PBC} \overset{t\to T/2}{\sim} W_{AP}\sinh\left(m_\pi(t-T/2)\right), \tag{3.259}$$

we can obtain the representation of the pion decay constant,

$$f_\pi = \frac{\langle 0|A_0(0)|E_\pi(\vec{p})\rangle}{m_\pi} = \frac{W_{AP}}{\sqrt{m_\pi e^{-m_\pi T/2}W_{PP}}}. \tag{3.260}$$

We will evaluate (3.260) using the gradient flow.

The Figure 12 shows the flow time dependence of the pion decay constant. As we mentioned,

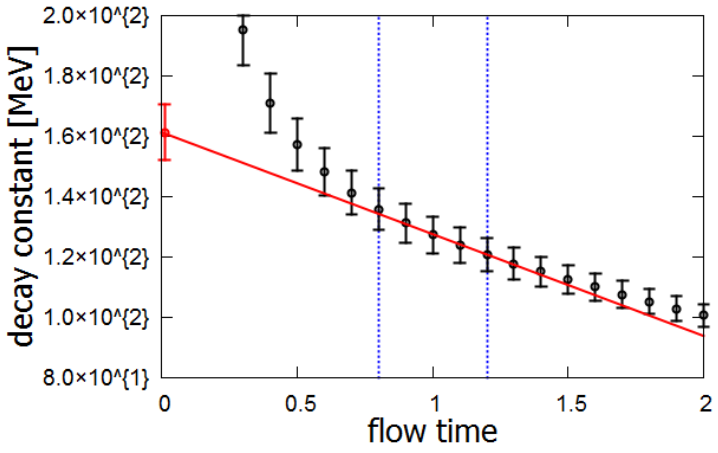

Figure 12: Pion decay constant and its $t \to 0$ limit.

we must take the flow time to 0 limits, because, our perturbative matching factor contains remnants which appear as $O(t)$ terms to the calculation. However, we cannot directly take the flow time to 0 limits, unlike the case of meson masses. In many cases, observables are contaminated by an artifact which is proportional to a^2/t. If we take the continuum limit before taking the flow time to 0 limit, the artifacts are successfully vanished. In [44], a way to skip formal procedures was suggested. According to the paper [44], once we find a window region in which the flow time dependence seem to linear, we can extrapolate the flow time to zero limit. We also apply the method and denote as the red solid line in the Figure 12. The window region which we used is denoted by the area between the blue dotted line in the Figure 12. We obtain the pion decay constant

$$f_\pi = 161.3(9.3)\text{MeV}. \tag{3.261}$$

At the physical point, the pion decay constant is $\sim$ 130MeV. Since our parameter setup is in the heavy quark region[13] our numerical result (3.261) is valid.

We also calculated the kaon decay constant as in the Figure 13. The result is

$$f_\pi = 168.7(9.3)\text{MeV}. \tag{3.262}$$

In this section, we measured the meson mass and the decay constant. We will advance to measurements of the operators which is related to some symmetry.

[13] $m_\pi \sim 630$MeV

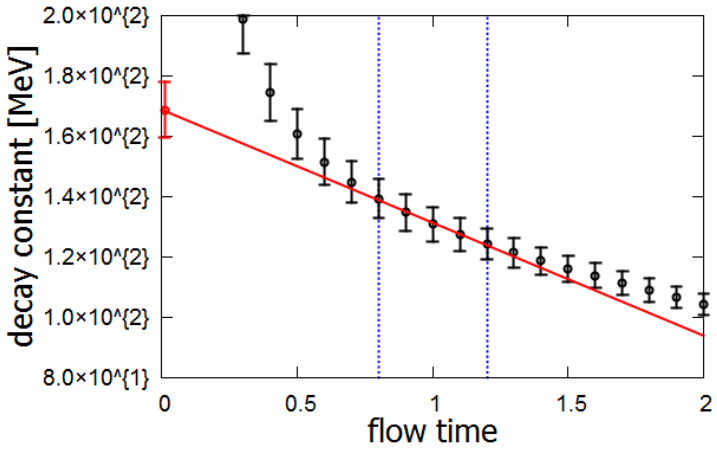

Figure 13: Kaon decay constant and its $t \to 0$ limit.

3.4 Previous Works with Gradient Flow

As we discussed in the section 2.2, Wilson fermion explicitly breaks the chiral symmetry. The effect is only $O(a)$, however, it grows combining with the divergence and we no longer ignore it even taking the continuum limit. We can define an operator in the $\overline{\text{MS}}$ scheme via the gradient flow method as

$$\left\langle O^{\overline{\text{MS}}} \right\rangle = \lim_{t \to 0} Z^{\text{GF} \to \overline{\text{MS}}}(t) \left\langle O^{\text{GF}}(t) \right\rangle . \tag{3.263}$$

Numerically, we measure $\left\langle O^{\text{GF}} \right\rangle$ on the lattice with the continuum limit. Our claim is that we can take the continuum limit even if the operator O relates to some symmetry which is broken on the lattice. In this section, we will see three previous works, energy momentum tensor [48], topological charge [49] and chiral condensate [48][57]. The each observable relate to breaking symmetry, however, the numerical results imply that the gradient flow works well even for such observables.

3.4.1 Energy momentum tensor

The energy momentum is Noether current with respect to the translational symmetry. In the thermodynamics of QCD, the energy momentum tensor is used as a convenient source of various thermodynamic quantities. For example, pressure and entropy density can be pulled out from the diagonal part of the energy momentum tensor. However, since the lattice regularization breaks the translational symmetry it is hard to define the energy momentum tensor on the lattice in naive ways.

In the finite temperature (continuum) QCD, the energy momentum tensor is written via the four

dimensional and gauge invariant symmetric operators,

$$
\begin{aligned}
O_{1\mu\nu}(x) &= F^a_{\mu\rho}(x)F^a_{\nu\rho}(x), && (3.264)\\
O_{2\mu\nu}(x) &= \delta_{\mu\nu}F^a_{\rho\sigma}(x)F^a_{\rho\sigma}(x), && (3.265)\\
O_{3\mu\nu}(x) &= \overline{\psi}(x)\left(\gamma_\mu \overleftrightarrow{D}_\nu + \gamma_\nu \overleftrightarrow{D}_\mu\right)\psi(x), && (3.266)\\
O_{4\mu\nu}(x) &= \delta_{\mu\nu}\overline{\psi}(x)\gamma_\rho \overleftrightarrow{D}_\rho\psi(x), && (3.267)\\
O_{5\mu\nu}(x) &= \delta_{\mu\nu}\overline{\psi}(x)\psi(x), && (3.268)
\end{aligned}
$$

as

$$
T_{\mu\nu}(x) = \frac{1}{g_0^2}\left(O_{1\mu\nu}(x) - \frac{1}{4}O_{2\mu\nu}(x)\right) + \frac{1}{4}O_{3\mu\nu}(x) - \frac{1}{2}O_{4\mu\nu}(x) - O_{5\mu\nu}(x). \tag{3.269}
$$

Because the energy momentum tensor takes an additive renormalization we can introduce a renormalization prescription for the energy momentum tensor as

$$
\left\{T_{\mu\nu}(x)\right\}_R = T_{\mu\nu}(x) - \left\langle T_{\mu\nu}(x)\right\rangle_{T=0}, \tag{3.270}
$$

where $\langle\cdot\rangle_{T=0}$ means the vacuum expectation value at zero temperature. However, we cannot use this definition on the lattice, since, the transnational invariance is no longer guaranteed. In [41], it is suggested that the gradient flow can play an important role to give the definition of the energy momentum tensor on the lattice. According to the general considerations of the gradient flow, if an operator is constructed from renormalized flowed fields the operator is free from the ultra violet divergence, that is, normalizations. Furthermore, we can expect that if we flow the definition (3.270) it can be diverted even on the lattice. Therefore, with the flowed operators,

$$
\begin{aligned}
\tilde{O}_{1\mu\nu}(t,x) &= G^a_{\mu\rho}(t,x)G^a_{\nu\rho}(t,x), && (3.271)\\
\tilde{O}_{2\mu\nu}(t,x) &= \delta_{\mu\nu}G^a_{\rho\sigma}(t,x)G^a_{\rho\sigma}(t,x), && (3.272)\\
\tilde{O}_{3\mu\nu}(t,x) &= \overset{\circ}{\overline{\chi}}(t,x)\left(\gamma_\mu \overleftrightarrow{D}_\nu + \gamma_\nu \overleftrightarrow{D}_\mu\right)\mathring{\chi}(t,x), && (3.273)\\
\tilde{O}_{4\mu\nu}(t,x) &= \delta_{\mu\nu}\overset{\circ}{\overline{\chi}}(t,x)\gamma_\rho \overleftrightarrow{D}_\rho\mathring{\chi}(t,x), && (3.274)\\
\tilde{O}_{5\mu\nu}(t,x) &= \delta_{\mu\nu}m\overset{\circ}{\overline{\chi}}(t,x)\mathring{\chi}(t,x), && (3.275)
\end{aligned}
$$

the energy momentum tensor is given by

$$
\begin{aligned}
\left\{T_{\mu\nu}(x)\right\}_R &= c_1(t)\left\{\tilde{O}_{1\mu\nu}(t,x) - \frac{1}{4}\tilde{O}_{2\mu\nu}(t,x)\right\} + c_2(t)\left\{\tilde{O}_{2\mu\nu}(t,x) - \left\langle\tilde{O}_{2\mu\nu}(t,x)\right\rangle\right\}\\
&+ c_3(t)\left\{\tilde{O}_{3\mu\nu}(t,x) - 2\tilde{O}_{4\mu\nu}(t,x) - \left\langle\tilde{O}_{3\mu\nu}(t,x) - 2\tilde{O}_{4\mu\nu}(t,x)\right\rangle\right\}\\
&+ c_4(t)\left\{\tilde{O}_{4\mu\nu}(t,x) - \left\langle\tilde{O}_{4\mu\nu}(t,x)\right\rangle\right\} + c_5(t)\left\{\tilde{O}_{5\mu\nu}(t,x) - \left\langle\tilde{O}_{5\mu\nu}(t,x)\right\rangle\right\},
\end{aligned} \tag{3.276}
$$

where the coefficients $c_i(t)$ mean the matching factor and given by for the $\overline{\text{MS}}$ scheme as

$$c_1(t) = \frac{1}{\overline{g}^2(1/\sqrt{8t})} - \frac{1}{(4\pi)^2}\left(\frac{11}{3}N - \frac{2}{3}N_f\right)(\gamma - 2\log(2)) - \frac{1}{(4\pi)^2}\left(\frac{7}{3}N - \frac{3}{4}N_f\right), \tag{3.277}$$

$$c_2(t) = \frac{1}{8(4\pi)^2}\left(\frac{11}{3}N + \frac{11}{6}N_f\right), \tag{3.278}$$

$$c_3(t) = \frac{1}{4}\left\{1 + \frac{\overline{g}^2(1/\sqrt{8t})}{(4\pi)^2}\frac{N^2-1}{2N}\left(\frac{3}{2} + \log(432)\right)\right\}, \tag{3.279}$$

$$c_4(t) = \frac{3}{4(4\pi)^2}\frac{N^2-1}{2N}\overline{g}^2(1/\sqrt{8t}), \tag{3.280}$$

$$c_5(t) = -\frac{\overline{m}(1/\sqrt{8t})}{m}\left\{1 + \frac{\overline{g}^2(1/\sqrt{8t})}{(4\pi)^2}\frac{N^2-1}{2N}\left(3\gamma - 6\log(2)\frac{7}{2} + \log(432)\right)\right\}. \tag{3.281}$$

The validation of the definition (3.276) have been concerned for $SU(3)$ Yang-Mills theory[14] in [44] and for full QCD in [48]. In this thesis, we review some of the results in QCD [48]. Figure 14

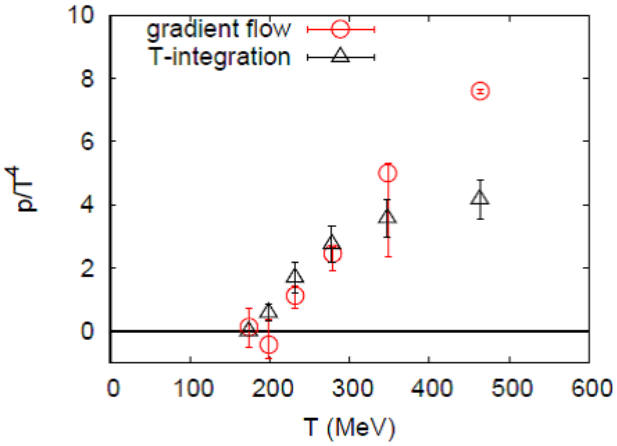

Figure 14: Pressure as a function of temperature [48].

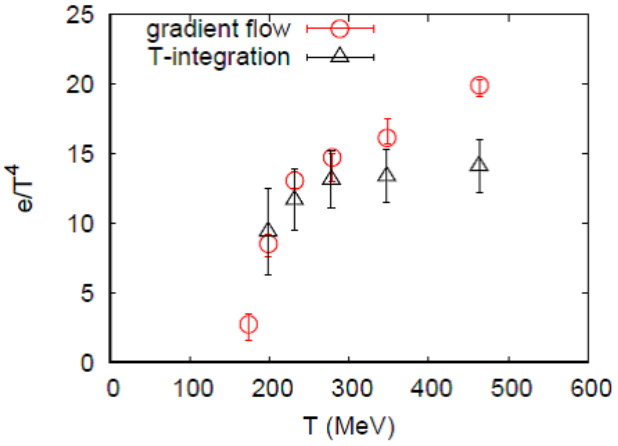

Figure 15: Entropy density as a function of temperature [48].

shows the numerical result of the pressure and Figure 15 shows the entropy density. The red points denote the results of the gradient flow method and the black points denote the results of the integral method. These two results are consistent in the region of $T \lesssim 279$MeV. It shows that the definition (3.276) which use the gradient flow works well. At the high temperature, because they used the fixed scale approach the lattice artifacts are severe and the two methods are not consistent.

[14] In Yang-Mills theory we must remove the quark fields from the representation (3.276).

3.4.2 Topological charge

The axion is a hypothetical elementary particle which was introduced to solve the strong CP problem in QCD. With the progress of the elementary particle theory, the axion also became a candidate for the dark matter. Since the axion mass relates to the topological susceptibility, there were many attempts to calculate the topological susceptibility on the lattice [69]-[73]. In [49], it is suggested that the gradient flow can contribute to the measurement of it.

The topological susceptibility can be defined via two different ways. One way is straightforward, and it is defined as a fluctuation of the topological charge,

$$Q = \int \mathrm{d}^4x \frac{1}{64\pi^2}\epsilon_{\mu\nu\rho\sigma}F^a_{\mu\nu}(x)F^a_{\rho\sigma}(x), \tag{3.282}$$

$$\chi_Q^{(\mathrm{gluonic})} = \frac{1}{V}\left(\left\langle Q^2\right\rangle - \langle Q\rangle^2\right). \tag{3.283}$$

In [49], this definition is called as gluonic definition.

The other way is using the chiral Ward-Takahashi identity

$$\chi_Q^{(\mathrm{fermionic})} = \frac{m^2}{VN_f^2}\left(\left\langle P^0P^0\right\rangle - N_f\left\langle P^aP^a\right\rangle^2\right), \tag{3.284}$$

$$P^a = \int \mathrm{d}^4x\overline{\psi}(x)T^a\psi(x). \tag{3.285}$$

In [49], it is called as fermionic definition. However, this definition has power divergence caused by the explicit chiral symmetry breaking for the Wilson fermion. They cared this problem by using the gradient flow. The two definitions evolve to

$$Q(t) = \int \mathrm{d}^4x \frac{1}{64\pi^2}\epsilon_{\mu\nu\rho\sigma}G^a_{\mu\nu}(t,x)G^a_{\rho\sigma}(t,x), \tag{3.286}$$

$$\chi_Q^{(\mathrm{gluonic})}(t) = \frac{1}{V}\left(\left\langle Q^2(t)\right\rangle - \langle Q(t)\rangle^2\right), \tag{3.287}$$

and

$$\chi_Q^{(\mathrm{fermionic})}(t) = \frac{m^2}{VN_f^2}\left(\left\langle P^0(t)P^0(t)\right\rangle - N_f\left\langle P^a(t)P^a(t)\right\rangle^2\right), \tag{3.288}$$

$$P^a(t) = c_s(t)\int \mathrm{d}^4x\mathring{\overline{\chi}}(t,x)T^a\mathring{\chi}(t,x), \tag{3.289}$$

$$c_s(t) = \left\{1 + \frac{\overline{g}^2(1/\sqrt{8t})}{(4\pi)^2}\left(4\gamma - 8\log(2) + 8 + \frac{4}{3}\log(432)\right)\right\}\frac{\overline{m}_{\mathrm{f}}(1/\sqrt{8t})}{\overline{m}_{\mathrm{f}}}. \tag{3.290}$$

After taking the flow time to 0 limit, the each expectation value are calculated as in Figure 16 which are the result of [49]. The red points show the gluonic definition (3.287) and the black points show the fermionic definition (3.288). They have good agreement, therefore, the gradient flow works well for the chiral Ward-Takahashi identity even for the Wilson fermion.

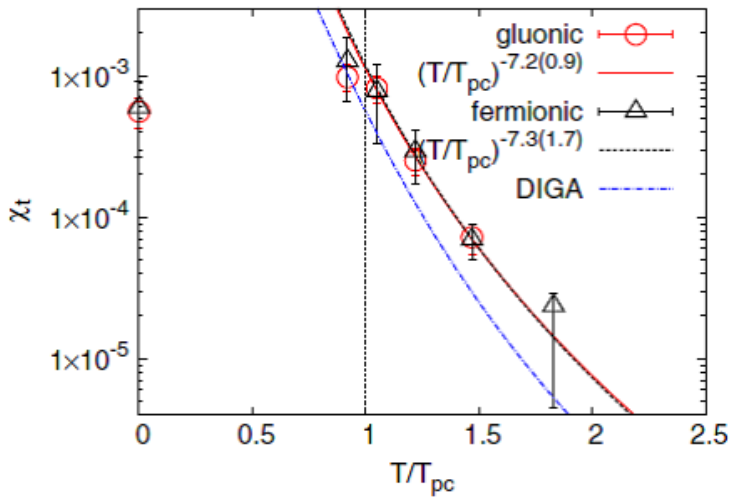

Figure 16: Topological susceptibility as a function of temperature [49].

3.4.3 Chiral condensate

Most of the Hadron mass comes from the spontaneous symmetry breaking of the chiral symmetry. However, when the temperature becomes very high the chiral symmetry is expected to recover. Such two phases are called as Hadron phase and Quark-Gluon plasma phase. The chiral condensate

$$\frac{1}{V}\sum_x \left\langle \overline{\psi}_{\rm f}(x)\psi_{\rm f}(x)\right\rangle, \tag{3.291}$$

is the order parameter of the phase transition. Since the Wilson fermion explicitly breaks the chiral symmetry (3.291) is taken an additive renormalization. When we consider the susceptibility of the chiral condensate, which shows a peak around the transition or crossover line,

$$\chi_{\rm f}^{\rm disc.} = \left\langle \left\{ \frac{1}{V}\sum_x \overline{\psi}_{\rm f}(x)\psi_{\rm f}(x)\right\}^2\right\rangle - \left\{\left\langle \frac{1}{V}\sum_x \overline{\psi}_{\rm f}(x)\psi_{\rm f}(x)\right\rangle\right\}^2. \tag{3.292}$$

must has a complicated structure for the Wilson fermion.

In [48], the renormalization was done by the gradient flow and realized the calculation of disconnected susceptibility. They defined it via the gradient flow as

$$\chi_{\rm f}^{\rm disc.}(t) = c_s^2(t)\varphi^2(t)\left\langle \left\{ \frac{1}{V}\sum_x \overline{\chi_{\rm f}(t,x)}\chi_{\rm f}(t,x)\right\}^2\right\rangle - \left\{\left\langle \frac{1}{V}\sum_x \overline{\chi_{\rm f}(t,x)}\chi_{\rm f}(t,x)\right\rangle\right\}^2, \tag{3.293}$$

where the matching coefficient is given by

$$c_s(t) = \left\{1 + \frac{\overline{g}^2(1/\sqrt{8t})}{(4\pi)^2}\left(4\gamma - 8\log(2) + 8 + \frac{4}{3}\log(432)\right)\right\}\frac{\overline{m}_{\rm f}(1/\sqrt{8t})}{\overline{m}_{\rm f}(2{\rm GeV})}. \tag{3.294}$$

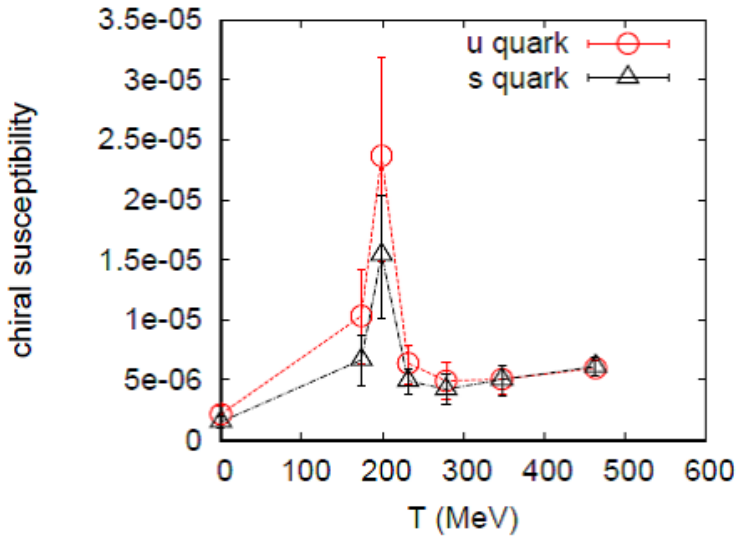

Figure 17: Disconnected chiral susceptibility as a function of temperature [48].

After taking the flow time to 0 limit, the disconnected chiral susceptibility become as in Figure 17. The red points show the disconnected chiral susceptibility for u, d quarks and the black points show for s quark. Moreover, there is a clear peak at $T \sim 199$MeV and this transition temperature is consistent with the previous work [68].

Their calculation was expanded to the connected part of the chiral susceptibility which includes the two point functions of flowed operators [57]. The flowed connected part is defined by

$$\chi_{\mathrm{f}}^{\mathrm{conn.}}(t) = c_s^2(t)\varphi^2(t)\left\langle \frac{1}{V}\sum_x \overline{\chi}_{\mathrm{f}}(t,x)\overline{\chi_{\mathrm{f}}(t,x)\overline{\chi}_{\mathrm{f}}(t,0)}\chi_{\mathrm{f}}(t,0)\right\rangle. \tag{3.295}$$

Combining these effects, the full chiral susceptibility can be calculated and the numerical results are denoted in Figure 18. The black points show the full chiral susceptibility for u, d quarks and the red points show for s quark. They also show a peak at $T \sim 199$MeV, however, the signal is mild at this time. It is notable that the same behavior can be seen for the Wilson fermion [74], the overlap fermion [75] and the HISQ [76].

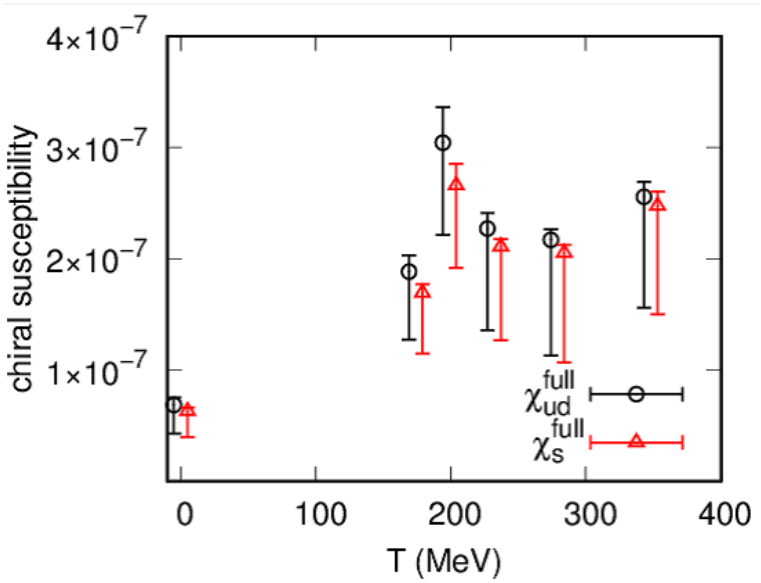

Figure 18: Full chiral susceptibility as a function of temperature [57].

3.5 PCAC Relation

In the section 3.2, we saw the two examples, axial vector current and the pseudo scalar density, which are important and concrete for PCAC[15] relation which is one representation of the chiral Ward-Takahashi identity. Since we are using Wilson fermion there are nontrivial renormalization to the equation. In some previous works with Wilson fermion[112]-[114], PCAC relation is used as a renormalization condition of the Schrödinger functional method[107][108], however, we expect that the PCAC relation will be automatically satisfied by using the gradient flow. We will obtain two important consequences in this section. (1) PCAC relation seems to be established. (2) PCAC mass calculated in gradient flow scheme and calculated in Schrödinger functional scheme are consistent within error bars.

3.5.1 Validation of PCAC relation

The gradient flow plays a role of ultraviolet cutoff for operators and such property is probably held even for the operator which relates to the broken symmetry by the lattice fermion. In the previous section we saw the three circumstantial evidence, energy momentum tensor, topological charge and chiral condensate. Since our target, the kaon bag parameter relates to the chiral symmetry, more study about chiral symmetry is important.

In this section, we will see that the PCAC relation is also held by using the gradient flow. The PCAC relation is a kind of Ward-Takahashi identity with respect to the chiral symmetry. The

[15]Abbreviation of partially conserved axial-vector current

infinitesimal chiral transformation is defined as

$$\begin{aligned}\psi'(x) &= \psi(x) + iT^a\theta^a(x)\gamma_5\psi(x),\\ \overline{\psi}'(x) &= \psi(x) + i\overline{\psi}(x)\gamma_5 T^a\theta^a(x),\end{aligned} \tag{3.296}$$

where $\theta(x)$ means the infinitesimal number. Assuming the invariance of the expectation value of an operator, $< 0|O(\psi,\overline{\psi})|0 >$, we obtain the chiral Ward-Takahashi identity

$$\left\langle 0|O(\psi,\overline{\psi})\delta S_F + \delta O|0\right\rangle = 0. \tag{3.297}$$

When we choose the operator $O(\psi,\bar{)}$ as $\overline{\psi}(y)\gamma_5 T^a\psi(y)$ and $\theta^a(x) = \theta = \text{const.}$,

$$\delta S_F = i\theta - \partial_\mu A^a_\mu(x) + 2mP^a(x), \tag{3.298}$$

$$\delta O = 2i\theta\delta(x-y)S^0(x), \tag{3.299}$$

where we defined the scalar density S^0, the pseudo scalar density P^a and the axial vector current A^a_μ as

$$S^0(x) = \overline{\psi}(x)\psi(x), \tag{3.300}$$

$$P^a(x) = \overline{\psi}(x)\gamma_5 T^a\psi(x), \tag{3.301}$$

$$A^a_\mu(x) = \overline{\psi}(x)\gamma_\mu\gamma_5 T^a\psi(x). \tag{3.302}$$

Performing a spacial integration, we obtain PCAC relation

$$2m\left\langle P^a(N_t)P^a(0)\right\rangle = -\left\langle \partial_0 A^a_0(N_t)P^a(0)\right\rangle. \tag{3.303}$$

We will evaluate its both sides numerically with Wilson fermion using gradient flow. As we saw in the previous section, the renormalized pseudo scalar density and the renormalized axial vector current are calculated via the flowed operator as

$$P^a_{\rm f}(t,x) = \lim_{t\to 0} c_P(t)\varphi_{\rm f}(t)\overline{\chi}_{\rm f}(t,x)\gamma_5 T^a\chi_{\rm f}(t,x), \tag{3.304}$$

$$A^a_{\mu,{\rm f}}(t,x) = \lim_{t\to 0} c_A(t)\varphi_{\rm f}(t)\overline{\chi}_{\rm f}(t,x)\gamma_\mu\gamma_5 T^a\chi_{\rm f}(t,x). \tag{3.305}$$

Flow time dependence of each operators are shown in Figure.20 and Figure 19. Figure 20 indicates $\langle P^a(N_t)P^a(0)\rangle$ and Figure 19 indicates $\left\langle A^a_0(N_t)P^a(0)\right\rangle$ with $N_t = 28$. We simply used linear extrapolation to take the flow time to 0 limit and the fit range is fixed for all N_t. The fit range is taken to $0.8\leq t\leq 1.2$. The AP indicates a clear signal and a wide window region, however, PP has severe flow time dependence as in Figure 20. We chose the fit range as the AP and PP seem to indicate a linear dependence at the same time.

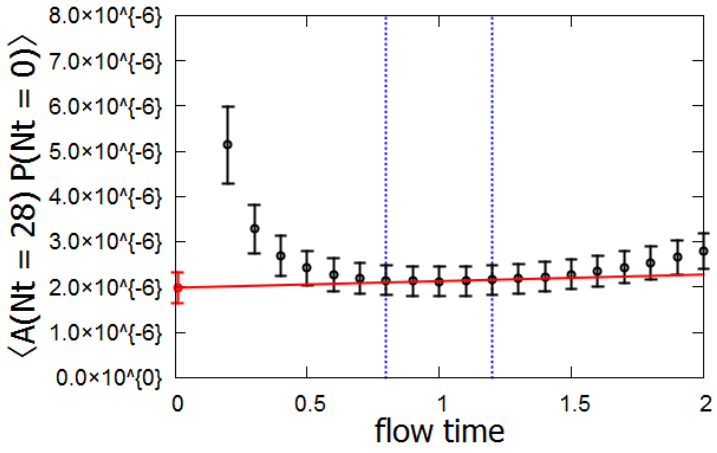

Figure 19: $\langle A_0(N_t = 28)P(N_t = 0)\rangle$ and its $t \to 0$ limit.

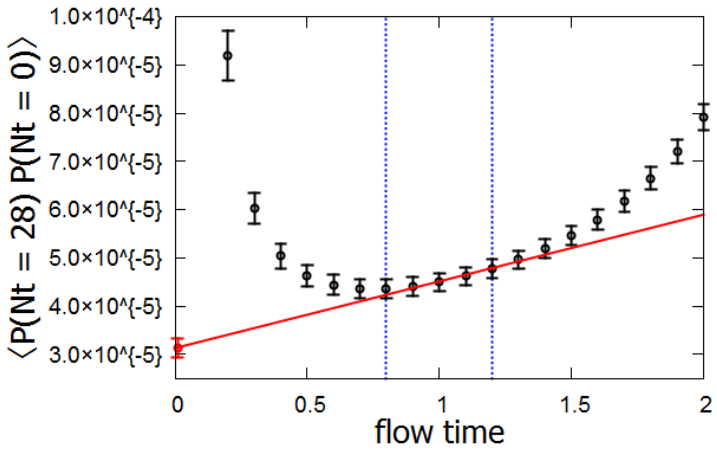

Figure 20: $\langle P(N_t = 28)P(N_t = 0)\rangle$ and its $t \to 0$ limit.

The numerical results of PCAC relation for u,d quarks are shown in Figure 21 and Figure 22. We used the same configuration with . The red points mean the left hand side of eq.(3.303) and the blue points mean the right hand side of eq.(3.303). We use the PCAC mass renormalized in Schrödinger functional scheme as quark mass $m = 82.3(4.1)$MeV. These two data are successfully consistent within error bars without $N_t \sim 0$.

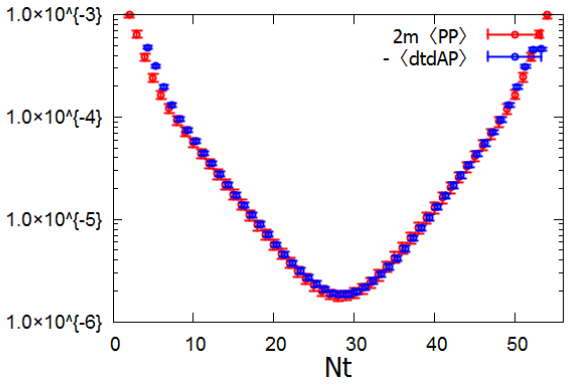

Figure 21: PCAC relation

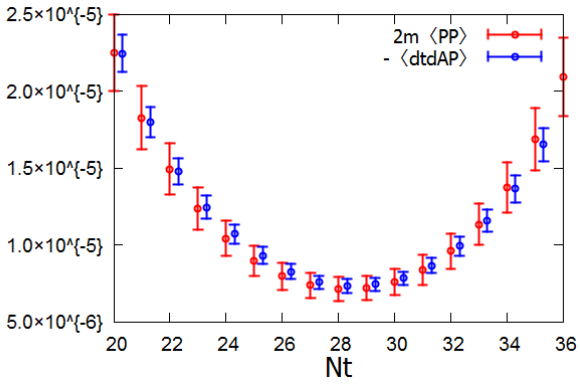

Figure 22: PCAC relation for $N_t \sim 28$

Our numerical results tells that the PCAC relation is held, although we are using the PCAC mass renormalized in Schrödinger functional scheme. However, we have still tested only the linear fit. We must apply the non-linear extrapolation to take the flow time to 0 limit, and the effect should be included as an systematic error.

3.5.2 PCAC mass

To estimate the renormalized PCAC mass, Schrödinger functional method is commonly used. In this section, we estimate the PCAC mass from the gradient flow method. Let us define the effective PCAC mass via the flowed operator as

$$m_{\mathrm{GF}}(t) = -\frac{c_A(t)c_P(t)\varphi^2(t)\left\langle \partial_0 A_0^a(N_t)P^a(0)\right\rangle}{2c_P^2(t)\varphi^2(t)\left\langle P^a(N_t)P^a(0)\right\rangle}. \tag{3.306}$$

At first, we look for a plateau with respect to the temporal distance N_t as in Figure 23. We specially pick up the case $t = 1.0$ in the Figure 23.

The renormalized PCAC mass can be estimated by

$$m_{\mathrm{GF}} = \lim_{t\to 0} m_{\mathrm{GF}}(t). \tag{3.307}$$

We also use the linear extrapolation to take the flow time to 0 limit for the calculation of the PCAC mass as shown in the Figure 24 for u,d quarks. We chose the fit range same as the AP and the PP.

Our final result of the renormalized PCAC mass for u,d quarks is that

$$m_{\mathrm{GF,ud}} = 76.9(5.2)\mathrm{MeV}. \tag{3.308}$$

This result is consistent with Schrödinger functional scheme

$$m_{\mathrm{SF,ud}} = 82.1(4.1)\mathrm{MeV}. \tag{3.309}$$

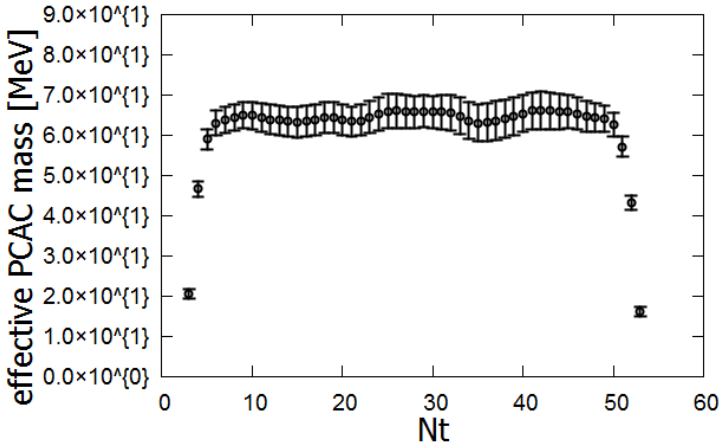

Figure 23: The effective PCAC mass for $t = 1.0$.

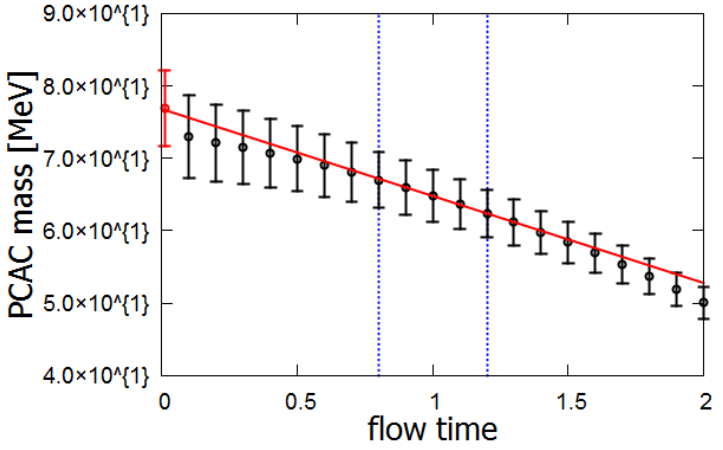

Figure 24: PCAC ud quark mass and its $t \to 0$ limit.

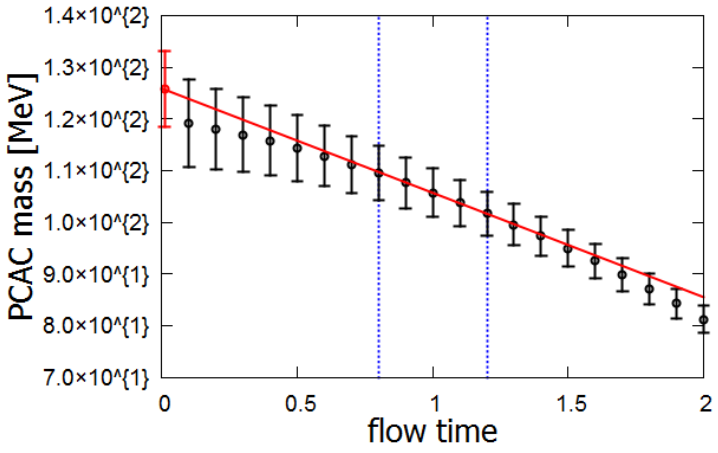

Figure 25: PCAC s quark mass and its $t \to 0$ limit.

With the same procedure, we can evaluate the renormalized PCAC mass for s quark. Figure 25 shows the linear extrapolation and the result is

$$m_{\mathrm{GF,s}} = 125.9(7.3)\mathrm{MeV}. \tag{3.310}$$

The Schrödinger functional scheme gives

$$m_{\mathrm{SF,s}} = 137.9(6.8)\mathrm{MeV}. \tag{3.311}$$

These results are also consistent within error bar.

In this section, we discussed about the PCAC relation which needs the nontrivial renormalization related to the chiral symmetry. We started from the validation of the PCAC relation and reached the PCAC mass. Our numerical result of the PCAC mass for u,d and s quarks are consistent with the Schrödinger functional scheme. It tells that the gradient flow works well even for the operator which is related to the chiral symmetry, and become a tailwind of the calculation of kaon bag parameter with gradient flow.

4 Four Fermion Operators

We saw a lot of applications of the gradient flow in the previous chapter. The point is that the gradient flow can be regarded as some kind of renormalization scheme, because the expectation value of flowed operators are finite. What we must calculate is matching factor of the each operator, since the most popular expression is given in the $\overline{\text{MS}}$ scheme. We have already discussed about the dominant techniques in the section 3.1 and practiced with fermion bi-linear examples in the section 3.2.

In the case of four fermion operators, the basic idea of the calculation is almost as same as the fermion bi-linear operators. However, when we consider one loop correction of the four fermion operators in naive way we can recognize that the spinor indices are disorganized. In general, we can expand a 4×4 Hermitian matrix with some base. Such reconstruction is known as Fierz rearrangement and we will see in the section 4.1.1. Fierz rearrangement recompose the spinor indeces and make the calculation possible. It is emphasized that Fierz rearrangement is effective in the four dimensional space time, therefore, the dimensional regularization scheme cannot be adopted just as it is. The dimensional regularization scheme changes to the dimensional reduction scheme in which only the internal loop momentums are reduced in the $D = 4-2\epsilon$ dimensional space time and the other Lorentz indices run for four dimensional space time. We will see more details of it in the section 4.1.2. After introducing Fierz rearrangement and the dimensional reduction scheme, the remaining calculation, integration of the internal momentum, will be smoothly done. Our calculation will be based on the small flow time expansion with the background field method. The key is calculation of $\langle O_{\text{flow}} - O_{\text{bare}} \rangle_{\text{1PI}}$, which is free from the infrared divergence as discussed in the section 3.2.3.

Our interest can be expanded to the other four fermion operators. Especially considering the importance of physics, we will pick up $\Delta S = 1$ four fermion operator in the section 4.2. It relates to the $K \to \pi\pi$ phenomenology and, therefore, also with CP-violation. When we consider the one loop correction of it we face to the new diagrams called QCD penguin diagrams. We will evaluate the internal momentum integration of penguin diagrams with the gradient flow in the section 4.2.2. We will see that integration of the internal momentum for the penguin diagram is more complicated than the $\Delta S = 2$ four fermion operator.

4.1 Kaon Bag Parameter

In this section, we calculate the matching factor of $\Delta S = 2$ four fermion operator which is the numerator of kaon bag parameter. Before the actual calculations, we will prepare two theoretical tools, Fierz rearrangement and the dimensional reduction scheme, which are needed for the calculation peculiar to the four fermion operators.

We also use the same notations with the previous section. T^a mean anti-Hermitian which satisfy

$$[T^a, T^b] = f^{abc}T^c, \tag{4.1}$$
$$Tr(T^aT^b) = -\frac{1}{2}\delta^{ab}, \tag{4.2}$$
$$T^aT^a = -\frac{N^2-1}{2N}\mathbb{1}, \tag{4.3}$$

for fundamental N representation of $SU(N)$. Gauge field A_μ and quark field ψ are decomposed into background fields and quantum fields

$$A_\mu(x) = \hat{A}_\mu(x) + a_\mu(x), \tag{4.4}$$
$$\psi(x) = \hat{\psi}(x) + p(x), \tag{4.5}$$
$$\overline{\psi}(x) = \hat{\overline{\psi}}(x) + \overline{p}(x), \tag{4.6}$$

where $\hat{A}_\mu$, $\hat{\psi}$, $\hat{\overline{\psi}}$ are background fields and a_μ, p, $\overline{p}$ are quantum fields.

The each fields evolve to flowed fields, $\hat{B}_\mu$, $\hat{\chi}$, $\hat{\overline{\chi}}$, b_μ, k, $\overline{k}$, along flow equations, where t means the flow time. The flow equation for the background fields are

$$\partial_t \hat{B}_\mu(t,x) = \hat{D}_\nu \hat{G}_{\nu\mu}(t,x) \ , \quad \hat{B}_\mu(t=0,x) = \hat{A}_\mu(x), \tag{4.7}$$
$$\partial_t \hat{\chi}(t,x) = \hat{D}^2 \hat{\chi}(t,x) \quad , \quad \hat{\chi}(t=0,x) = \hat{\psi}(x), \tag{4.8}$$
$$\partial_t \hat{\overline{\chi}}(t,x) = \hat{\overline{\chi}}(t,x)\overleftarrow{\hat{D}}^2 \quad , \quad \hat{\overline{\chi}}(t=0,x) = \hat{\overline{\psi}}(x), \tag{4.9}$$

and for the quantum fields are

$$\partial_t b_\mu(t,x) = \hat{D}^2 b_\mu(t,x) + 2[\hat{G}_{\mu\nu}(t,x), b_\nu(t,x)] + \hat{R}_\mu(t,x) \ , \ \hat{b}_\mu(t=0,x) = \hat{a}_\mu(x), \tag{4.10}$$
$$\begin{aligned}\partial_t k(t,x) = &\left\{D^2 - \hat{D}_\mu b_\mu(t,x)\right\} k(t,x) \\ &+ \left\{2b_\mu(t,x)\hat{D}_\mu + b^2(t,x)\right\} \hat{\chi}(t,x) \quad , \ k(t=0,x) = p(x),\end{aligned} \tag{4.11}$$
$$\begin{aligned}\partial_t \overline{k}(t,x) = &\ \overline{k}(t,x)\left\{\overleftarrow{D}^2 + \hat{D}_\mu b_\mu(t,x)\right\} \\ &+ \hat{\overline{\chi}}(t,x)\left\{-2\overleftarrow{\hat{D}}_\mu b_\mu(t,x) + b^2(t,x)\right\} \quad , \ \overline{k}(t=0,x) = \overline{p}(x),\end{aligned} \tag{4.12}$$

where we define that

$$\begin{aligned}
\hat{G}_{\mu\nu}(t,x) &= \partial_t \hat{B}_\nu(t,x) - \partial_t \hat{B}_\mu(t,x) + [\hat{B}_\mu(t,x),\, \hat{B}_\nu(t,x)], && (4.13)\\
\hat{D}_\mu &= \partial_\mu + [\hat{B}_\mu(t,x), \cdot]\ , \text{(for gauge fields)} && (4.14)\\
\hat{D}_\mu &= \partial_\mu + \hat{B}_\mu(t,x) \qquad , \text{(for quark fields)} && (4.15)\\
\hat{R}_\mu(t,x) &= +2[b_\nu(t,x),\, \hat{D}_\nu b_\mu(t,x)] \\
&\quad -[b_\nu(t,x),\, \hat{D}_\mu b_\nu(t,x)] + \left[b_\nu(t,x),\, \left[b_\nu(t,x),\, b_\mu(t,x)\right]\right]. && (4.16)
\end{aligned}$$

The four fermion operator we will consider throughout this section is defined as

$$\begin{aligned}
O_\pm &= \left[\left(\overline{\psi}_1 \gamma_\mu^L \psi_2\right)\left(\overline{\psi}_3 \gamma_\mu^L \psi_4\right) \pm \left(\overline{\psi}_1 \gamma_\mu^L \psi_4\right)\left(\overline{\psi}_3 \gamma_\mu^L \psi_2\right)\right], && (4.17)\\
\gamma_\mu^L &:= \gamma_\mu \frac{(1-\gamma_5)}{2}, && (4.18)
\end{aligned}$$

and its flowed one is defined as

$$O_\pm(t) = \left[\left(\overline{\chi}_1 \gamma_\mu^L \chi_2\right)\left(\overline{\chi}_3 \gamma_\mu^L \chi_4\right) \pm \left(\overline{\chi}_1 \gamma_\mu^L \chi_4\right)\left(\overline{\chi}_3 \gamma_\mu^L \chi_2\right)\right]. \tag{4.19}$$

The subscript $1 \cdots 4$ means the flavor index of the quark fields.

4.1.1 Fierz rearrangement

For perturbative calculation of four fermion operator, we will consider some product

$$\left(\overline{\psi}_1 \Lambda^{(1)} \psi_2\right)\left(\overline{\psi}_3 \Lambda^{(2)} \psi_4\right). \tag{4.20}$$

If $\Lambda^{(1)}$ and $\Lambda^{(2)}$ take simple form, there is no problem at all. However, we will evaluate the more complicated spinor structure as

$$\left(\overline{\psi}_1 \gamma_\mu \psi_2\right)\left(\overline{\psi}_3 \gamma_\mu \psi_4\right), \tag{4.21}$$

and we must take a summation with respect to the spinor index μ. Firtz rearrangement makes such calculation possible.

Let us consider an arbitrary 4×4 Hermitian matrix Λ. In general terms, Λ can be expanded by 16 linearly independent matrices. We choose them as

$$\lambda^A = \left\{\mathbb{1},\, \gamma_5,\, \gamma_\mu,\, i\gamma_\mu\gamma_5, i\sigma_{\mu\nu}\right\}. \tag{4.22}$$

We can verify that they are normalized as

$$\mathrm{tr}[\lambda^A \lambda^B] = 4\delta^{AB}, \tag{4.23}$$

and Λ is written by

$$\Lambda = \frac{1}{4}\sum_A \mathrm{tr}[\lambda^A\Lambda]\lambda^A. \tag{4.24}$$

When we regard the product of $\Lambda^{(1)}$ and $\Lambda^{(2)}$ as a 4×4 matrix,

$$\Lambda^{(il)}_{jk} := \Lambda^{(1)}_{ij}\Lambda^{(2)}_{kl}, \tag{4.25}$$

four fermion operator (4.20) is rewritten as

$$\begin{aligned}\left(\overline{\psi}_1\Lambda^{(1)}\psi_2\right)\left(\overline{\psi}_3\Lambda^{(2)}\psi_4\right) &= \overline{\psi}_{1i}\Lambda^{(1)}_{ij}\psi_{2j}\overline{\psi}_{3k}\Lambda^{(2)}_{kl}\psi_{4l}\\ &= \frac{1}{4}\sum_A \mathrm{tr}[\lambda^A\Lambda^{(il)}]\lambda^A_{jk}\overline{\psi}_{1i}\psi_{2j}\overline{\psi}_{3k}\psi_{4l}\\ &= -\frac{1}{4}\sum_A\left(\overline{\psi}_1\Lambda^{(1)}\lambda^A\Lambda^{(2)}\psi_4\right)\left(\overline{\psi}_3\lambda^A\psi_2\right),\end{aligned} \tag{4.26}$$

where we used equation (4.24) in the second line and imposed that the spinor index run in the four dimensional space time. If we define the 4×4 matrix by (4.27) instead of (4.25),

$$\Lambda^{(jk)}_{il} := \Lambda^{(1)}_{ij}\Lambda^{(2)}_{kl}, \tag{4.27}$$

we obtain another form of Fierz rearrangement,

$$\left(\overline{\psi}_1\Lambda^{(1)}\psi_2\right)\left(\overline{\psi}_3\Lambda^{(2)}\psi_4\right) = -\frac{1}{4}\sum_A\left(\overline{\psi}_1\lambda^A\psi_4\right)\left(\overline{\psi}_3\Lambda^{(2)}\lambda^A\Lambda^{(1)}\psi_2\right). \tag{4.28}$$

Fierz rearrangement also lead formulae,

$$S\odot S = -\frac{1}{4}\left(S\otimes S + P\otimes P + V\otimes V - A\otimes A - T\otimes T\right), \tag{4.29}$$

$$P\odot P = -\frac{1}{4}\left(S\otimes S + P\otimes P - V\otimes V + A\otimes A - T\otimes T\right), \tag{4.30}$$

$$S\odot P = -\frac{1}{4}\left(S\otimes P + P\otimes S - V\otimes A + A\otimes V - \tilde{T}\otimes T\right), \tag{4.31}$$

$$P\odot S = -\frac{1}{4}\left(S\otimes P + P\otimes S + V\otimes A - A\otimes V - \tilde{T}\otimes T\right), \tag{4.32}$$

$$V\odot V = -\frac{1}{4}\left(4S\otimes S - 4P\otimes P - 2V\otimes V - 2A\otimes A\right), \tag{4.33}$$

$$A\odot A = -\frac{1}{4}\left(-4S\otimes S + 4P\otimes P - 2V\otimes V - 2A\otimes A\right), \tag{4.34}$$

$$V\odot A = -\frac{1}{4}\left(-4S\otimes P + 4P\otimes S - 2V\otimes A - 2A\otimes V\right), \tag{4.35}$$

$$A\odot V = -\frac{1}{4}\left(4S\otimes P - 4P\otimes S - 2V\otimes A - 2A\otimes V\right), \tag{4.36}$$

$$T\odot T = -\frac{1}{4}\left(-6S\otimes S - 6P\otimes P - 4V\otimes V + 4A\otimes A\right) \tag{4.37}$$

$$T\odot \tilde{T} = -\frac{1}{4}\left(-6S\otimes P - 6P\otimes S + 4V\otimes A - 4A\otimes V\right). \tag{4.38}$$

4.1.2 Dimensional reduction

We reviewed Fierz rearrangement which organizes the spinor indeces by the complete set (4.22) in the previous section. Since we considered a 4×4 Hermitian matrix, the spinor indeces must run in the four dimensional space time. We impose that only the internal loop momentums are reduced in the $D = 4-2\epsilon$ dimension and the other Lorentz indices run for four dimensional space time, which condition is called as the dimensional reduction scheme. We denote the gamma matrices in four dimension as γ_μ, and the gamma matrices in D dimensional as $\overline{\gamma}_\mu$. When we denote the remaining part as $\tilde{\gamma}_\mu$, the gamma matrices are separated as

$$\gamma_\mu = \overline{\gamma}_\mu + \tilde{\gamma}_\mu. \tag{4.39}$$

We define the γ_5 matrix which anti-commute with every gamma matrices in this scheme.

$$\left\{\gamma_5, \gamma_\mu\right\} = 0, \tag{4.40}$$
$$\left\{\gamma_5, \overline{\gamma}_\mu\right\} = 0, \tag{4.41}$$
$$\left\{\gamma_5, \tilde{\gamma}_\mu\right\} = 0. \tag{4.42}$$

When we consider an anti-commutation relation between γ_μ and $\overline{\gamma}_\nu$, it can be calculated as

$$\left\{\gamma_\mu, \overline{\gamma}_\nu\right\} = \left\{\left(\overline{\gamma}_\mu + \tilde{\gamma}_\mu\right), \overline{\gamma}_\nu\right\} = 2\overline{\delta}_{\mu\nu}, \tag{4.43}$$

where the $\overline{\delta}_{\mu\nu}$ means the Kronecker delta in D dimension. The other relation can be calculated almost the same manner. For example,

$$\overline{\gamma}_\mu\gamma_\nu\overline{\gamma}_\mu = D\gamma_\nu - 2\overline{\gamma}_\nu, \tag{4.44}$$
$$\gamma_\mu\overline{\gamma}_\nu\gamma_\mu = -2\overline{\gamma}_\nu. \tag{4.45}$$

In the previous chapter, we calculated the renormalization factor of the quark field with the dimensional regularization scheme(DREG). The renormalization condition of flowed quark fields is

$$\mathring{\chi}(t,x) = \sqrt{\frac{-8N_f}{(4\pi)^2t^2\left\langle\overline{\chi}(t,x)\gamma_\mu\overleftrightarrow{D}_\mu\chi(t,x)\right\rangle}}\chi(t,x) := \varphi^{1/2}(t)\chi(t,x). \tag{4.46}$$

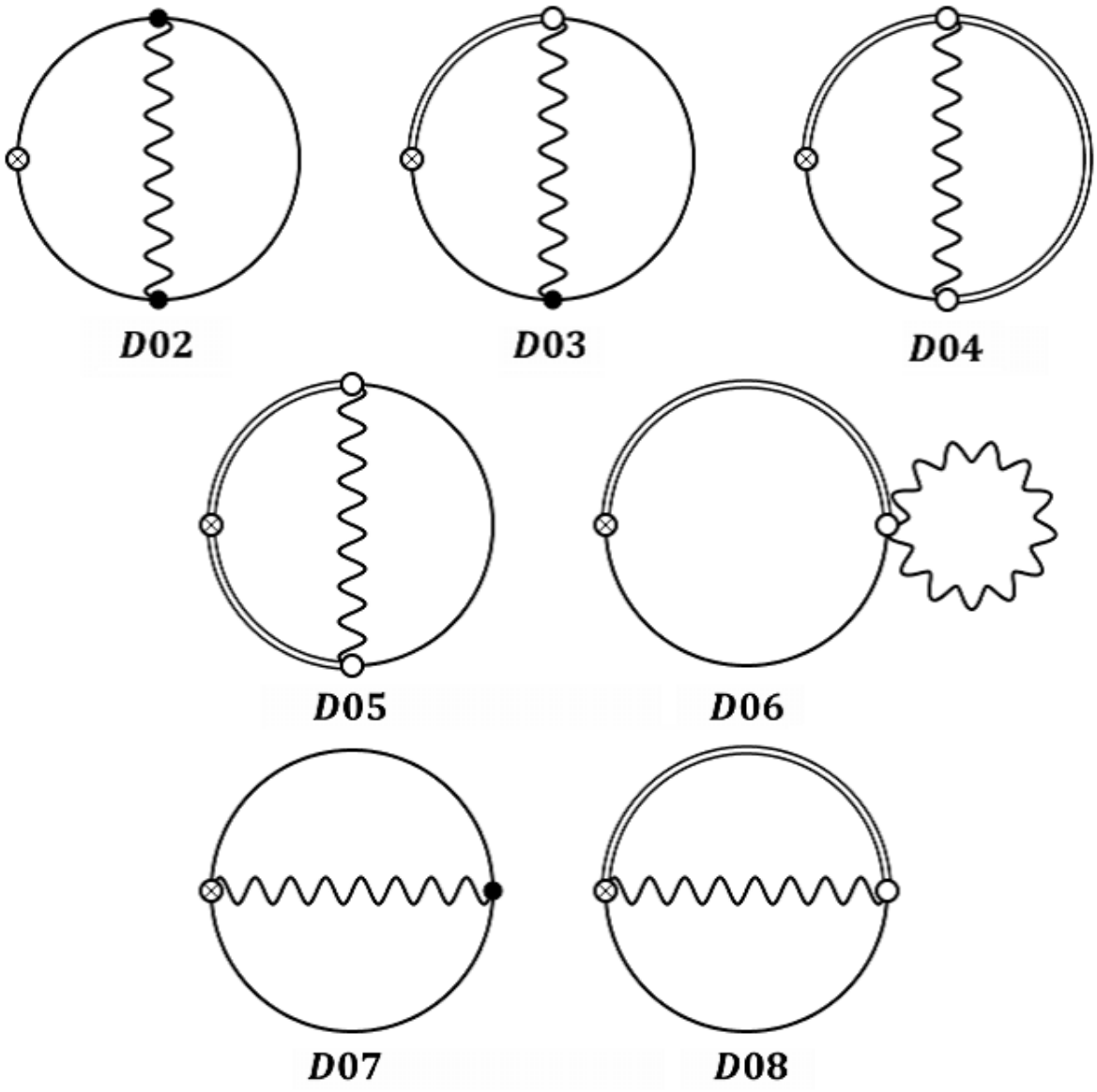

Figure 26: One loop diagrams for the fermion renormalization factor.

Feynman diagrams are drawn as Figure26. The contribution of each diagram is given by

$$
\begin{aligned}
D02|_{\mathrm{DERG}} &: -\frac{1}{\epsilon} - 2\log(8\pi t), && (4.47)\\
D03|_{\mathrm{DERG}} &: 2\frac{1}{\epsilon} + 4\log(8\pi t) + 2 + 4\log 2 - 2\log 3, && (4.48)\\
D04|_{\mathrm{DERG}} &: -20\log(2) + 16\log(3), && (4.49)\\
D05|_{\mathrm{DERG}} &: 12\log(2) - 5\log(3), && (4.50)\\
D06|_{\mathrm{DERG}} &: -4\frac{1}{\epsilon} - 8\log(8\pi t) - 2, && (4.51)\\
D07|_{\mathrm{DERG}} &: 8\log(2) - 4\log(3), && (4.52)\\
D08|_{\mathrm{DERG}} &: -2\log(3), && (4.53)
\end{aligned}
$$

in the unit of

$$
\frac{-8N_f}{(4\pi)^2 t^2}\frac{g_0^2}{(4\pi)^2}\frac{N^2-1}{2N}. \tag{4.54}
$$

Summing up all, we obtain

$$
\varphi(t)|_{\mathrm{DREG}} = (8\pi t)^{-\epsilon}\left\{1 + \frac{g^2}{(4\pi)^2}\,\frac{N^2-1}{2N}\left(\frac{3}{\epsilon} + 3\log\left(8\pi\mu^2 t\right) - \log\left(432\right)\right)\right\}. \tag{4.55}
$$

It is emphasized that this calculation is done in the dimensional regularization scheme and the result must be changed in the dimensional reduction scheme with finite value. The contribution of each diagram in the dimensional reduction scheme is

$$
\begin{aligned}
D02|_{\mathrm{DERD}} &: -\frac{1}{\epsilon} - 2\log(8\pi t) - 1, && (4.56)\\
D03|_{\mathrm{DERD}} &: 2\frac{1}{\epsilon} + 4\log(8\pi t) + 2 + 4\log 2 - 2\log 3, && (4.57)\\
D04|_{\mathrm{DERD}} &: -20\log(2) + 16\log(3), && (4.58)\\
D05|_{\mathrm{DERD}} &: 12\log(2) - 5\log(3), && (4.59)\\
D06|_{\mathrm{DERD}} &: -4\frac{1}{\epsilon} - 8\log(8\pi t) - 4, && (4.60)\\
D07|_{\mathrm{DERD}} &: 8\log(2) - 4\log(3), && (4.61)\\
D08|_{\mathrm{DERD}} &: -2\log(3), && (4.62)
\end{aligned}
$$

and the renormalization factor is

$$
\varphi(t)|_{\mathrm{DRED}} = (8\pi t)^{-\epsilon}\left\{1 + \frac{g^2}{(4\pi)^2}\,\frac{N^2-1}{2N}\left(\frac{3}{\epsilon} + 3\log\left(8\pi\mu^2 t\right) + 3 - \log\left(432\right)\right)\right\}. \tag{4.63}
$$

The difference emerges in diagram D02 and D06. We use this renormalization factor for the calculation of four fermion operator.

4.1.3 Feynman diagrams

The purpose of this section is finding Feynman diagrams which effect on the calculation of of $\langle O_\pm(t) - O_\pm\rangle_{\rm 1PI}$. $O_\pm$ and $O_\pm(t)$ are defined at (4.17) and (4.19).

Let us review the procedure of perturbative calculation of the flowed field. At first, we denote the flowed operator via the bare operator with small flow time,

$$O_\pm(t) \sim c(t)O_\pm + O(t)\ , \quad (\text{for } t \to 0), \tag{4.64}$$

where the coefficient $c(t)$ is available later. A convenient combination is $O_\pm(t) - O_\pm$ and its one particle irreducible vertex correction. When we use the background field method vertex correction is proportional to the operator which is written by the background field. In this case,

$$\begin{aligned} \langle O_\pm(t) - O_\pm\rangle_{\rm 1PI} &= I_{\rm GF}(t)\hat{O}_\pm, & (4.65)\\ \hat{O}_\pm &= \left[\left(\hat{\bar{\psi}}_1\gamma_\mu^L\hat{\psi}_2\right)\left(\hat{\bar{\psi}}_3\gamma_\mu^L\hat{\psi}_4\right) \pm \left(\hat{\bar{\psi}}_1\gamma_\mu^L\hat{\psi}_4\right)\left(\hat{\bar{\psi}}_3\gamma_\mu^L\hat{\psi}_2\right)\right], & (4.66)\end{aligned}$$

where we denote the proportional constant as $I_{\rm GF}(t)$. The right hand side, in other wards, proportional constant $I_{\rm GF}(t)$ is calculated in the section 4.1.4 and 4.1.5. We can also calculate the left hand side by using the relation (4.64) as

$$\begin{aligned} \langle O_\pm(t) - O_\pm\rangle_{\rm 1PI} &= (c(t)-1)\langle O_\pm\rangle_{\rm 1PI} \\ &= (c(t)-1)Z_{O_\pm}\hat{O}_\pm \sim (c(t)-1)\hat{O}_\pm \end{aligned} \tag{4.67}$$

In the second line, we considered one loop perturbation theory and used the fact that $c(t) - 1$ is $O(g^2)$, because the tree level contributions of the flowed operator and the bare operator are same,

$$\begin{aligned} \langle O_\pm(t)\rangle_{\rm 1PI}|_{\rm tree} &= \hat{O}_\pm\ , \quad (\text{for } t \to 0), & (4.68)\\ \langle O_\pm\rangle_{\rm 1PI}|_{\rm tree} &= \hat{O}_\pm. & (4.69)\end{aligned}$$

Comparing (4.65) and (4.67) we obtain $c(t)$, therefore, the representation of the small flow time expansion,

$$O_\pm(t) \sim (1 + I_{\rm GF}(t))O_\pm + O(t)\ , \quad (\text{for } t \to 0). \tag{4.70}$$

When we define the renormalization of the flowed quark field $\chi(t,x)$ by

$$\mathring{\chi}(t,x) = \sqrt{\frac{-8N_f}{(4\pi)^2t^2\left\langle\overline{\chi}(t,x)\gamma_\mu\overleftrightarrow{D}_\mu\chi(t,x)\right\rangle}}\chi(t,x) := \varphi^{1/2}(t)\chi(t,x), \tag{4.71}$$

the relation between the gradient flow scheme and the $\overline{\rm MS}$ scheme are given as

$$\begin{aligned} \mathring{O}_\pm(t) &= (1 + I_{\rm GF}(t))\varphi^2(t)O_\pm \\ &= \frac{(1 + I_{\rm GF}(t))}{Z_{O_\pm}^{\overline{\rm MS}}}\left(\frac{\varphi(t)}{Z_\psi^{\overline{\rm MS}}}\right)^2 O_\pm^{\overline{\rm MS}}, \end{aligned} \tag{4.72}$$

where we define the ringed four fermion operator $\mathring{O}_\pm(t)$,

$$\mathring{O}_\pm = \left[\left(\mathring{\overline{\chi}}_1\gamma_\mu^L\mathring{\chi}_2\right)\left(\mathring{\overline{\chi}}_3\gamma_\mu^L\mathring{\chi}_4\right) \pm \left(\mathring{\overline{\chi}}_1\gamma_\mu^L\mathring{\chi}_4\right)\left(\mathring{\overline{\chi}}_3\gamma_\mu^L\mathring{\chi}_2\right)\right]. \tag{4.73}$$

The other factor, $Z_{O_\pm}^{\overline{\rm MS}}$ and $Z_\psi^{\overline{\rm MS}}$, mean renormalization factor for the four fermion operator $O_\pm$ and the renormalization factor of the quark field $\psi(x)$ in the $\overline{\rm MS}$ scheme.

Eq. (4.72) tells us a representation of the matching factor from the gradient flow to the $\overline{\rm MS}$,

$$Z_{O_\pm}^{{\rm GF}\to\overline{\rm MS}} = \frac{Z_{O_\pm}^{\overline{\rm MS}}}{(1+I_{\rm GF}(t))}\left(\frac{Z_\psi^{\overline{\rm MS}}}{\varphi(t)}\right)^2. \tag{4.74}$$

We have already calculated the renormalization factor $\varphi(t)$ at (4.63) in the dimensional reduction scheme. What we want to calculate are $Z_{O_\pm}^{\overline{\rm MS}}$, $Z_\psi^{\overline{\rm MS}}$ and $I_{\rm GF}(t)$. We postpone the calculation in the $\overline{\rm MS}$ scheme, we consider the coefficient of small flow time expansion $I_{\rm GF}(t)$ in this section.

Our starting point is the solution of flow equations of quantum field (4.10), (4.11) and (4.12). According to background field method, we can freely choose the background fields to a certain degree. It is emphasized that our calculation needs contributions from one loop and 1PI diagrams. Therefore, we can set the background gauge field to zero and the background quark field to be constant. They evolve along the flow equation of the background field (4.7), (4.8) and (4.9). The solution are

$$\hat{B}(t,x) = \hat{A}(x) = 0, \tag{4.75}$$

$$\hat{\chi}(t,x) = \hat{\psi}(x) = (\text{const.}), \tag{4.76}$$

$$\hat{\overline{\chi}}(t,x) = \hat{\overline{\psi}}(x) = (\text{const.}). \tag{4.77}$$

Let us review the formal solutions of flow equations discussed in the section 3.1.3,

$$b_\mu^a(t,x) = \int {\rm d}^D y\,\left\{K_t^{ab}(x,y)_{\mu\nu}a_\nu^b(y) + \int_0^t {\rm d}s\, K_{t-s}^{ab}(x,y)_{\mu\nu}\hat{R}_\nu^b(s,y)\right\}, \tag{4.78}$$

$$\begin{aligned} k(t,x) &= e^{t\hat{D}^2}p(x) \\ &\quad + \int_0^t {\rm d}s\, e^{(t-s)\hat{D}^2}\left\{2b_\mu(s,x)\hat{D}_\mu + b^2(s,x)\right\}\left\{e^{s\hat{D}^2}\hat{\psi}(x) + k(s,x)\right\}, \end{aligned} \tag{4.79}$$

$$\begin{aligned} \overline{k}(t,x) &= \overline{p}(x)e^{t\hat{\overline{D}}^2} \\ &\quad + \int_0^t {\rm d}s\left\{\hat{\overline{\psi}}(x)e^{s\hat{\overline{D}}^2} + \overline{k}(s,x)\right\}\left\{-2\hat{\overline{D}}_\mu b_\mu(s,x) + b^2(s,x)\right\}e^{(t-s)\hat{\overline{D}}^2}, \end{aligned} \tag{4.80}$$

where we define heat kernel $K_t^{ab}(x,y)_{\mu\nu}$,

$$
\begin{aligned}
K_t(x,y) &= e^{t\left\{\hat{\mathcal{D}}_x + 2\hat{\mathcal{F}}(x)\delta(x-y)\right\}}, && (4.81)\\
\hat{\mathcal{D}}_\mu^{ab} &= \delta^{ab}\partial_\mu + \hat{B}_\mu^c(t,x) f^{acb}, && (4.82)\\
\hat{\mathcal{F}}_{\mu\nu}^{ab}(x) &= \hat{F}_{\mu\nu}^c(x) f^{acb}, && (4.83)\\
\hat{R}_\mu^a(t,x) &= 2 f^{abc} b_\nu^b(t,x)\hat{\mathcal{D}}_\nu^{cd} b_\mu^d(t,x) - f^{abc} b_\nu^b(t,x)\hat{\mathcal{D}}_\mu^{cd} b_\nu^d(t,x) \\
&\qquad + f^{abc} f^{cde} b_\nu^b(t,x) b_\nu^d(t,x) b_\mu^e(t,x). && (4.84)
\end{aligned}
$$

Combining them with the solutions for the background fields, we obtain the propagator between $b(t,l)$ and $b(s,l)$ as

$$
G(t,s;l) \sim e^{-(t+s)l^2} G(l), \tag{4.85}
$$

where $G(l)$ means gluon propagator at zero flow time with l momentum,

$$
G(l) = g_0^2 \frac{1}{l^2} \delta^{ab}\delta_{\mu\nu}. \tag{4.86}
$$

The quantum quark fields k and $\overline{k}$ can be simplified as,

$$
\begin{aligned}
k(t,x) &\sim e^{t\partial^2} p(x) + \int_0^t \mathrm{d}s\, e^{(t-s)\partial^2} \left(b^2(s,x)\hat{\psi} + 2 b_\mu(s,x)\partial_\mu e^{s\partial^2} p(x) \right), && (4.87)\\
\overline{k}(t,x) &\sim \overline{p}(x)\, e^{t\overleftarrow{\partial^2}} + \int_0^t \mathrm{d}s\, \left(\hat{\overline{\psi}} b^2(s,x) - 2\overline{p}(x)\, e^{s\overleftarrow{\partial^2}} \overleftarrow{\partial}_\mu b_\mu(s,x) \right) e^{(t-s)\overleftarrow{\partial^2}}. && (4.88)
\end{aligned}
$$

It is enough to use these three results for the later calculation.

Our purpose of this section is a preliminary arrangement for the calculation of $\langle O_\pm(t) - O_\pm \rangle_{1\mathrm{PI}}$. We set the external momentum to zero for simplicity. With such conditions, it is enough to consider five types of diagrams to calculate the one loop corrections, and name the each diagram (a) to (e) as in Figure 27. We denote the heat kernel $e^{(t-s)\partial^2}$ as double solid line with vertex in white circle. We can denote the each diagrams as

$$
\begin{aligned}
(a) &: \int_0^t \mathrm{d}s \left(\gamma_\sigma^L \overline{\gamma}_\rho V_{1\mu}^a\right)_{12} \left(\gamma_\sigma^L \overline{\gamma}_\lambda V_{1\nu}^b\right)_{34} (-2l^2) e^{-2sl^2} S_{F\rho}(l) S_{F\lambda}(-l) G_{\mu\nu}^{ab}(l) \pm \{\text{Fierz}\}, && (4.89)\\
(b) &: \int_0^t \mathrm{d}s \left(V_{1\mu}^a \overline{\gamma}_\rho \gamma_\sigma^L\right)_{12} \left(\gamma_\sigma^L \overline{\gamma}_\lambda V_{1\nu}^b\right)_{34} (-2l^2) e^{-2sl^2} S_{F\rho}(l) S_{F\lambda}(l) G_{\mu\nu}^{ab}(l) \pm \{\text{Fierz}\}, && (4.90)\\
(c) &: \int_0^t \mathrm{d}s \left(V_{1\mu}^a \overline{\gamma}_\rho \gamma_\sigma^L \overline{\gamma}_\lambda V_{1\nu}^b\right)_{12} \left(\gamma_\sigma^L\right)_{34} (-2l^2) e^{-2sl^2} S_{F\rho}(l) S_{F\lambda}(l) G_{\mu\nu}^{ab}(l) \pm \{\text{Fierz}\}, && (4.91)\\
(d) &: 2\int_0^t \mathrm{d}s \left(\gamma_\sigma^L (-i) l_\mu T^a \overline{\gamma}_\nu V_{1\rho}^b\right)_{12} \left(\gamma_\sigma^L\right)_{34} e^{-sl^2} S_{F\nu}(l) G_{\mu\rho}^{ab}(s.0;l) \pm \{\text{Fierz}\}, && (4.92)\\
(e) &: \int_0^t \mathrm{d}s \left(\gamma_\sigma^L T^a T^b\right)_{12} \left(\gamma_\sigma^L\right)_{34} G_{\mu\mu}^{ab}(s,s;l) \pm \{\text{Fierz}\}, && (4.93)
\end{aligned}
$$

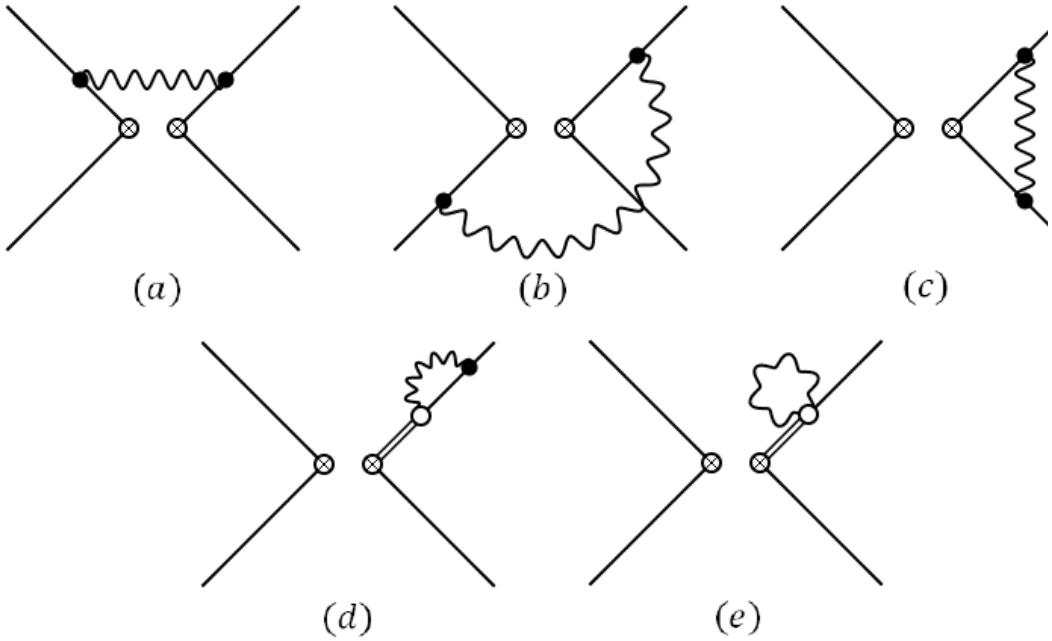

Figure 27: One loop and 1PI diagrams for zero external momentum.

where we abbreviate the quark propagator $S_{F\mu}(l)$, quark-gluon vertex $V^a_{1\mu}$ and fermion bi-linear term $(\Gamma)_{12}$ to

$$S_{F\mu}(l) = -i\frac{l_\mu}{l^2}, \tag{4.94}$$

$$V^a_{1\mu} = \gamma_\mu T^a, \tag{4.95}$$

$$(\Gamma)_{12} = \hat{\bar{\psi}}_1 \, \Gamma \, \hat{\psi}_2. \tag{4.96}$$

The symbol {Fierz} of each equations (4.89)-(4.93) means the Fierz partner of the original operator, for example

$$(\Gamma^A)_{12}(\Gamma^B)_{34} \pm \{\text{Fierz}\} := (\Gamma^A)_{12} \pm (\Gamma^B)_{34} \pm (\Gamma^A)_{14} \pm (\Gamma^B)_{32}. \tag{4.97}$$

Estimation of each diagram will be shown in the next sections.

4.1.4 Calculation of diagram c, d and e

In this section, we evaluate the diagram (c), (d) and (e). The calculation is almost same as of fermion bi-linear operators discussed in the section 3.2. As we discussed in the section 3.2.3, we must take care the order of the integrations. For example,

$$\int_0^t \mathrm{d}s \int_l \frac{1}{l^2} e^{-2sl^2} \neq \int_l \int_0^t \mathrm{d}s \, \frac{1}{l^2} e^{-2sl^2}. \tag{4.98}$$

The right hand side of (4.98) are ill-defined integration because the integrand has infrared divergence. If we introduce a regulator of the infrared divergence such as gluon mass, there is no need to care the order. More discussion is given in the section 3.2.3.

The biggest difference comes from $O(\epsilon)$ term called evanescent operator. Evanescent operator is a byproduct of the dimensional reduction scheme, and it must be removed from the calculation. The spinor factor of the diagram (c) is calculated as,

$$\left(\gamma_\mu \overline{\gamma}_\rho \gamma_\sigma^L \overline{\gamma}_\rho \gamma_\mu\right)_{12} \left(\gamma_\sigma^L\right)_{34} = 2D \left(\gamma_\sigma^L\right)_{12} \left(\gamma_\sigma^L\right)_{34} - 4 \left(\overline{\gamma}_\sigma^L\right)_{12} \left(\overline{\gamma}_\sigma^L\right)_{34}. \tag{4.99}$$

We can define the evanescent operator $\hat{E}$ by

$$\hat{E} := \left(\gamma_\sigma^L\right)_{12} \left(\gamma_\sigma^L\right)_{34} - \frac{4}{D} \left(\overline{\gamma}_\sigma^L\right)_{12} \left(\overline{\gamma}_\sigma^L\right)_{34}. \tag{4.100}$$

We can check that the evanescent operator $\hat{E}$ is $O(\epsilon)$. At first, we transform the evanescent operator,

$$\hat{E} = \left(\tilde{\gamma}_\sigma^L\right)_{12} \left(\tilde{\gamma}_\sigma^L\right)_{34} - \frac{\epsilon}{2} \left(\gamma_\sigma^L\right)_{12} \left(\gamma_\sigma^L\right)_{34} + O(\epsilon^2). \tag{4.101}$$

We defined that the remnant gamma matrix $\tilde{\gamma}_\mu$ live in the 2ϵ dimension. Therefore, we can consider that the first term is (ϵ). We choose the evanescent operator with (4.100), we can adopt another definition which vanishes in the limit of $\epsilon \to 0$.

Removing the evanescent operator, the spinor factor of the diagram (c) become

$$\left(\gamma_\mu \overline{\gamma}_\rho \gamma_\sigma^L \overline{\gamma}_\rho \gamma_\mu\right)_{12} \left(\gamma_\sigma^L\right)_{34} = D \left(\gamma_\sigma^L\right)_{12} \left(\gamma_\sigma^L\right)_{34}. \tag{4.102}$$

The integrations of the internal momentum are given by the formula,

$$\int \frac{\mathrm{d}^D l}{(2\pi)^D} \frac{1}{l^2} e^{-tl^2} = \frac{t^{1-D/2}}{(4\pi)^{D/2}} \frac{\Gamma(D/2-1)}{\Gamma(D/2)}, \tag{4.103}$$

where $\Gamma(\cdot)$ means the gamma function. Combing them all, we can evaluate (4.91)-(4.93),

$$(c) \quad : \quad \frac{N^2-1}{2N} \frac{-g_0^2}{(4\pi)^2} \left\{ \frac{1}{\epsilon} + \log(8\pi t) + 1 \right\} \hat{O}_\pm, \tag{4.104}$$

$$(d) \quad : \quad \frac{N^2-1}{2N} \frac{g_0^2}{(4\pi)^2} \left\{ \frac{1}{\epsilon} + \log(8\pi t) + 1 \right\} \hat{O}_\pm, \tag{4.105}$$

$$(e) \quad : \quad \frac{N^2-1}{2N} \frac{-2g_0^2}{(4\pi)^2} \left\{ \frac{1}{\epsilon} + \log(8\pi t) + 1 \right\} \hat{O}_\pm. \tag{4.106}$$

The above calculations are in essence same as of fermion bi-linear operator. Since we used the dimensional reduction scheme, the spinor factor causes a gap in $O(\epsilon)$. We rewrite such gap as the evanescent operator $\hat{E}$ defied in (4.100).

In the next section, we go forward to the calculation of the diagram (a) and (b) which are specific to the four fermion operators.

4.1.5 Calculation of diagram a and b

For the evaluation of (a) and (b), Fierz rearrangement make a significant contribution, since the spinor and the color indeces of (4.89) and (4.90) take a complicated structure. Calculation of the color factor is easier, because we know a formula,

$$T^a_{ij}T^a_{kl} = -\frac{1}{2}\delta_{il}\delta jk + \frac{1}{2N}\delta ijkl. \tag{4.107}$$

The spinor factor can be calculated using Fierz rearrangement (4.26) and the formulae of gamma matrix (4.44) and (4.45),

$$\begin{aligned}
(a): \left(\gamma^L_\sigma\overline{\gamma}_\rho\gamma_\mu\right)_{12}\left(\gamma^L_\sigma\overline{\gamma}_\rho\gamma_\mu\right)_{34} &= 4D\left(\gamma^L_\sigma\right)_{14}\left(\gamma^L_\sigma\right)_{32} \\
&= 4D\left(\gamma^L_\sigma\right)_{12}\left(\gamma^L_\sigma\right)_{34}, \qquad (4.108)\\
(b): \left(\gamma_\mu\overline{\gamma}_\rho\gamma^L_\sigma\right)_{12}\left(\gamma^L_\sigma\overline{\gamma}_\rho\gamma_\mu\right)_{34} &= 2D\left(\gamma^L_\sigma\right)_{14}\left(\gamma^L_\sigma\right)_{32} - 4\left(\overline{\gamma}^L_\sigma\right)_{14}\left(\overline{\gamma}^L_\sigma\right)_{32} \\
&= D\left(\gamma^L_\sigma\right)_{14}\left(\gamma^L_\sigma\right)_{32} = D\left(\gamma^L_\sigma\right)_{12}\left(\gamma^L_\sigma\right)_{34}. \qquad (4.109)
\end{aligned}$$

The evanescent operator is removed in the second line of equation (4.109). We use the same definition of $\hat{E}$ with (4.100).

We obtain the contributions of the diagram (a), (b),

$$(a) \quad : \quad \mp\frac{N\mp 1}{2N}\frac{-4g_0^2}{(4\pi)^2}\left\{\frac{1}{\epsilon} + \log(8\pi t) + 1\right\}\hat{O}_\pm, \tag{4.110}$$

$$(b) \quad : \quad \mp\frac{N\mp 1}{2N}\frac{g_0^2}{(4\pi)^2}\left\{\frac{1}{\epsilon} + \log(8\pi t) + 1\right\}\hat{O}_\pm. \tag{4.111}$$

Since the (a), (b), (c) type diagrams exist two and the (d), (e) type diagrams exist four, the coefficient of the small expansion method $I_{\rm GF}(t)$ is estimated as

$$I_{\rm GF} = -3\frac{N^2\mp N}{N}\frac{g^2}{(4\pi)^2}\left\{\frac{1}{\epsilon} + \log(8\pi\mu^2 t) + 1\right\}, \tag{4.112}$$

where we replace the bare gauge coupling g_0 by

$$g_0^2 = \mu^{2\epsilon}g^2. \tag{4.113}$$

In the calculation until now, we obtained the renormalization factor of the flowed quark field $\varphi(t)$ and the the coefficient of the small expansion method $I_{\rm GF}(t)$. The last pieces are renormalization factor for the four fermion operator $O_\pm$ and the renormalization factor of the quark field $\psi(x)$ in the $\overline{\rm MS}$ scheme.

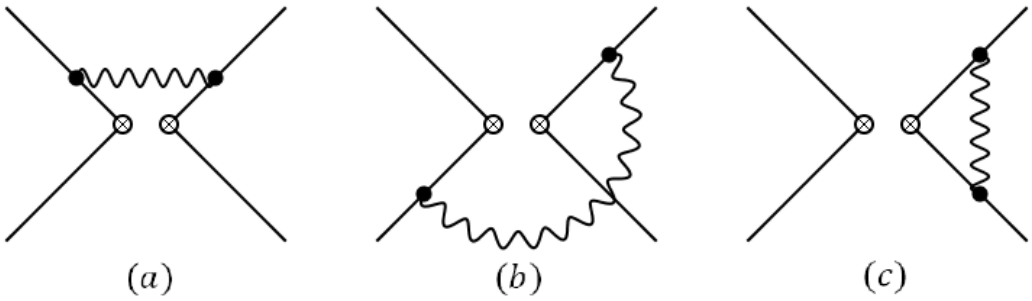

Figure 28: One loop and 1PI diagrams for zero external momentum.

4.1.6 Result in $\overline{\text{MS}}$ scheme

The remaining part of our calculation is $Z_{O_\pm}^{\overline{\text{MS}}}$ and $Z_\psi^{\overline{\text{MS}}}$. We will estimate them in this section.

To calculate the renormalization factor $Z_{O_\pm}^{\overline{\text{MS}}}$, we must consider the 1PI vertex corrections of O_{pm}. Diagrams what we need to evaluate for the calculation are the diagrams (a), (b), (c) in the Figure 28. The other diagrams do not emerge since they are peculiar for the calculation of the gradient flow. We again set the external momentum to zero for simplicity. However, we must also regularize the infrared divergence as same as previous calculation. We introduce a gluon mass λ and rewrite the propagator $G(l)$ as

$$G_{\mu\nu}^{ab}(l;\lambda) \quad = \quad g_0^2 \frac{1}{l^2+\lambda^2}\delta^{ab}\delta_{\mu\nu}. \tag{4.114}$$

Using this replacement, we can denote the contribution from each type of diagrams as

$$(a) \quad : \quad \left(\gamma_\mu^L \overline{\gamma}_\rho V_{1\mu}^a\right)_{12}\left(\gamma_\mu^L \overline{\gamma}_\lambda V_{1\nu}^b\right)_{34} S_{F\rho}(l) S_{F\lambda}(-l) G_{\mu\nu}^{ab}(l;\lambda) \pm \{\text{Fierz}\}\,, \tag{4.115}$$

$$(b) \quad : \quad \left(V_{1\mu}^a \overline{\gamma}_\rho \gamma_\mu^L\right)_{12}\left(\gamma_\mu^L \overline{\gamma}_\lambda V_{1\nu}^b\right)_{34} S_{F\rho}(l) S_{F\lambda}(l) G_{\mu\nu}^{ab}(l;\lambda) \pm \{\text{Fierz}\}\,, \tag{4.116}$$

$$(c) \quad : \quad \left(V_{1\mu}^a \overline{\gamma}_\rho \gamma_\mu^L \overline{\gamma}_\lambda V_{1\nu}^b\right)_{12}\left(\gamma_\mu^L\right)_{34} S_{F\rho}(l) S_{F\lambda}(l) G_{\mu\nu}^{ab}(l;\lambda) \pm \{\text{Fierz}\}\,. \tag{4.117}$$

Calculations for spinor factors and color factors can be done in the same way. We again use Fierz rearrangement and the dimensional reduction scheme, and the definition of the evanescent operator is same as (4.100). The difference comes from the integration of the internal momentum. The convenient formula is

$$\int \frac{\mathrm{d}^D l}{(2\pi)^D} \frac{1}{(l^2)^a (l^2+\lambda^2)} = \frac{1}{(4\pi)^{D/2}} \lambda^{D-2a-2} \frac{\Gamma(D/2-a)\Gamma(a+1-D/2)}{\Gamma(D/2)}. \tag{4.118}$$

After all, we obtain

$$(a) \quad : \quad \mp\frac{N\mp 1}{2N}\,\frac{4g_0^2}{(4\pi)^2}\left\{\frac{1}{\epsilon}-\gamma+\log\left(\frac{4\pi}{\lambda^2}\right)+1\right\}\hat{O}_{\pm}, \tag{4.119}$$

$$(b) \quad : \quad \mp\frac{N\mp 1}{2N}\,\frac{-g_0^2}{(4\pi)^2}\left\{\frac{1}{\epsilon}-\gamma+\log\left(\frac{4\pi}{\lambda^2}\right)+1\right\}\hat{O}_{\pm}, \tag{4.120}$$

$$(c) \quad : \quad \frac{N^2-1}{2N}\,\frac{g_0^2}{(4\pi)^2}\left\{\frac{1}{\epsilon}-\gamma+\log\left(\frac{4\pi}{\lambda^2}\right)+1\right\}\hat{O}_{\pm}, \tag{4.121}$$

and the one loop 1PI vertex corrections

$$\langle O_{\pm}\rangle_{1\mathrm{PI}} = \left[1+\frac{N^2\mp 3N+2}{N}\,\frac{g^2}{(4\pi)^2}\left\{\frac{1}{\epsilon}-\gamma+\log\left(\frac{4\pi\mu^2}{\lambda^2}\right)+1\right\}\right]\hat{O}_{\pm}. \tag{4.122}$$

The renormalization factor is extracted,

$$Z_{O_{\pm}}^{\overline{\mathrm{MS}}} = 1+\frac{N^2\mp 3N+2}{N}\,\frac{g^2}{(4\pi)^2}\left\{\frac{1}{\epsilon}-\gamma+\log(4\pi)+1\right\}. \tag{4.123}$$

Renormalization factor of the quark field is defined via the self energy,

$$\begin{aligned}\left\langle\psi(x)\overline{\psi}(y)\right\rangle &= \int_p \frac{1}{ip_\mu\overline{\gamma}_\mu+m}e^{-p\cdot(x-y)} \\ &- \frac{N^2-1}{2N}g_0^2\int_{p,q}\frac{1}{ip_\mu\overline{\gamma}_\mu+m}\gamma_\nu\frac{1}{iq_\mu\overline{\gamma}_\mu+m}\gamma_\nu\frac{1}{ip_\mu\overline{\gamma}_\mu+m}\,\frac{1}{(p-q)^2+\lambda^2}e^{ip\cdot(x-y)}.\end{aligned} \tag{4.124}$$

Integration of the internal momentum q can be performed as

$$\begin{aligned}&\int_q \gamma_\nu\frac{1}{iq_\mu\overline{\gamma}_\mu+m}\gamma_\nu\frac{1}{(p-q)^2+\lambda^2} \\ &= \int_q \frac{iq_\mu\overline{\gamma}_\mu+m}{q^2+m^2}\,\frac{1}{(p-q)^2+\lambda^2} \\ &= \frac{1}{(4\pi)^2}ip_\mu\overline{\gamma}_\mu\left\{\frac{1}{\epsilon}-\gamma+\log\left(\frac{4\pi}{\lambda^2}\right)+\frac{1}{2}\right\}+\frac{1}{(4\pi)^2}4m\left\{\frac{1}{\epsilon}-\gamma+\log\left(\frac{4\pi}{\lambda^2}\right)+1\right\}.\end{aligned} \tag{4.125}$$

Reading the renormalization factor of the quark field, we obtain

$$Z_{\psi}^{\overline{\mathrm{MS}}} = 1+\frac{N^2-1}{2N}\,\frac{g^2}{(4\pi)^2}\left\{\frac{1}{\epsilon}-\gamma+\log(4\pi)+\frac{1}{2}\right\}. \tag{4.126}$$

We have already seen the renormalization factor for the quark field in the $\overline{\mathrm{MS}}$ scheme in the section 3.2, however the result is changed only with finite value, because we are using the dimensional reduction scheme for the spinor factor.

4.1.7 Matching factor

We get all pieces which are required to calculate the matching factor in the previous sections. Before seeing the result, let us consider the ultraviolet divergence. We have faced many divergences $1/\epsilon$ in the calculation of 1PI vertex corrections of $\{O_\pm(t) - O_\pm\}$, such as (4.110), (4.111), (4.104), (4.105) and (4.106). These divergences can be classified into two types, derived from bare operator $O_\pm$ or derived from flowed field $O_\pm(t)$. Indeed, the divergence of (4.110), (4.111), (4.104) corresponds to the divergence of (4.119), (4.120), (4.121), because the diagrams (a), (b), (c) are composite combination and must be renormalized by the gradient flow. The other divergences relate to the renormalization of quark fields, and cared by $\varphi(t)$ and $Z_\psi^{\overline{\rm MS}}$. After all, the ultra violet divergence is removed and the matching factor of $O_\pm$ is given by

$$\begin{aligned} Z_{O_\pm}^{\mathrm{GF}\to\overline{\mathrm{MS}}} &= \frac{Z_{O_\pm}^{\overline{\mathrm{MS}}}}{(1+I_{\mathrm{GF}}(t))}\left(\frac{Z_\psi^{\overline{\mathrm{MS}}}}{\varphi(t)}\right)^2 \\ &= 1+\frac{g^2}{(4\pi)^2}\left\{-3\frac{\mp N+1}{N}\left(\log(8t\mu^2)+\gamma-\log 4+1\right)\right. \\ &\qquad \left. +\frac{N^2\mp 6N+5}{2N}+\frac{N^2-1}{N}\log 432\right\}. \end{aligned} \tag{4.127}$$

We can see that the finiteness of the gradient flow indirectly, since the matching factor (4.127) does not depend on $1/\epsilon$. In other words, the gradient flow scheme and the $\overline{\rm MS}$ is bounded by a finite gap.

We have calculated the matching factor throughout this section with some steps. At first, we considered the one loop and one particle irreducible vertex corrections of the combination $\{O_\pm(t)-O_\pm\}$ and obtained the representation of the small flow time expansion of the four fermion operator $O_\pm(t) = (1+I_{\mathrm{GF}})O_\pm$. The coefficient I_{GF} is defined via the $\langle O_\pm(t)-O_\pm\rangle_{1\mathrm{PI}}$. Combining with the renormalization factor of the flowed quark field $\varphi(t)$, the relation between bare operator $O_\pm$ and the ringed operator $\mathring{O}_\pm$ becomes obvious. When we consider another operator the difference should emerge in the representation of I_{GF}. In the next section, we will calculate it against $\Delta S = 1$ four fermion operator which is important for $K\to\pi\pi$ phenomenology.

Our perturbative calculation is justified by applying a renormalization group argument. As discussed in [120], we can replace the coupling constant g by the running coupling constant $\overline{g}(q)$ in (4.127). Moreover, we can set the scale $q = 1/\sqrt{8t}$, because the expression (4.127) does not depend on the scale q.

$$\begin{aligned} &Z_{O_\pm}^{\mathrm{GF}\to\overline{\mathrm{MS}}}\left(t,\overline{g}(1/\sqrt{8t})\right) \\ &\quad = 1+\frac{\overline{g}(1/\sqrt{8t})^2}{(4\pi)^2}\left\{-3\frac{\mp N+1}{N}\left(\gamma-\log 4+1\right)\right. \\ &\qquad \left. +\frac{N^2\mp 6N+5}{2N}+\frac{N^2-1}{N}\log 432\right\}. \end{aligned} \tag{4.128}$$

Since we adopted the small flow time expansion, the flow time must be restricted to small. Therefore, the running coupling constant $\overline{g}(1/\sqrt{8t})^2$ is also small because of the asymptotic freedom of QCD, and our expression of matching factor (4.128) goes to the perturbative region.

4.2 $\Delta S = 1$ Operator

In the previous section, we calculated the matching factor of the $\Delta S = 2$ four fermion operator. Our interesting can be expanded to the $\Delta S = 1$ four fermion operator, which is important to the kaon decay phenomenology. Lattice calculation of it is also suffering from the chiral symmetry breaking of Wilson fermion, and we can expect that the gradient flow is effective. We will calculate the matching factor of the $\Delta S = 1$ four fermion operator in this section.

The $\Delta S = 1$ four fermion operator has almost same form of the $\Delta S = 2$ four fermion operator. The definition is given by

$$O^{\Delta S=1} = \left(\overline{\psi}_s \gamma_\mu^L \psi_d\right)\left(\overline{\psi}_q \gamma_\mu^L \psi_q\right), \tag{4.129}$$

$$\gamma_\mu^L := \gamma_\mu \frac{(1-\gamma_5)}{2}, \tag{4.130}$$

where the subscript q means u, d, s flavor. It is also convenient to consider the operator

$$O_\pm = \left[\left(\overline{\psi}_1 \gamma_\mu^L \psi_2\right)\left(\overline{\psi}_3 \gamma_\mu^L \psi_4\right) \pm \left(\overline{\psi}_1 \gamma_\mu^L \psi_4\right)\left(\overline{\psi}_3 \gamma_\mu^L \psi_2\right)\right]. \tag{4.131}$$

When we consider the Feynman diagrams, we will recognize that the subscript q makes a new Wick contraction possible. Such new contribution is called as (QCD) penguin diagrams. We will discuss the internal momentum integration of the penguin diagrams.

4.2.1 Penguin diagram

We consider the Green function without the gradient flow. The flowed penguin diagrams are treated in the next section.

The Feynman diagrams are distributed in the Figure 29-31. The gluon exchange diagrams in the Figure 29 are same as the Figure 28. At the one loop perturbation theory, we can show that the contribution of them are same as previous ones. Therefore, we omit their estimation.

Let us consider the penguin diagram in the Figure 30. When we set the external momentum as p and denote the internal momentum as l, we can denote them as

$$\gamma_\sigma^L \overline{\gamma}_\rho V_{1\mu}^a \overline{\gamma}_\lambda \gamma_\sigma^L \otimes V_{1\nu}^b \, S_{F\rho}(l) S_{F\lambda}(l-p) G_{\mu\nu}^{ab}(p;\lambda), \tag{4.132}$$

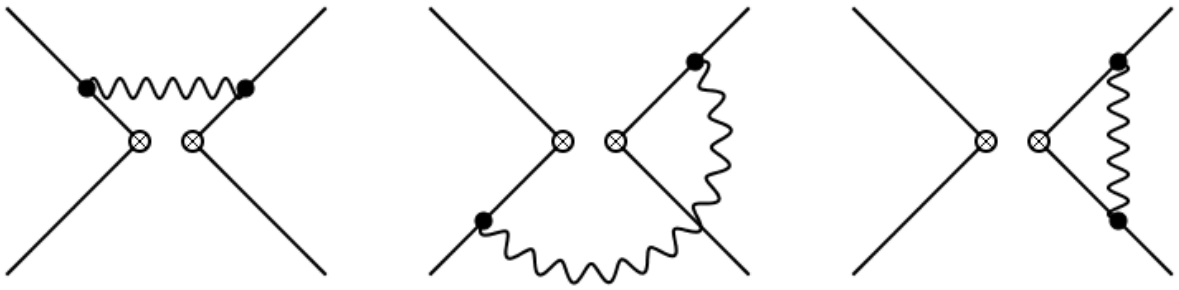

Figure 29: Gluon exchange diagrams.

with the notations,

$$S_{F\mu}(l) = -i\frac{l_\mu}{l^2}, \tag{4.133}$$

$$V^a_{1\mu} = \gamma_\mu T^a, \tag{4.134}$$

$$G^{ab}_{\mu\nu}(l;\lambda) = g_0^2 \frac{1}{l^2+\lambda^2}\,\delta^{ab}\delta_{\mu\nu}. \tag{4.135}$$

We took the massless limit of quarks and denote their propagator simply as $S_u = S_d = S_s \equiv S_F$. Since we also use the dimensional reduction scheme, only the gamma matrix accompanies to the internal momentum live at the $D = 4 - 2\epsilon$ dimensional space time. We denote such gamma matrix by $\overline{\gamma}_\mu$ as we did in the section 4.1.2.

The remaining contribution is disconnected diagrams described in the Figure 31. We can see that

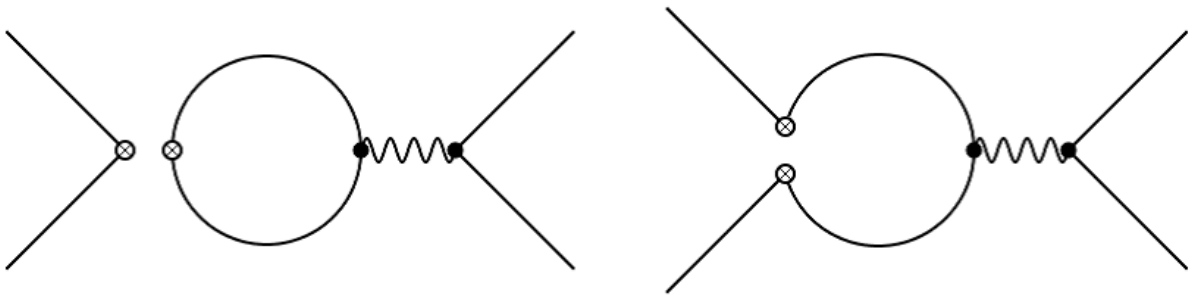

Figure 30: Penguin diagrams.

the disconnected diagram is proportional to the quark mass. Therefore, it will be vanished in the massless limit.

Let us evaluate the internal momentum integration of the penguin diagram (4.132),

$$I_{\mu\nu} = \int_l \frac{l_\mu - p_\mu}{(l-p)^2}\,\frac{l_\nu}{l^2}. \tag{4.136}$$

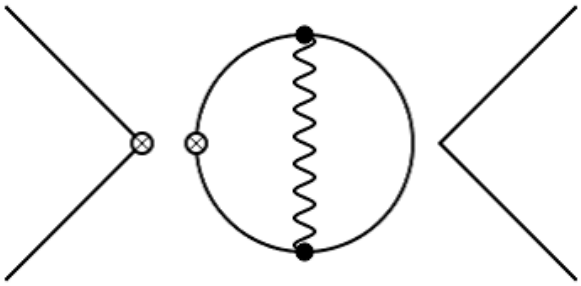

Figure 31: Disconnected diagram.

Using the Feynman parameter integral and completing the square, we get

$$\begin{aligned} I_{\mu\nu} &= \int_l \int_0^1 \mathrm{d}x \, \frac{(l_\mu - p_\mu) l_\nu}{\{x(l-p)^2 + (1-x)l^2\}^2} \\ &= \int_l \int_0^1 \mathrm{d}x \, \frac{(l_\mu - p_\mu) l_\nu}{\{(l-xp)^2 + x(1-x)p^2\}^2} \\ &= \int_l \int_0^1 \mathrm{d}x \, \frac{l_\mu l_\nu - x(1-x) p_\mu p_\nu}{\{l^2 + x(1-x)p^2\}^2}. \end{aligned} \tag{4.137}$$

We can use the useful formula,

$$\int_l \frac{\left(l^2\right)^a}{\left(l^2+\lambda^2\right)^b} = \frac{\left(\lambda^2\right)^{a-b+D/2}}{(4\pi)^{D/2}} \frac{\Gamma(a+D/2)\Gamma(b-a-D/2)}{\Gamma D/2 \Gamma(b)}, \tag{4.138}$$

and the $I_{\mu\nu}$ is

$$\begin{aligned} I_{\mu\nu} &= \frac{1}{(4\pi)^2} \int_0^1 \mathrm{d}x \, p^2 \frac{-g_{\mu\nu}}{2} x(1-x) \left\{ \frac{1}{\epsilon} - \gamma + \log\left(\frac{4\pi}{p^2}\right) - \log(x(1-x)) + 1 \right\} \\ &\quad + \frac{1}{(4\pi)^2} \int_0^1 \mathrm{d}x \, p_\mu p_\nu x(1-x) \left\{ \frac{1}{\epsilon} - \gamma + \log\left(\frac{4\pi}{p^2}\right) - \log(x(1-x)) \right\} \\ &= -\frac{1}{6} \frac{1}{(4\pi)^2} \frac{g_{\mu\nu}}{2} p^2 \left\{ \frac{1}{\epsilon} - \gamma + \log\left(\frac{4\pi}{p^2}\right) + \frac{8}{3} \right\} - \frac{1}{6} \frac{1}{(4\pi)^2} p_\mu p_\nu \left\{ \frac{1}{\epsilon} - \gamma + \log\left(\frac{4\pi}{p^2}\right) + \frac{5}{3} \right\}. \end{aligned} \tag{4.139}$$

We also calculate the flowed penguin diagram in the next section.

4.2.2 Flowed penguin diagram

According to the discussion of the section 4.1, the new calculation is concentrated on the I_{GF} which is defined via the flowed operator and the original operator, $\langle O_\pm(t) - O_\pm \rangle_{1\mathrm{PI}}$. The other calculation specific to the gradient flow, the renormalization factor of the quark field, have been calculated in

the section 4.1.2.

We emphasized that the pare $O_\pm(t) - O_\pm$ has no infrared divergence and rewrote the flowed kernel e^{-tl^2} as

$$e^{-tl^2} - 1 = -l^2 \int_0^t \mathrm{d}s\, e^{-sl^2}. \tag{4.140}$$

This replacement was effective, because we set the external momentum to zero in the previous computation. In the meaning of it, we can separate the pair at this time, because our calculation here has nonzero external momentum p. Moreover, the flowed penguin diagram can be considered as a composite type diagram at the one loop calculation. Therefore, we can take the $\epsilon \to 0$ limit in the calculation of it.

We start from the flowed disconnected diagrams shown in the Figure 32. We can show that the flowed disconnected diagrams are proportional to the quark mass, therefore, contributions of them are also vanished in the massless limit.

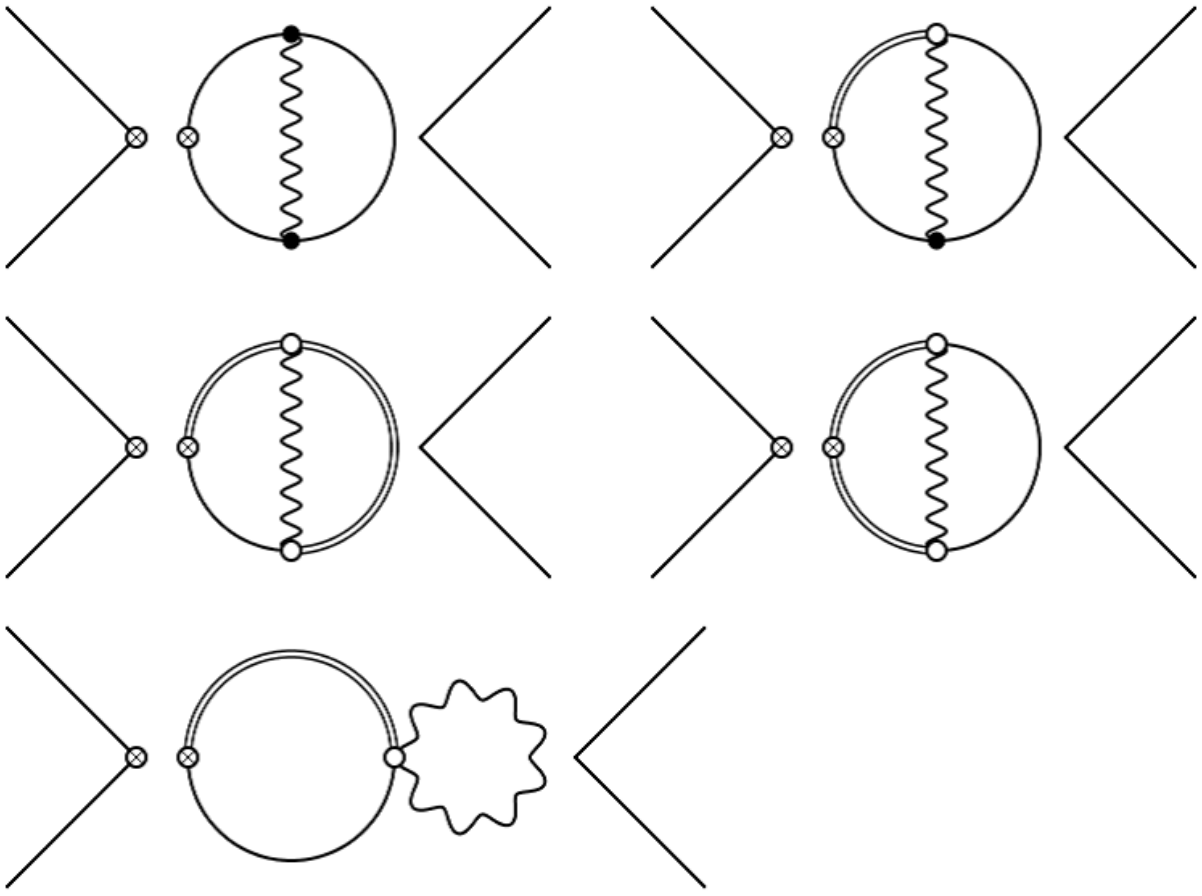

Figure 32: Disconnected diagrams with gradient flow.

When we consider the flow time evolution of the penguin diagram there are two types of the flowed diagrams described in the Figure 33. The left diagram has the same shape with the original one, however, the flow kernel is accompanied to the solid line.

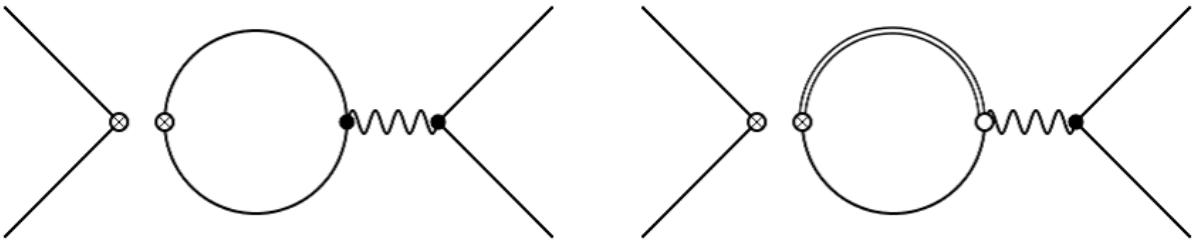

Figure 33: Flowed penguin diagram.

Contributions from the left diagram is written as

$$\gamma_\sigma^L \overline{\gamma}_\rho V_{1\mu}^a \overline{\gamma}_\lambda \gamma_\sigma^L \otimes V_{1\nu}^b \, S_{F\rho}(l) S_{F\lambda}(l-p) e^{-t(l-p)^2} e^{-tl^2} G_{\mu\nu}^{ab}(p;\lambda). \tag{4.141}$$

The internal momentum integration is denoted by

$$I_{\mu\nu}(t) = \int_l \frac{l_\mu - p_\mu}{(l-p)^2} \frac{l_\nu}{l^2} e^{-t(l-p)^2} e^{-tl^2}. \tag{4.142}$$

As we mentioned, we estimate the integral without subtraction of the original operator.[16] Moreover, we can take $\epsilon \to 0$ limit, because, the penguin diagrams are composite combination of the contraction. Indeed, the internal momentum integration $I_{\mu\nu}(t)$ can be performed free from the ultra violet divergence as follows. At first, we put the denominator on the shoulder of the exponential,

$$\begin{aligned} I_{\mu\nu}(t) &= \int_l \int_0^\infty \mathrm{d}\alpha \int_0^\infty \mathrm{d}\beta (l_\mu - p_\mu) l_\nu e^{-(t+\alpha)(l-p)^2} e^{-(t+\beta)l^2} \\ &= \int_l \int_t^\infty \mathrm{d}\alpha \int_t^\infty \mathrm{d}\beta (l_\mu - p_\mu) l_\nu e^{-\alpha(l-p)^2} e^{-\beta l^2}. \end{aligned} \tag{4.143}$$

Using complete the squared,

$$\alpha(l-p)^2 + \beta l^2 = (\alpha+\beta)\left(l - \frac{\alpha}{\alpha+\beta}p\right)^2 + \frac{\alpha\beta}{\alpha+\beta}p^2, \tag{4.144}$$

the integration of the internal momentum l can be performed,

$$\begin{aligned} I_{\mu\nu}(t) &= \int_l \int_t^\infty \mathrm{d}\alpha \int_t^\infty \mathrm{d}\beta \left(l_\mu l_\nu - \frac{\alpha\beta}{\alpha+\beta} p_\mu p_\nu\right) e^{-(\alpha+\beta)l^2} e^{-\frac{\alpha\beta}{\alpha+\beta}p^2} \\ &= \int_t^\infty \mathrm{d}\alpha \int_t^\infty \mathrm{d}\beta \left\{ \frac{1}{2} g_{\mu\nu} \frac{1}{(\alpha+\beta)^3} - p_\mu p_\nu \frac{\alpha\beta}{(\alpha+\beta)^3} \right\} e^{-\frac{\alpha\beta}{\alpha+\beta}p^2}, \end{aligned} \tag{4.145}$$

[16] It is very difficult to evaluate the difference $I_{\mu\nu}(t) - I_{\mu\nu}$ in the $4-2\epsilon$ dimensional space time. We decide to evaluate $I_{\mu\nu}(t)$ in the $D=4$ dimension and $I_{\mu\nu}$ in $D = 4-2\epsilon$ dimension. In the $D = 4-2\epsilon$ dimension, the integrand of (4.147) takes more complicated structure. Such operation is justified by the general property of the gradient flow.

where we used the formula

$$\int_l \left(l^2\right)^a \; e^{-tl^2} = \frac{t^{-2-a}}{(4\pi)^2}\frac{\Gamma(2+a)}{\Gamma(2)}, \quad \text{for } a > -2 \text{ and } \quad D = 4. \tag{4.146}$$

In the second line of (4.145), we can replace $\alpha\beta/(\alpha+\beta)$ by $\partial/\partial p^2$ as

$$I_{\mu\nu}(t) \;=\; \int_t^\infty \mathrm{d}\alpha \int_t^\infty \mathrm{d}\beta \left\{ \frac{1}{2} g_{\mu\nu} \frac{1}{(\alpha+\beta)^3} + p_\mu p_\nu \frac{1}{(\alpha+\beta)^2} \frac{\partial}{\partial p^2} \right\} e^{-\frac{\alpha\beta}{\alpha+\beta}p^2}. \tag{4.147}$$

Performing the integration of β for the first term, we obtain

$$\begin{aligned} I_1 &= \int_t^\infty \mathrm{d}\alpha \int_t^\infty \mathrm{d}\beta \frac{1}{(\alpha+\beta)^3} e^{-\frac{\alpha\beta}{\alpha+\beta}p^2} \\ &= \int_t^\infty \mathrm{d}\alpha \left\{ \frac{1}{p^2} \frac{1}{\alpha^2(\alpha+t)} e^{-\frac{\alpha t}{\alpha+t}p^2} + \frac{1}{(p^2)^2} \frac{1}{\alpha^4} e^{-\frac{\alpha t}{\alpha+t}p^2} - \frac{1}{(p^2)^2} \frac{1}{\alpha^4} e^{-\alpha p^2} \right\}. \end{aligned} \tag{4.148}$$

When we make the substitution $\tau \equiv \alpha t/(\alpha+t)$ we get

$$\begin{aligned} I_1 &= -\frac{1}{(p^2)^2} \int_t^\infty \mathrm{d}\alpha \, \frac{1}{\alpha^4} e^{-\alpha p^2} + \frac{1}{p^2} \int_{t/2}^t \mathrm{d}\tau \, \frac{t-\tau}{t^2\tau^2} e^{-\tau p^2} - \frac{1}{(p^2)^2} \int_{t/2}^t \mathrm{d}\tau \, \frac{(t-\tau)^2}{t^2\tau^4} e^{-\tau p^2} \\ &= -\frac{1}{t^3(p^2)^2} \int_1^\infty \mathrm{d}x \, \frac{1}{x^4} e^{-tp^2 x} + \frac{1}{t^2 p^2} \int_{1/2}^1 \mathrm{d}x \, \frac{1-x}{x^2} e^{-tp^2 x} - \frac{1}{t^3(p^2)^2} \int_{1/2}^1 \mathrm{d}x \, \frac{(1-x)^2}{x^4} e^{-tp^2 x}. \end{aligned} \tag{4.149}$$

Since we are applying the small flow time expansion, we need a power series with respect to the flow time. We can recognize that I_1 is constructed from the $n-$th order exponential integral,

$$E_n(z) \equiv \int_1^\infty \mathrm{d}x \, \frac{1}{x^n} e^{-zx}. \tag{4.150}$$

Its alternating series are

$$E_1(z) \;=\; -\gamma - \log(z) + \sum_{k=1}^\infty \frac{(-1)^{k+1} z^k}{k \, k!}, \tag{4.151}$$

$$E_n(z) \;=\; \frac{1}{n} e^{-z} - \frac{z}{n} E_{n-1}(z). \tag{4.152}$$

Using them all, we obtain

$$\begin{aligned} I_1 &= \frac{1}{t^3(p^2)^2} \left(-2E_3(tp^2) + E_2(tp^2) \right) - \frac{1}{8t^3(p^2)^2} \left(E_4(2tp^2) - 4E_3(2tp^2) + 4E_2(2tp^2) \right) \\ &\quad - \frac{1}{t^2 p^2} \left(E_2(tp^2) - E_1(tp^2) \right) + \frac{1}{2t^2 p^2} \left(E_2(2tp^2) - 2E_1(2tp^2) \right) \\ &= \frac{p^2}{6} \left(\frac{3}{2tp^2} + \log(2tp^2) + \gamma - \frac{25}{12} \right) + O(t). \end{aligned} \tag{4.153}$$

With the almost same calculation, the second term of (4.147) and we finally obtain

$$\begin{aligned} I_{\mu\nu}(t) &= -\frac{1}{6}\frac{1}{(4\pi)^2}\frac{g_{\mu\nu}}{2}p^2\left\{-\frac{3}{2tp^2}-\gamma-\log\left(2tp^2\right)+\frac{25}{12}\right\} \\ &\quad -\frac{1}{6}\frac{1}{(4\pi)^2}p_\mu p_\nu\left\{-\gamma+\log\left(\frac{4\pi}{p^2}\right)+\frac{13}{12}\right\}. \end{aligned} \tag{4.154}$$

It is no wonder that $1/t$ is appearing in the result, because the right diagrams in the Figure 33 cancels such term. Contributions from it are written as

$$2\int_0^t \mathrm{d}s\ \gamma_\sigma^L\overline{\gamma}_\rho T^a\gamma_\sigma^L\otimes V_{1\nu}^b\ (-il_\mu)S_{F\rho}(l)e^{-(t-s)(p+l)^2}e^{-sl^2}e^{-tl^2}e^{-sp^2}G_{\mu\nu}^{ab}(p;\lambda). \tag{4.155}$$

The integration of the internal momentum l is

$$I_{\mu\nu}(t)=\int_0^t \mathrm{d}s\ \int_l \frac{l_\mu l_\nu}{l^2}e^{-(t-s)(p+l)^2}e^{-sl^2}e^{-tl^2}e^{-sp^2}. \tag{4.156}$$

Computational procedure is almost same as previous one,

$$\begin{aligned} I_{\mu\nu}(t) &= \int_0^t \mathrm{d}s\ \int_0^\infty \mathrm{d}\alpha\ \int_l l_\mu l_\nu e^{-(t-s)(p+l)^2}e^{-sl^2}e^{-(t+\alpha)l^2}e^{-sp^2} \\ &= \int_0^t \mathrm{d}s\ \int_0^\infty \mathrm{d}\alpha\ \int_l l_\mu l_\nu e^{-(2t+\alpha)\left(l+\frac{t-s}{2t+\alpha}p\right)^2-tp^2+\frac{(t-s)^2}{2t+\alpha}p^2} \\ &= \int_0^t \mathrm{d}s\ \int_0^\infty \mathrm{d}\alpha\ \int_l \left\{l_\mu l_\nu+\frac{(t-s)^2}{(2t+\alpha)^2}p_\mu p_\nu\right\}e^{-(2t+\alpha)l^2}e^{-tp^2}e^{\frac{(t-s)^2}{2t+\alpha}p^2} \\ &= \int_0^t \mathrm{d}s\ \int_{2t}^\infty \mathrm{d}\alpha\ \int_l \left\{l_\mu l_\nu+\frac{s^2}{\alpha^2}p_\mu p_\nu\right\}e^{-\alpha l^2}e^{-tp^2}e^{\frac{s^2}{\alpha}p^2} \\ &= \int_0^t \mathrm{d}s\ \int_{2t}^\infty \mathrm{d}\alpha\ \left\{\frac{1}{2}\frac{1}{\alpha^3}l_\mu l_\nu+\frac{s^2}{\alpha^4}p_\mu p_\nu\right\}e^{-tp^2}e^{\frac{s^2}{\alpha}p^2}. \end{aligned} \tag{4.157}$$

Replacing s^2/α by $\partial/\partial p^2$,

$$I_{\mu\nu}(t) = \int_0^t \mathrm{d}s\ \int_{2t}^\infty \mathrm{d}\alpha\ e^{-tp^2}\left\{\frac{1}{2}l_\mu l_\nu\frac{1}{\alpha^3}+\frac{1}{\alpha^3}p_\mu p_\nu\frac{\partial}{\partial p^2}\right\}e^{\frac{s^2}{\alpha}p^2}. \tag{4.158}$$

After performing the integration for α, we apply expand the exponential with respect to s,

$$\begin{aligned} I_2 &= \int_{2t}^\infty \mathrm{d}\alpha\ \frac{1}{\alpha^3}e^{\frac{s^2}{\alpha}p^2} \\ &= \frac{1}{s^4(p^2)^2}\left\{1-\left(1-\frac{s^2}{2t}p^2\right)e^{\frac{s^2}{2t}p^2}\right\} \\ &= -\frac{1}{8t^2}-\frac{s^2p^2}{24t^3}+\cdots. \end{aligned} \tag{4.159}$$

Therefore, the integration of the right diagram is

$$I_{\mu\nu}(t) = -\frac{1}{6}\frac{1}{(4\pi)^2}\frac{g_{\mu\nu}}{2}p^2\left(\frac{3}{4tp^2}-\frac{2}{3}\right)-\frac{1}{6}\frac{1}{(4\pi)^2}p_\mu p_\nu\left(-\frac{1}{12}\right). \tag{4.160}$$

Let us finally the $1/t$ term in (4.154) is canceled out by the $1/t$ term in (4.154). Since such terms are proportional to $g_{\mu\nu}$ the spinor factor of (4.141) can be written

$$\begin{aligned}
&\gamma_\sigma^L \overline{\gamma}_\rho V_{1\mu}^a \overline{\gamma}_\lambda \gamma_\sigma^L \otimes V_{1\nu}^b \, g_{\rho\lambda} G_{\mu\nu}^{ab}(p;\lambda) \\
&\quad = \gamma_\sigma^L \gamma_\rho V_{1\mu}^a \gamma_\lambda \gamma_\sigma^L \otimes V_{1\nu}^b \, g_{\rho\lambda} G_{\mu\nu}^{ab}(p;\lambda) \\
&\quad = -2\gamma_\sigma^L \gamma_\mu T^a \gamma_\sigma^L \otimes V_{1\nu}^b \, G_{\mu\nu}^{ab}(p;\lambda) \\
&\quad = -2\gamma_\sigma^L \gamma_\rho T^a \gamma_\sigma^L \otimes V_{1\nu}^b \, g_{\mu\rho} G_{\mu\nu}^{ab}(p;\lambda). \qquad (4.161)
\end{aligned}$$

This spinor factor is same as (4.155). Including the symmetric factor 2 the (4.160), the $1/t$ is just canceled out.

5 Summary and Outlook

In the elementary particle physics, the CP violation has an important meaning involved with new physics. The missions of the lattice QCD are giving the first principle calculation of quantities. Especially for the kaon bag parameter, since it indicates the QCD corrections of the $K^0 - \overline{K^0}$ mixing the expectation of the lattice QCD is great. Unfortunately, the $\Delta S = 2$ four fermion operator involves with the chiral symmetry, and is incompatible with the naive Wilson fermions.

The purpose of this study is preparations towards calculations of the kaon bag parameter with the gradient flow. In particular, we performed two preparations in the thesis. One is the calculation of the PCAC mass for a numerical practice. One is perturbative evaluation of the $\Delta S = 2$ four fermion operator. These studies have the meaning as follows.

As we mentioned, the $\Delta S = 2$ four fermion operator causes the operator mixing and the origin is the chiral symmetry breaking of the Wilson fermion. Similarly, the PCAC relation needs an additive renormalization, since it is defined via the PCAC relation. Our numerical results in the section 3.5 use only the gradient flow instead of the additive renormalization. Nevertheless, the both sides of the PCAC relation have good agreement with each other as in Figure 22, and the PCAC mass is consistent with the one calculated in the Schrödinger functional scheme. Although there is a problem related to the linear window, the gradient flow method is reasonable for calculations of the PCAC mass. Note that we simply apply the gradient flow without the other special techniques and the renormalization is automatically done. It implies that the gradient flow removes the details of the lattice fermion and make it possible to take a continuum limit with no concern from the renormalization. We can also expect that the gradient flow can be applied to the operator mixing, in other words, the kaon bag parameter. However, we must take care of the linear window discussed in the section 3.3.3. We should research the fit range dependence and fitting function dependence of the operator, and include it as a systematic error of the results. There is also possibility that such analyses make the error large. It is the future work of our study.

We should calculate the matching factor which gives the conversion factor to the $\overline{\text{MS}}$ scheme to define the $\overline{\text{MS}}$ operator via the gradient flow. In numerical studies of the section 3, we used the previously calculated matching factors of the fermion bi-linear operators. However, we must construct it for four fermion operators. To calculate them, we used the small flow time expansion combining with the background field method in the section 4.1. Our result is (4.127) with the dimensional reduction scheme. In addition to the $\Delta S = 2$ four fermion operator, we discussed about the $\Delta S = 1$ four fermion operator in the section 4.2. According to the general considerations of the small flow time expansion, it is enough to see the one particle irreducible vertex of the difference between the bare operator and the flowed operator. We evaluated the internal momentum integration as (4.154) and (4.160). Of cause, the numerical studies of them are our future works.

Acknowledgments

I would like to show my greatest appreciation to Prof. Y. Taniguchi for the great supervision. I am also grateful to the all members of WHOT-QCD Collaboration for helpful discussions. Finally, I would like to thank Dr. T. Matsumoto for the long office times with me.

This work was in part supported by JSPS KAKENHIGrant Numbers JP18K03607, JP17K05442, JP16H03982, JP15K05041, JP26400251, JP26400244, and JP26287040. This research used computational resources of COMA and Oakforest-PACS provided by the Interdisciplinary Computational Science Program of Center for Computational Sciences, University of Tsukuba, Oakforest-PACS at JCAHPC through the HPCI System Research Project (Project ID:hp17208), OCTOPUS at Cybermedia Center, Osaka University, and ITO at R.I.I.T., Kyushu University. The simulations were in part based on Lattice QCD common code Bridge++ [127].

References

[1] F. Englert and R. Brout, Phys. Rev. Lett. 13 (1964) 321.

[2] P. W. Higgs, Broken symmetries, Phys. Lett. 12 (1964) 132.

[3] S. L. Glashow, Nucl. Phys. 22 (1961) 579.

[4] S. Weinberg, Phys. Rev. Lett. 19 (1967) 1264.

[5] A. Salam, Originally printed in *Svartholm: Elementary Particle Theory, Proceedings of the Nobel Symposioum Held 1968 at Lerum, Sweden*, Stockholm 1968, 367-377.

[6] S. L. Glashow, J. Iliopoulos and L. Maiani, Phys. Rev. D 2 (1970) 1285.

[7] O. W. Greenberg, Phys. Rev. Lett. 13 (1964) 598.

[8] M. Y. Han and Y. Nambu, Phys. Rev. 139 (1965) B1006.

[9] H. Fritzsch, M. Gell-Mann and H. Leutwyler, Phys. Lett. B 47 (1973) 365.

[10] ATLAS Collaboration, Phys.Lett. B716 1-29 [1207.7214[hep-ex]].

[11] CMS Collaboration, Phys.Lett. B716 30-61 [arXiv:1207.7235[hep-ex]].

[12] J.H.Christenson,J.W.Cronin, V.L.Fitch, and R.Turlay, Phys. Rev. Lett.13,138 (1964).

[13] A. Alavi-Harati et al., (KTeV Collaboration), Phys. Rev. Lett. 83, 917 (1999).

[14] N. Cabibbo, Phys. Rev. Lett. 10 (1963) 531.

[15] M. Kobayashi and T. Maskawa, Prog. Theor. Phys.49, 652 (1973).

[16] K. Hagiwara et al. [Particle Data Group Collaboration], Phys. Rev. D 66 (2002) 010001.

[17] L. Wolfenstein, Phys. Rev. Lett. 51, 1945 (1983).

[18] A. J. Buras, M. Jamin and P. H. Weisz, Nucl. Phys. B 347 (1990) 491.

[19] J. Urban, F. Krauss, U. Jentschura and G. Soff, Nucl. Phys. B 523 (1998) 40 [arXiv:hep-ph/9710245].

[20] K. G. Wilson, Phys. Rev. D10 (1974) 2445-2459.

[21] M. Creutz, Phys. Rev. Lett 45 (1980) 313-316 .

[22] M. Creutz, Phys. Rev. D 21, 2308-2315 (1980).

[23] L.H. Karsten, Phys. Lett. B104 (1981) 315-319.

[24] P. H. Ginsparg and K. G. Wilson, Phys. Rev. D 25, 2649-2657 (1982).

[25] M. Bochicchio, L. Maiani, G. Martinelli, G. Rossi and M. Testa , Nucl. Phys. B262 (1985) 331.

[26] H. B. Nielsen and M. Ninomiya, Phys. Lett. B105 219 (1981).

[27] D. Friedan, Commun. Math. Phys. 85 481 (1982).

[28] C. Itzykson and J.-M. Drouffe, Cambridge Monographs on Mathematical Physics, Vol. 1 (1989).

[29] J. Kogut and L. Susskind, Phys. Rev. D 11, 395 (1975).

[30] P. H. Ginsparg and K. G. Wilson, Phys. Rev. D25 (1982) 2649.

[31] D. B. Kaplan, Phys. Lett. B288 (1992) 342 [hep-lat/9206013].

[32] R. Narayanan and H. Neuberger, Nucl. Phys. B412, 574-606 (1994) [hep-lat/9307006].

[33] R. Narayanan and H. Neuberger, JHEP 0603, 064 (2006) [hep-th/0601210].

[34] M. Lüscher, JHEP 1304, 123 (2013) [arXiv:1302.5246 [hep-lat]].

[35] M. Lüscher, Commun. Math. Phys. 293, 899 (2010) [arXiv:0907.5491[hep-lat]].

[36] M. Lüscher, JHEP 1008, 071 (2010) Erratum: [JHEP 1403, 092 (2014)] [arXiv:1006.4518 [hep-lat]].

[37] M. Lüscher and P. Weisz, JHEP 1102, 051 (2011) [arXiv:1101.0963[hep-th]].

[38] M. Lüscher, Proc. Sci. LATTICE 2013, 016 (2014) [arXiv:1308.5598 [hep-lat]].

[39] H. Suzuki, PTEP 2013, no. 8, 083B03 (2013) [arXiv:1304.0533 [hep-lat]].

[40] S. Borsanyi, S. Durr, Z. Fodor, C. Hoelbling, S. D. Katz, S. Krieg, T. Kurth, L. Lellouch, T. Lippert, C. McNeile and K. K. Szabo, JHEP 1209 (2012) 010 [arXiv:1203.4469[haep-lat]].

[41] H. Makino and H. Suzuki, Progr. Theor. Exp. Phys. 2014, 063B02 (2014) Erratum: [Progr. Theor. Exp. Phys. 2015, 079202 (2015)] [arXiv:1403.4772 [hep-lat]].

[42] H. Makino, H. Suzuki, [arXiv: 1404.2758 [hep-lat]].

[43] MILC Collaboration: A. Bazavov, C. Bernard, N. Brown, C. DeTar, J. Foley, Steven Gottlieb, U.M. Heller, J. Komijani, J. Laiho, L. Levkova, R.L. Sugar, D. Toussaint and R.S. Van de Water, Phys. Rev. D 93, 094510 (2016) [arXiv:1503.02769[hep-lat]].

[44] FlowQCD Collaboration: M. Asakawa, T. Hatsuda, E. Itou, M. Kitazawa, H. Suzuki, Phys.Rev. D90 (2014) no.1, 011501 [Erratum: Phys.Rev. D92 (2015) no.5, 059902] [arXiv:1312.7492 [hep-lat]].

[45] M. Kitazawa, M. Asakawa, T. Hatsuda, T. Iritani, E. Itou and H. Suzuki, PoS LATTICE 2015, 162 (2016) [arXiv:1511.05235 [hep-lat]].

[46] V. G. Bornyakov, R. Horsley, R. Hudspith, Y. Nakamura, H. Perlt, D. Pleiter, P. E. L. Rakow, G. Schierholz, A. Schiller, H. Stüben and J. M. Zanotti, PoS LATTICE 2015 (2016) 264 [arXiv:1512.05745 [hep-lat]].

[47] F. Capponi, L. Del Debbio, A. Patella and A. Rago, PoS LATTICE 2015, 302 (2016) [arXiv:1512.04374[hep-lat]].

[48] Y. Taniguchi, S. Ejiri, R. Iwami, K. Kanaya, M. Kitazawa, H. Suzuki, T. Umeda and N. Wakabayashi, Phys. Rev. D 96, 014509 (2017) [arXiv:1609.01417[hep-lat]].

[49] Y. Taniguchi, K. Kanaya, H. Suzuki and T. Umeda, Phys. Rev. D 95, 054502 (2017) [arXiv:1611.02411[hep-lat]].

[50] M. Kitazawa, T. Iritani, M. Asakawa and Tetsuo Hatsuda, Phys. Rev. D 96, 111502 (2017) [arXiv:1708.01415[hep-lat]].

[51] R. Yanagihara, T. Iritani, M. Kitazawa, M. Asakawa and T. Hatsuda, Phys. Lett. B 789 (2019) 210-214 [arXiv:1803.05656[hep-lat]].

[52] K. Kanaya, S. Ejiri, R. Iwami, M. Kitazawa, H. Suzuki, Y. Taniguchi, T. Umeda and N. Wakabayashi, PoS LATTICE 2016, 063 (2017) [arXiv:1610.09518[hep-lat]].

[53] K. Kanaya, S. Ejiri, R. Iwami, M. Kitazawa, H. Suzuki, Y. Taniguchi and T. Umeda, EPJ Web of Conferences 175, 07023 (2018) [arXiv:1710.10015[hep-lat]].

[54] Y. Taniguchi, S. Ejiri, K. Kanaya, M. Kitazawa, A. Suzuki, H. Suzuki and T. Umeda, EPJ Web of Conferences 175, 07013 (2018) [arXiv:1711.02262[hep-lat]].

[55] M. Shirogane, S. Ejiri, R. Iwami, K. Kanaya, M. Kitazawa, H. Suzuki, Y. Taniguchi and T. Umeda, PoS LATTICE2018 164 (2019) [arXiv:1811.04220[hep-lat]].

[56] Y. Taniguchi, A. Baba, S. Ejiri, K. Kanaya, M. Kitazawa, T. Shimojo, A. Suzuki, H. Suzuki and T. Umeda, PoS LATTICE2018 166 (2019) [arXiv:1901.01666[hep-lat]].

[57] A. Baba, S. Ejiri, K. Kanaya, M. Kitazawa, T. Shimojo, A. Suzuki, H. Suzuki, Y. Taniguchi and T. Umeda, PoS LATTICE2018 173 (2019) [arXiv:1901.02294[hep-lat]].

[58] R. V. Harlander, Y. Kluth and F. Lange, Eur. Phys. J. C (2018) 78: 944 [arXiv:1808.09837[hep-lat]].

[59] K. Hieda, H. Makino and H. Suzuki, Nucl. Phys. B 918 (2017) 23-51 [arXiv:1604.06200 [hep-lat]].

[60] K. Kikuchi and T. Onogi, JHEP11(2014)094 [arXiv:1408.2185[hep-th]].

[61] D. Kadoh and N. Ukita, [arXiv:1812.02351[hep-th]].

[62] H. Makino and H. Suzuki, PTEP 2015, Issue 3, 033B08 (2015) [arXiv:1410.7538[hep-lat]].

[63] G. 't Hooft, In *Karpacz 1975, Proceedings, Acta Universitatis Wratislaviensis No.368, Vol.1*, Wroclaw 1976, 345-369.

[64] B. S. DeWitt, In *Oxford 1980, Proceedings, Quantum Gravity 2*, 449-487 and Calif. Univ. Santa Barbara - NSF-ITP-80-031 (80,REC.AUG.) 54 P. (009106) (SEE CONFERENCE INDEX)

[65] D. G. Boulware, Phys. Rev. D 23, 389 (1981).

[66] L. F. Abbott, Nucl. Phys. B 185, 189 (1981).

[67] S. Ichinose and M. Omote, Nucl. Phys. B 203, 221 (1982).

[68] T. Umeda, S. Aoki, S. Ejiri, T. Hatsuda, K. Kanaya, Y. Maezawa and H. Ohno, Phys. Rev. D 85, 094508 (2012) [arXiv:1202.4719 [hep-lat]].

[69] E. Berkowitz, M. I. Buchoff and E. Rinaldi, Phys. Rev. D 92, no. 3, 034507 (2015) [arXiv:1505.07455 [hep-ph]].

[70] R. Kitano and N. Yamada, J. High Energy Phys. 1510, 136 (2015) [arXiv:1506.00370 [hep-ph]].

[71] S. Borsanyi, M. Dierigl, Z. Fodor, S.D. Katz, S.W. Mages, D. Nogradi, J. Redondo, A. Ringwald, and K.K. Szabo, Phys. Lett. B 752, 175 (2016) [arXiv:1508.06917 [hep-lat]].

[72] C. Bonati, M. D'Elia, M. Mariti, G. Martinelli, M. Mesiti, F. Negro, F. Sanfilippo and G. Villadoro, J. High Energy Phys. 1603, 155 (2016) [arXiv:1512.06746 [hep-lat]].

[73] P. Petreczky, H. P. Schadler and S. Sharma, Phys. Lett. B 762, 498 (2016) [arXiv:1606.03145 [hep-lat]].

[74] G. Aarts, C. Allton, A. Amato, P. Giudice, S. Hands and J.-I. Skullerud, JHEP 1502, 186 (2015) [arXiv:1412.6411[hep-lat]].

[75] O. A. Kochetkov, V. G. Bornyakov, P. V. Buividovich and N. Cundy, PoS LATTICE2014, 047 (2015) [arXiv:1412.4341[hep-lat]].

[76] S.-T. Li and H.-T. Ding (Bielefeld-BNL-CCNU Collaboration), PoS LATTICE2016, 372 (2017) [arXiv:1312.0119 [hep-lat]].

[77] P. E. Crouch and R. Grossman, Journal of NonLinear Science 3 (1993), 1-33.

[78] Hans Munthe-Kaas, Applied Numerical Mathematics 29.1 (1999). Proceedings of the NSF/CBMS Regional Conference on Numerical Analysis of Hamiltonian Differential Equations, 115-127.

[79] M. B. Gavela, L. Maiani, S. Petrarca and F. Rapuano, Nucl. Phys. B 306 (1988) 677; Nucl. Phys. B (Proc. Suppl.) I7 (1990) 769.

[80] C. Bernard and A. Soni, Nucl. Phys. B (Proc. Suppl.) 17 (1990) 49.5; Nucl. Phys. B (Proc. Suppl.) 42 (1995) 391.

[81] R. Gupta, D. Daniel, G. W. Kilcup, A. Patel, and S. R. Sharpe, Phys. Rev. D 47 (1993) 5113 [arXiv:hep-lat/9210018].

[82] A. Donini, G. Martinelli, C. T. Sachrajda, M. Talevi and A. Vladikas, Phys. Lett. B360 (1995) 83 [arXiv:hep-lat/9508020].

[83] M. Crisafulli, A. Donini, V. Lubicz, G. Martinelli F. Rapuano, M. Talevi, C. Ungarelli and A. Vladikas, Phys. Latt. B369 (1996) 325 [arXiv:hep-lat/9509029].

[84] A. Donini, V. Giménez, G. Martinelli, G. C. Rossi, M. Talevi, M. Testa and A. Vladikas, Nucl. Phys. B (Proc. Suppl.) 53 (1997) 883 [arXiv:hep-lat/9608108].

[85] L. Conti, A. Donini, V. Gimenez, G. Martinelli, M. Talevi and A. Vladikas, Nucl. Phys. B (Proc. Suppl.) 63 (1998) 880 [arXiv:hep-lat/9710023]; Phys.Lett. B421 (1998) 273 [arXiv:hep-lat/9711053].

[86] T. Bhattacharya and S. Sharpe, Phys. Rev. D55 (1997) 4036 [arXiv:hep-lat/9611023].

[87] R. Gupta, Nucl.Phys. B (Proc.Suppl.) 63 (1998) 278 [arXiv:hep-lat/9710090].

[88] JLQCD Collaboration, S. Aoki, M. Fukugita, S. Hashimoto, N. Ishizuka, Y. Iwasaki, K. Kanaya, Y. Kuramashi, M. Okawa, A. Ukawa, T. Yoshié, Nucl. Phys. B (Proc.Suppl.) 63 (1998) 281 [arXiv:hep-lat/9709136]; Phys. Rev. Lett. 80 (1998) 5271 [arXiv:hep-lat/9710073]; Phys.Rev. D58 (1998) 054503 [arXiv:hep-lat/9711046].

[89] JLQCD Collaboration, S. Aoki, M. Fukugita, S. Hashimoto, N. Ishizuka, Y. Iwasaki, K. Kanaya, Y. Kuramashi, M. Okawa, A. Ukawa, T. Yoshié, Nucl.Phys. B(Proc.Suppl.) 60A (1998) 67 [arXiv:hep-lat/9711014], Phys.Rev. D60 (1999) 034511 [arXiv:hep-lat/9901018].

[90] D. Becirevic, Ph. Boucaud, V. Gimenez, V. Lubicz and M. Papinutto, Eur. Phys. J.C37 315-321 (2004), [hep-lat/0407004].

[91] F. Mescia, V. Gimenez, V. Lubicz, G. Martinelli, S. Simula and C.Tarantino, PoS LAT2005 (2005) 365, [hep-lat/0510096].

[92] G. Martinelli, C. Pittori, C. T. Sachrajda, M. Testa, and A. Vladikas, Nucl. Phys. B445, 81 (1995) [hep-lat/9411010].

[93] Y. Aoki, T. Blum, N. H. Christ, C. Dawson, T. Izubuchi, R. D. Mawhinney, J. Noaki, S. Ohta, K. Orginos, A. Soni and N. Yamada, Phys.Rev.D 73 (2006) 094507 [hep-lat/0508011].

[94] Y. Aoki, P.A. Boyle, N.H. Christ, C. Dawson, M.A. Donnellan, T. Izubuchi, A. Juttner, S. Li, R.D. Mawhinney, J. Noaki, C.T. Sachrajda, A. Soni, R. J. Tweedie and A. Yamaguchi, Phys. Rev. D78 (2008) 054510 [arXiv:0712.1061[hep-lat]].

[95] P. Dimopoulos, [arXiv:1101.3069[hep-lat]].

[96] C. Aubin, J. Laiho and R. S. Van de Water, Phys. Rev. D 81 (2010) 014507 [arXiv:0905.3947 [hep-lat]].

[97] T. Bae, Y.-C. Jang, C. Jung, H.-J. Kim, J. Kim, K. Kim, W. Lee, S. R. Sharpe and B. Yoon, Phys. Rev. D 82 (2010) 114509 [arXiv:1008.5179 [hep-lat]].

[98] Y. Aoki, R. Arthur, T. Blum, P.A. Boyle, D. Brömmel, N. H. Christ, C. Dawson, T. Izubuchi, C. Jung, C. Kelly, R. D. Kenway, M. Lightman, R. D. Mawhinney, S. Ohta, C. T. Sachrajda, E. E. Scholz, A. Soni, C. Sturm, J. Wennekers and R. Zhou, Phys. Rev. D84 (2011) 014503 [arXiv:1012.4178 [hep-lat]].

[99] R. Frezzotti, P. A. Grassi, S. Sint and P. Weisz, J. High Energy Phys. 08 (2001) 058 [hep-lat/0101001].

[100] R. Frezzotti, S. Sint and P. Weisz, J. High Energy Phys. 07 (2001) 048 [hep-lat/0104014].

[101] M. Constantinou, P. Dimopoulos, R. Frezzotti, K. Jansen, V. Gimenez, V. Lubicz, F. Mescia, H. Panagopoulos, M. Papinutto, G.C. Rossi, S. Simula, A. Skouroupathis, F. Stylianou and A. Vladikas, Phys. Rev. D83 (2011) 014505 [arXiv:1009.5606[hep-lat]].

[102] N. Carrasco, P. Dimopoulos, R. Frezzotti, V. Lubicz, G.C Rossi, S. Simula, C. Tarantino, Phys. Rev. D 92 (2015) 034516 [arXiv:1505.06639[hep-lat]].

[103] P. Vilaseca, M. Dalla Brida, and M. Papinutto, PoS LATTICE2015 (2016) 252 [arXiv:1605.09053 [hep-lat]].

[104] T. Ishikawa, S. Aoki, M. Fukugita, S. Hashimoto, K-I. Ishikawa, N. Ishizuka, Y. Iwasaki, K. Kanaya, T. Kaneko, Y. Kuramashi, M. Okawa, Y. Taniguchi, N. Tsutsui, A. Ukawa, N. Yamada, and T. Yoshié (CP-PACS and JLQCD Collaborations), Phys. Rev. D 78, 011502(R) (2008) [arXiv:0704.1937[hep-lat]].

[105] B. Sheikholeslami and R. Wohlert, Nucl. Phys. B259 (1985) 572.

[106] Y. Iwasaki, Nucl. Phys. B258, 141 (1985); University of Tsukuba Report No. UTHEP-118 (1983).

[107] M. Lüscher, R. Narayanan, P. Weisz, and U. Wolff, Nucl. Phys. B384 (1992) 168-228 [hep-lat/9207009].

[108] S. Sint, Nucl. Phys. B421 (1994) 135-158 [hep-lat/9312079]; Phys. B 451 (1995) 416 [arXiv:hep-lat/9504005].

[109] T.Kaneko, S.Aoki, M.Della Morte, S.Hashimoto, R.Hoffmann, R.Sommer , JHEP 0704 (2007) 092 [arXiv:hep-lat/0703006].

[110] M. Lüscher and P. Weisz, Nucl. Phys. B479 (1996) 429-458, [hep-lat/9606016].

[111] M. Lüscher, S. Sint, R. Sommer, and H. Wittig, Nucl. Phys. B491 (1997) 344-364 [hep-lat/9611015].

[112] M. Della Morte, R. Hoffmann, F. Knechtli, R. Sommer, and U. Wolff, JHEP 0507 (2005) 007 [hep-lat/0505026].

[113] S. Sint, Nucl. Phys. B847 (2011) 491-531, [arXiv:1008.4857 [hep-lat]].

[114] J. G. Lopez, K. Jansen, D. Renner, and A. Shindler, Nucl. Phys. B867 (2013) 567-608 [arXiv:1208.4591 [hep-lat]]; Nucl. Phys. B867 (2013) 609-635, [arXiv:1208.4661 [hep-lat]].

[115] F. Butler, H. Chen, J. Sexton, A. Vaccarino, D. Weingarten, Nucl.Phys. B421 (1994) 217-240 [hep-lat/9302012]; Nucl.Phys. B421 (1994) 217-240 [arXiv:hep-lat/9310009]

[116] UKQCD Collaboration: C.R. Allton, L. Lellouch, C.T. Sachrajda, H. Wittig, R.M. Baxter, S.P. Booth, K.C. Bowler, D.S. Henty, R.D. Kenway, C. McNeile, B.J. Pendleton, D.G. Richards, J.N. Simone, A.D. Simpson, Phys.Rev.D49:474-485,1994 [arXiv:hep-lat/9309002]

[117] S. Hashimoto, Phys.Rev. D50 (1994) 4639-4648 [arXiv:hep-lat/9403028].

[118] JLQCD collaboration: S. Aoki, M. Fukugita, S. Hashimoto, N. Ishizuka, Y. Iwasaki, K. Kanaya, Y. Kuramashi, M. Okawa, A. Ukawa, T. Yoshié, KEK-CP-71, KEK-CP-071, KEK-PREPRINT-97-217 [arXiv:hep-lat/9711041]

[119] J. C. Collins, Renormalization. An Introduction to Renormalization, the Renormalization Group, and the Operator Product Expansion (Cambridge University Press, Cambridge, UK, 1984).

[120] T. Endo, K. Hieda, D. Miura and H. Suzuki, PTEP 2015, no. 5, 053B03 (2015) [arXiv:1502.01809 [hep-lat]].

[121] H. Suzuki, PTEP 2015, no. 10, 103B03 (2015) [arXiv:1507.02360 [hep-lat]].

[122] H. Suzuki, PoS LATTICE 2015, 304 (2016) [arXiv:1510.08675 [hep-lat]].

[123] K. Hieda and H. Suzuki, Mod. Phys. Lett. A 31, no. 38, 1650214 (2016) [arXiv:1606.04193 [hep-lat]].

[124] G. Martinelli, Phys. Lett. B141 (1984) 395.

[125] S. Herrlich and U. Nierste, Nucl. Phys. B 455 (1995) 39 [arXiv:hep-ph/9412375].

[126] Y. Taniguchi, JHEP 04 (2012) 143 [arXiv:1203.1401[hep-lat]].

[127] http://bridge.kek.jp/Lattice-code/index_e.html